STRUCTURAL ANALYSIS OF J-AGGREGATING MOLECULES BY ABSORPTION, RAMAN, AND NMR SPECTROSCOPIES

By

PHILIPPE HELI MERCIER

A dissertation submitted to the Graduate Faculty in Chemistry in partial fulfillment of the requirements for the degree of Doctor of Philosophy, The City University of New York

2008

This manuscript has been read and accepted for the
Graduate Faculty in Chemistry in satisfaction of the
dissertation requirement for the degree of Doctor of Philosophy.

Daniel L. Akins

Date	Chair of Examining Committee

Gerald Koeppl

Date	Executive Officer

Daniel L. Akins

Nan-Loh Yang

Chwen-Yang Shew

Supervisory Committee

THE CITY UNIVERSITY OF NEW YORK

Abstract

STRUCTURAL ANALYSIS OF J-AGGREGATING MOLECULES BY ABSORPTION, RAMAN, AND NMR SPECTROSCOPIES.

by

Philippe Heli Mercier

Adviser: Professor Daniel L. Akins

Structural properties of J-aggregating molecules were studied using absorption, Raman and NMR spectroscopies. Results for PIC and 2,2'-carbocyanine showed that although the molecules were similar structurally, their NMR spectra showed fundamental differences in the bonding character of the bonds connecting the moieties in both molecules, these differences affected their conjugation, and also had consequences in the molecules' Raman spectra. TTBC and TDBC-4 were also studied and it was shown through absorption studies that in silver colloidal formulations, J-aggregates of TTBC formed preferentially on the silver nanoparticles rather than in solution. Similarities between Raman spectra of aggregated TTBC in colloidal silver and on silver electrode supported that conclusion and suggested that the optical coherence length of the J-aggregate was sufficiently short as to not be affected by the curvature of the nanoparticle. Structural isomers were found to exist in solutions of both TTBC and TDBC-4 indicating the greater pi bond character of the bonds in the polymethine chain compared to those of 2,2'-carbocyanine. A simple model arguing for both an optical and orbital coupling of

adjacent molecules in order to obtain all the special characteristics of J-aggregates was presented and was used to discuss intrinsic limitations to the coherence length that were unrelated to structural defects. This model was also used to explain the occurrence of disordered aggregates and other similar structures as well. Based on the concepts proposed, it was possible to develop a systematic method to elucidate a credible structure for the TSPP J-aggregate that agreed with conclusions advanced in the literature. Cyclic voltammetry was conducted on two metal porphyrins, Fe-TSPP and Co-protoporphyrin with the intent to use their aggregating properties to synthesize uniform-sized metal nanoparticles. Although the cyclic voltammograms did not show that the porphyrins released the metal ions from their core, it was determined that such a process could still occur and that further study with other metal porphyrins was needed. The combined data from Raman and NMR methods provided the necessary information on conjugation and conformational differences between similar molecules to make determinations that had not been previously possible with either method individually.

Acknowledgements

There are countless many to whom I owe a debt of gratitude and although there is not enough space for me to properly honor their contributions to my development as a thinker, a scientist, and more importantly, as human being, I must say a few things about them. Teachers are not given enough credit for their role in creating the next generation of leaders and there were many teachers who gave encouraged me to pursue excellence in anything that I did because they saw in me the potential to be great. In this regard, I would like to thank my middle-school and high school mathematics teachers Mme. Smith and Dr. Weill, my history and geography teacher Mme Lamerain, and my economics teacher Veronique, for all of their encouragement.

As an undergraduate student at City College and as a graduate student at the CUNY Graduate Center I had the privilege of meeting and learning from many professors who often taught me not only in their classes but also outside of the classroom. I would like to thank Professor Stephen Julich who at the time was in the Anthropology department, Professor Stanley Kaplan of the Mathematics department, Professors Frederick Smith, Harold Falk, and the late Philip Baumel of the Physics department, Professor Joseph Osinchak formerly of the Biology department, Professors Vernon G.S. Box, John Lombardi, Ronald Birke, Glen Kowach, and Maria Tamargo of the Chemistry department. I would like to give special thanks to the dedicated people in the Chemistry department at the Graduate Center, Professor Gerald Koeppl, Mrs Diane Adebowale, and Ms. Vivian Mason.

This research could not have progressed without the encouragement, advice and guidance from my committee members, Distinguished Professor Robert Alfano of the Physics department who serve on my committee for three years, Professors Nan-Loh Yang and Chwen-Yang Shew of the College of Staten Island Chemistry department, and of course my advisor, Distinguished Service Professor Daniel L. Akins. I would also like to thank the many people who helped me at the Center for Analysis of Structures and Interfaces, also known as CASI, during all these years and they include Mrs. Sandra Smith, Dr. Ronald H. Brown, and Ms. Diane Beckford. I am grateful to the many graduate students I shared time with in graduate school and they include my lab mates Dr. Fleumingue Jean-Mary, Dr Haiquan Guo, Dr, Xiaoming Zhang, Dr. Shiunchin Wang, Dr. Yanting Liao, Dr. Sheuli Zakia, Dr. Dionne Miller, and Dr. Nathan Stevens. I would like thank Dr. Mohammed Sohel, Dr. Benjamin Davis, Dr. Richard Foucault, Dr. Danh Nguyen-Thanh and soon-to-be, Dr. Richard Livingston for their solidarity in this shared experience. I must also thank Mr. Derrick Quinlan for all his help and friendship. It is very possible that I may have unintentionally omitted some names but I ask for their understanding and I also offer them my many thanks.

I hope to have the opportunity to demonstrate my gratitude for all the kindness, friendship, and counsel I received from all of you who contributed to my development as a scholar by doing what I can to help someone else, and perhaps many others, achieve their goals as well. Again, thanks.

In a larger context I would like to give thanks to my Lord and Savior Jesus Christ who ensured that before I was to know success, I was to learn humility so that whatever I were to accomplish, I would remember that ultimately it was all for His glory and honor.

This work is dedicated to the two people who did everything for me

My Mother Caroline Michel Mercier

My Grandmother Rose-Marie Fils-Aimé

Table of Contents

List of figures

Chapter 1: Introduction

1.1 Overview and motivation

The growth of nanotechnology relies on the discovery, characterization, and use of systems and materials that have, among many other characteristics, some combination of nanoscale dimensionality, high electrical, optical and thermal efficiencies, and ultrafast responsiveness to excitation. With the growing demand in industry for products that have higher performance, lower power consumption, and reduced production cost, nanoscale materials and processes are increasingly being sought-after[1]. Reducing the size of components in devices helps dissipate the heat generated from a mechanical or an electrical process more easily and reduces the power necessary to perform these processes. As a consequence of this need for smaller, more energy-efficient, and affordable components and materials, there has been a significant increase in academia, government, and industry in interdisciplinary research efforts as it has become apparent that skills from all areas of science and engineering are required to make important advances in nanotechnology[2].

Some of the major challenges in harnessing the capabilities of nanoscale systems and materials include synthesizing them and controlling their formation, along with arranging and incorporating them into larger functional systems. Because the nanoscale is within two orders of magnitude or less of the molecular scale for instance, nanomaterials often exhibit quantum mechanical behavior that cannot be duplicated in bulk materials where classical physics and bulk properties of matter dominate[3]. Similarly, although there have

been many advances particularly in energy and consumer electronic industries there is still a significant amount of basic scientific research that has not yet been done on many of the nanoscale systems that are already in use today [4]. It remains essential to conduct original basic scientific research to better understand and use the relevant properties of those systems. As an example, although carbon nanotubes (CNT) are at the heart of fuel cell technology because of their potential capacity to store fuels such as liquid hydrogen, there is still much basic information on CNT properties to understand before fuel cell systems can be optimized for highest efficiency and cost-effectiveness. Additionally, there are still no synthetic methods available to selectively form carbon nanotubes and this remains a key challenge for researchers. Other difficulties concerning CNT synthesis and use will be discussed in section 1.3.

Among the molecules in which many of the aforementioned desirable nanotechnological properties are present are the cyanine dyes and porphyrins; many have the ability to aggregate, under the proper conditions, by self-assembly into well-ordered structures called J-aggregates (named after one of their co-discoverers). These aggregates have interesting non-linear optical properties as well as dynamical properties that may potentially lead to future device applications[5]. J-aggregates can potentially used as nanomaterials and with their optical properties may provide the opportunity to create new all-optical pathways for processes that today are being performed by bulkier, heavier, and less efficient materials such as the silicon-based semiconductor systems that are prevalent today.

There are many useful optical properties of J-aggregates, included among them are high fluorescence efficiencies; in the case of some J-aggregates there is also the phenomenon

of amplified spontaneous emission, also known as superradiance. The potential, for instance, of cyanine dyes to serve as core components in mirrorless laser systems because of their superradiant properties is extremely important. The possibility of mirrorless lasing opens the door for true all-optical networks where optical switches could replace, or at least reduce, the electrical components in current-day transistor technology and lead to previously unimaginable processing scales while also drastically reducing heat output. In addition to the fact that cyanine dyes, because of their relatively simple shapes and relatively small sizes, could potentially be synthesized for specific systems depending on what properties were needed, cyanine dyes are also interesting to study for basic scientific research[6].

Porphyrins have for a long time been known to be important molecules in biological research and similarly to the cyanine dyes, still have many areas of basic scientific interest that have yet to be fully addressed, particularly concerning their J-aggregates through which for instance charge-transfer processes are facilitated[7]. Structural properties of molecular aggregates have not been studied to the same degree as their corresponding optical and dynamical properties; aggregate morphology for instance, likely an important factor in potential device applications, is an area that remains fertile ground for investigation. As an example of how much basic work on aggregate morphology remains to be done only recently have techniques such as dynamic light scattering (DLS) and atomic force microscopy (AFM) been used to make measurements and determinations on smooth surfaces[8].

J-aggregates are ubiquitous in forming in various environments and it is essential to obtain comprehensive structural data on them. J-aggregates of many molecules form in

basic[9] as well as acidic solvents[10], in colloidal suspensions[11], embedded in micellar media[12], occluded in vesicles and mesoporous materials[13], on electrode surfaces[14] and layered onto solid substrates[15]. Their versatility makes them essential for nanoscience research. While many J-aggregates have been characterized in these environments and much research has been conducted on the dynamics of these systems, very little data has been obtained on the structure of the single molecule within the aggregate. In recent decades techniques such as Raman and conventional NMR spectroscopy have been improved to widen their applicability. Today these techniques can be used to study increasingly complex molecular systems including J-aggregates and the combined data obtained with these spectroscopic techniques in conjunction with theoretical methods can significantly augment the quality and amount of structural data available for J-aggregating molecules.

1.2 Background

1.2.1 Molecular exciton theory

In an effort to understand the optical properties of molecular crystals a theory on the resonance interaction of excited states of weakly coupled molecular systems was developed by Davydov and the central concept used to describe this interaction was that of the exciton. This comprehensive theory was termed molecular exciton theory and ever since the exciton concept has been used to describe optical properties of numerous coupled molecular systems, including that of H- and J-aggregates. Although investigations into the structural properties of H-aggregates will not be explicitly

presented in this work molecular exciton theory has been the foundation on which both types of aggregates have been studied. There were essentially two problems that were considered when developing the theory of molecular excitons: firstly, a method had to be developed to construct an energy level scheme for these systems and secondly a model had to be developed that described the transitions between these energy levels[16].

The exciton concept used today to describe the optical properties of H- and J-aggregates is of the Frenkel type, introduced in 1931. The exciton's state and energy are represented by an electronic excited-state delocalization over an extended space covering a range within the physical dimensions of the system of interest[17]. In the case of molecular aggregates, the exciton extends within the range allowed by the coupling of the available transition dipoles. As the intermolecular forces holding the aggregate together are much weaker than those within individual molecules, the structure and energy of the monomers in H- and J-aggregates can be considered as unchanged to a first approximation. This approach allows exciton concepts to be applied to their theoretical analysis using perturbation methods and this is particularly useful because molecular exciton theory can describe the essential optical properties of both aggregates by using the simplest aggregate, the molecular dimer, as a model.

1.2.2 Optical properties of J-aggregates

The theoretical underpinning of self-assembled ordered aggregates relies on interpreting the aggregate as a collection of oscillators with the transition dipoles of the monomers aligned in a presumed "head-to-head" (H-aggregates) or "head-to-tail" (J-aggregates) fashion[18] (Fig 1-1).

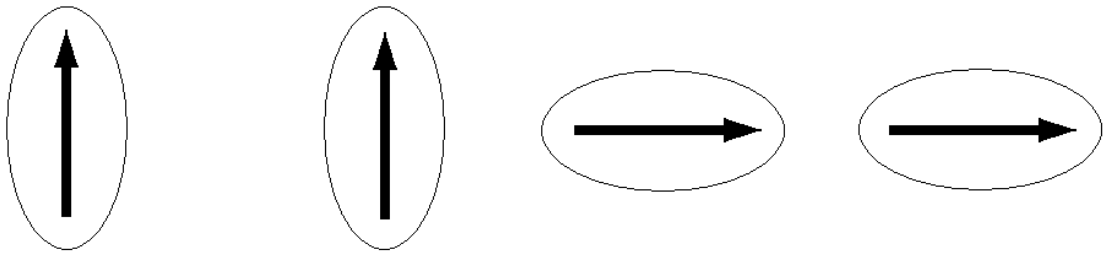

Figure 1-1. a) Head-to-Head alignment of transition dipoles. b) Head-to-Tail alignment of transition dipoles.

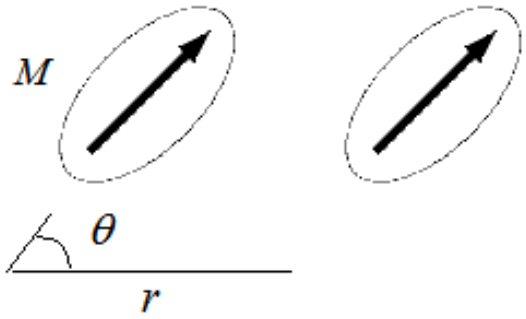

Figure 1-2. The simplified point-dipole model. The size of the transitions dipoles is enlarged only to illustrate their parallelism however the validity of the point-dipole model applies when the "length" of the transition dipoles is much shorter than the distance between them.

Qualitatively, the point-dipole approximation can properly describe the affect of aggregation on the energy of the molecular system because the general features of dipoles and molecular alignments are represented (Fig 1-2). Mathematically, the energy difference between the combined energies of two individual monomers and that of a molecular dimer can be represented thusly.

$$\Delta\varepsilon = c\frac{M^2}{r^3}\left(1-3\cos^2\theta\right) \qquad [1.1]$$

Here $\Delta\varepsilon$ is the energy difference, θ is the angle between parallel transition dipole vectors and the line of centers between the molecules in the aggregate, r is the distance between the two molecules and M is the transition dipole of each molecule.

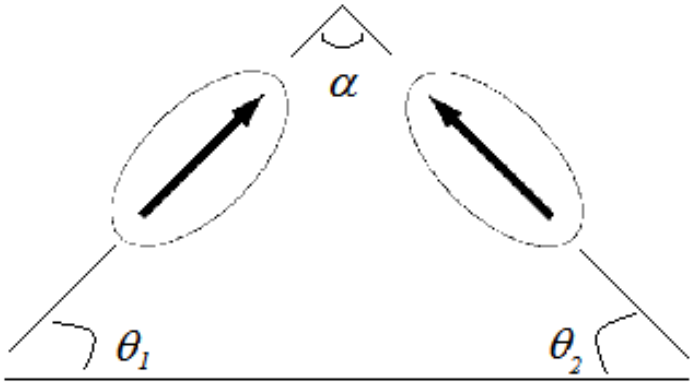

Figure 1-3. Generalized point-dipole model.

A more generalized point-dipole expression can be used where the transition dipoles are not necessarily parallel to each other (Fig 1-3).

$$\Delta\varepsilon = \frac{2M^2}{r^3}\left(\cos\alpha + 3\cos\theta_1\cos\theta_2\right) \qquad [1.2]$$

Here α is the angle between the transition dipole moment vectors and θ_1 and θ_2 are the angles of the respective transition dipoles and the line of centers between the molecules. In both models, the result of aligning both of the molecules with respect to the line of centers at less than 54.7°, the so-called magic angle, leads to a lowering of the aggregate energy with respect to the monomers, a J-aggregate configuration. An alignment where the transition dipoles are at an angle greater than 54.7°, an H-aggregate configuration, leads to an increase in the aggregate's energy with respect to that of the monomers. This simple model easily illustrates why the allowed electronic absorption transition for an H-

aggregate is blue-shifted relative to that of the monomer absorption, and why in the case of the J-aggregate the absorption is red-shifted.

Absorption spectroscopy is often the first technique used to study a molecule because of the relative ease with which a spectrum can be obtained and an interpretation of that spectrum can be made.

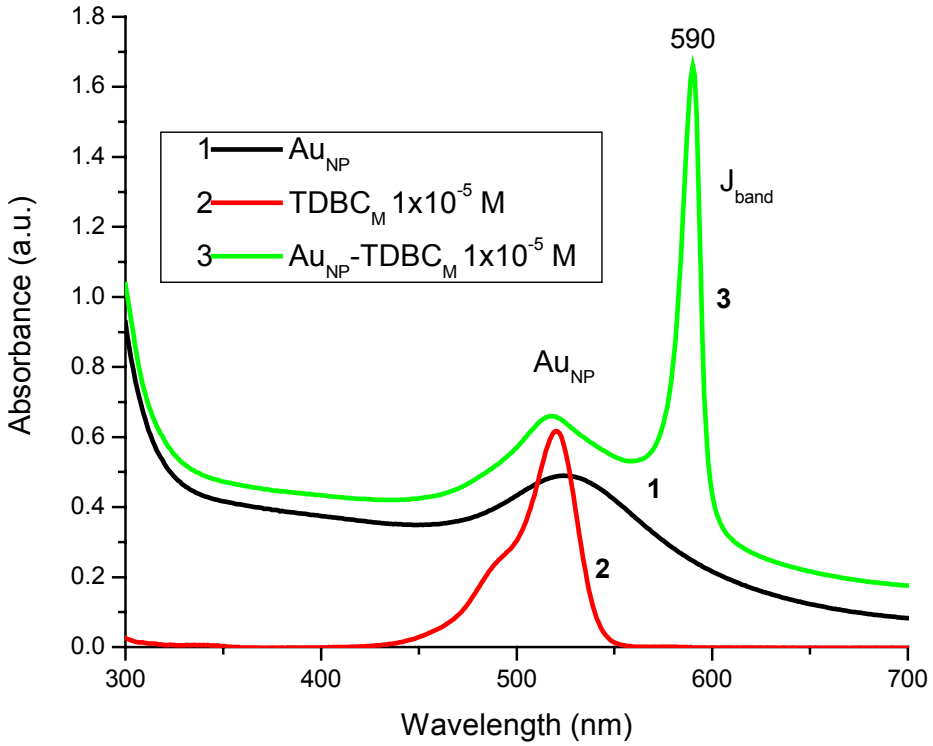

Figure 1-4. Absorption spectra of 1.) gold nanoparticles, 2.) TDBC in methanol and 3.) TDBC on gold nanoparticles. The J-aggregate of TDBC produces a sharp and red-shifted peak relative to the absorption peak of the TDBC monomer.

Dyes in particular are highly responsive to excitation in the ultraviolet and visible region and significant information on structure and dynamics can be gathered from absorption and fluorescence measurements. Because of their activity in this region cyanine dyes for

instance have been used for a long time in the photographic industry and in recent decades have been used as sensitizers for metal surfaces[19]. The special ability of cyanine dyes to self-assemble into ordered aggregates also causes them to have both different spectroscopic and structural properties compared to those of the single molecule such as the previously mentioned appearance of a sharp and red-shifted peak relative to the single molecule transition (Fig 1-4). Emission properties of J-aggregated cyanine dyes include emission intensities that are much greater than those of the monomer and emission profiles that are nearly the mirror image of the respective absorption profiles[20]. The fact that the J-aggregate emission peak is virtually the mirror image of its absorption peak indicates that the individual molecules effectively lose many torsional, rotational, and vibrational degrees of freedom, reducing the number of available non-radiative relaxation pathways for the excited species.

One of the most important matters that continues to be an area of very active research concerning the optical properties of J-aggregates relates to what is termed the optical coherence length of the aggregate[21], a property that is intimately related to the stability and structural integrity of the aggregate. The optical coherence length is interpreted as being the delocalization of the excited state over the space occupied by a certain number of monomer units in the aggregate whose transition dipoles have coupled and thus respond coherently to electronic excitation. There have been many attempts to determine the coherence length of various molecules by spectroscopic means[22] however no method has provided conclusive evidence to validate it over the results of other methods. The primary obstacle in determining not only the aggregate's coherence length but all the optical properties of these self-assembled structures is that there is no highly detailed

structural data available that clearly shows how the molecules arrange themselves in space and how this arrangement affects the aggregate's response to electronic excitation. For instance, it is unclear what role irregularities in the conformations of the individual molecules play, if any, in limiting the coherence length of the aggregate. Similarly, it is unclear if the coherence length is in some way an inherent property of the aggregate being studied. More specifically, it is unclear if the coherence length is variable, has a minimum value specific to each aggregate or does not. It is furthermore unclear if there is some kind of relationship between the coherence length and the actual physical length of the aggregate.

1.2.3 Structural properties of J-aggregates

The study of J-aggregate structure is of fundamental importance to the understanding of all their physical and spectroscopic properties however, there are many challenges to overcome before a comprehensive structural analysis can be done. As mentioned before it is still unknown how individual molecules arrange themselves upon formation of the aggregate and most methods used so far have been useful to the extent that they have provided some support for proposed models (Fig 1-5).

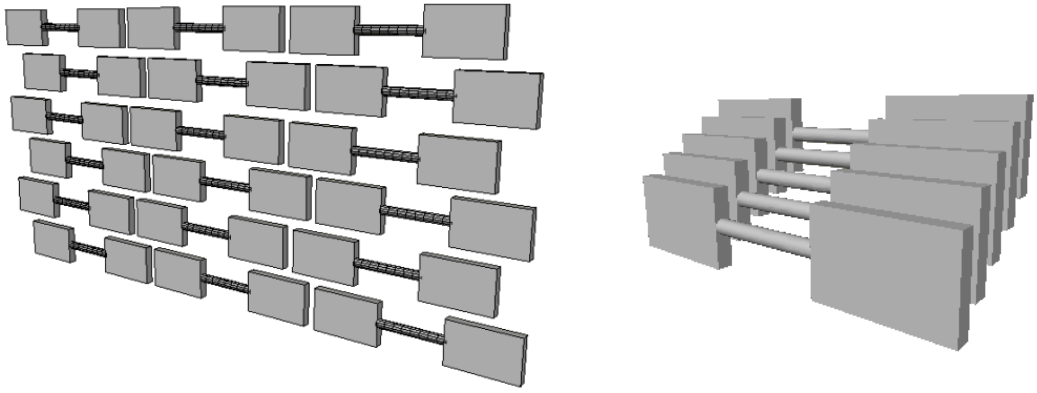

a. Staircase model b. Spread-deck-of-cards model

Figure 1-5. Conceptual models of J-aggregate arrangements

The primary reason why it is not clear how these molecules self-assemble is that there is no obvious driving force. One common aspect of the environments in which J-aggregates of cyanine dyes have formed is that there seems to be a negative electric field that serves as an attractor to the dyes. The fact that these dyes are usually cations suggests an electrostatic interaction triggers the aggregation process however this is an overly simplified explanation that does not address the behavior of cyanine dyes in specific situations such as in a basic solution or on a glass substrate. As an example, there is no obvious reason why colloidal silver or colloidal silica serve as such favorable surfaces for aggregation of dyes even in minimally basic solutions while the same dye may not easily aggregate in aqueous solutions even with very high ionic strength or pH. Said differently, even though electrostatics can explain to some degree the attraction of a molecule to a surface it does not totally explain the attraction of a molecule to another. A change occurs in the aggregating molecule that alters its energy; in particular, the energies of the pi-orbitals in the molecules are affected in a manner that promotes a coupling of one molecule with another. Clearly thermodynamic considerations are important in understanding J-aggregation[23] such as solubility in a solution, entropy change upon aggregation, etc, however it is clear that the quantum mechanical properties of the molecules cannot be ignored and that a comprehensive description of J-aggregation would address both aspects. The fact that one cannot simply view the molecules involved as classical objects that collide and stick together makes it more difficult to theoretically model the self-assembly process. When structural changes occur within a molecule, it is possible that the result of the change affect the portion of the molecule that contains the chromophore in a systematic or predictable way. In this area Raman spectroscopy has

been an essential tool in determining the areas in a molecule where changes occur that lead to differences in the relative intensities of vibrations between the monomer and the aggregate[24]. Sometimes however, the changes that occur cannot be easily interpreted and require further study. Despite the fact that many questions remain unanswered concerning aggregate morphology on surfaces, and concerning the structure of the monomer within the aggregate, there are nonetheless many details that have already been uncovered. It is known for instance that J-aggregates are typically linear structures, helical in shape, and with a degree of slippage between neighboring molecules. Additionally, J-aggregating molecules produce peaks in the low energy region of their Raman spectra that are attributable to the coupling of molecular vibro-excitonic modes. These vibrations that can be understood conceptually as being similar to lattice modes in molecular crystals. In Raman spectra of most J-aggregates, the intermolecular vibrations lead to a pair of peaks in the low energy region although the set of motions that lead to these vibrations has not yet been conclusively determined.

1.3 Preview of chapters

Molecules that J-aggregate are unique in many ways. Not only do these molecules form ordered structures by self-assembly and can do so in various environments under differing conditions, but what is particularly interesting is that the integrity and stability of their structures rely primarily on weak, non-covalent forces. Ordinarily aggregates that are held together by weak interactions are usually disordered, unstable, and do not display any unique spectroscopic properties. J-aggregates on the other hand are ordered structures, can be relatively stable even in solution, and display spectroscopic properties

that are very different from those of the single molecule. The coupling of transition dipoles of neighboring molecules requires an environment that facilitates the process but also requires that the molecules themselves readjust to compensate for their proximity. One of the difficulties in studying the structural changes that occur within the single molecule upon aggregation is that traditional spectroscopic methods that have been used so far do not give sufficient clues.

Absorption spectroscopy, while used extensively to demonstrate the validity of theoretical models that try to predict the optical response of J-aggregates is not really a reliable tool to ascertain the optical coherence length of the exciton. Furthermore, absorption spectroscopy is even less reliable for structural assessments because it is rather insensitive to subtle changes in molecular conformations and small differences in molecular constitution. Most research on J-aggregate structure has focused on vibrational band assignments using Raman spectroscopy, often with the aggregating species on an electrode surface in an electrochemical system whereby different vibro-excitonic states can be tuned to resonance with the excitation source. In using Raman spectroscopy to study cyanine dyes and certain porphyrins it was possible to determine the presence of aggregated species even in systems where it was not possible to make such a confirmation through absorption spectroscopy[25]. With the advent of more powerful and sensitive instrumentation, NMR techniques have increasingly been used to verify the composition and general structure of newly synthesized cyanine dyes[26]. Curiously, Raman and NMR methods have not been used together to provide a clearer understanding of cyanine dye structure especially concerning the differences between dyes that are similar in composition. Previously published NMR work on monomer and

aggregated cyanines offered some insight into the dyes' structure[27-29] however, there were certain erroneous conclusions concerning the arrangement of the molecules in the aggregate that could have been avoided had Raman spectra of such dyes been available as well. The absence of an independent source of structural information with which to corroborate the NMR data limited the reliability of the analysis in those studies. It is the intent of this work to show how the combined data obtained from absorption, Raman and NMR spectroscopies will serve to demonstrate how differences in the pi-orbital distribution affects the flexibility, deformability, and shape of cyanine dyes and porphyrins, and ultimately, formation of the J-aggregates. These differences show how the process of self-assembly depends largely on the nature of the conjugation of the pi-orbitals and in large part explains why similarly structured molecules do not necessarily aggregate in the same way, or to the same degree, under the same conditions. Furthermore, it will be shown to a first approximation that there are essentially two types of coupling that take place in a J-aggregate, there is a physical type that ensures the cohesion and structural integrity of the aggregate, and there is an optical type that gives the aggregate its optical properties. It is possible to treat the two forms of coupling independently in order to facilitate a theoretical analysis of the system however it is understood that ultimately the physical coupling that takes place in a J-aggregate greatly affects not only the aggregate's physical stability but also its coherence length.

In chapter two all the experimental techniques and apparatuses are described. An effort is made to provide the sufficient background information for each experimental technique so that all results in subsequent chapters can be discussed without the need for additional background material.

In chapter three UV-Vis, Raman and NMR results will be presented on the monomeric forms of 2,2-cyanine, herein referred to as PIC (pseudoisocyanine), and 2,2'-carbocyanine, the carbocyanine analogue of PIC. It will be shown how the pi-character of the electrons near the center of both molecules is fundamentally different in each molecule and this information will provide an interesting vantage point to understand the nature of J-aggregation from a structural perspective. The choice of using 2,2'-carbocyanine is helpful in two ways as not only can its structural properties be compared to those of PIC but also to those of other carbocyanine dyes. It is known that cyanine dyes that J-aggregate very often do so on surfaces without the need for any special surface treatment or derivatization. In solution however factors such as pH, ionic strength and solubility affect the potential for a particular dye to aggregate and also affects the stability of that aggregate. PIC and 2,2'-carbocyanine are two cyanine dyes that do not easily J-aggregate at low concentrations in simple solutions however are known to aggregate in colloidal suspensions and in concentrated solutions with high ionic strength. By studying NMR spectra of the monomers of PIC and 2,2'-carbocyanine the similarities, differences, and trends in their spectra will help support the comparative analysis of their Raman spectra. The results obtained will also serve as a good foundation for the work presented in chapter four.

The carbocyanines 1,1',3,3'-tetraethyl,5,5', 6,6'-tetrachlorobenzimidazolocarbocyanine iodide, known as TTBC, and 5,5',6,6'-tetrachloro-l,l'-diethyl-3,3'-

di(4-sulfobutyl)-benzimidazolocarbocyanine, also known as TDBC-4, are two dyes with similar characteristics. These two dyes form J-aggregates in solution relatively easily as opposed to PIC or 2,2'-carbocyanine and are therefore better candidates to study J-

aggregate structure with NMR methods. It will be shown how the aromatic character of the polymethine bridge electrons help explain the relative ease of J-aggregation of these molecules compared to PIC and 2,2'-carbocyanine and the NMR spectrum of J-aggregated TDBC-4 will be analyzed with the objective of finding clues to the arrangement of the monomer in the aggregate. Raman spectra of TTBC and TDBC-4 will be presented and analyzed along with UV-Visible spectra of TTBC in colloidal silver where the nature of the J-aggregate/Ag nanoparticle interaction will be discussed. Overall, the intent of the work presented in this chapter will have been to show that there are trends in the spectra of these dyes, particularly in the NMR spectra, that make it possible for one to deduce or confirm certain structural characteristics of J-aggregates that are otherwise at best suggestive without this data. Two additional results from this study will be used to demonstrate the importance of conjugation and pi orbital character to the stability of a J-aggregate and to show in a different way that the regions of the molecules that give a J-aggregate its structural and optical properties are, for practical purposes, independent of each other. With this data arguments will be made that support a molecular assemblage that should generally apply to all J-aggregates. Theoretical models of the way quantum mechanics governs the optical properties of J-aggregates have been proposed and refined ever since the discovery of J-aggregates. While the concept of the exciton remains the central element in any J-aggregate theory and many conceptual advances have been made to understand the nature and properties of excitons very little work has been done that intrinsically associates them to the structure of the molecules that form a particular aggregate[30]. There are many reasons for this although the principal obstacle that prevents a well-developed model from including structural

considerations is that basic details of J-aggregated structures are still unknown. As a substitute, data obtained from crystal forms of some dyes are used in exciton theory equations, however, there are sufficient differences between the conditions under which J-aggregates and molecular crystals are formed that there remains an incomplete picture of J-aggregate structure. Similarly, attempts to determine the chiralities and symmetry groups of J-aggregates have been unsuccessful; only relatively recently have high-level quantum chemical calculations been possible on molecules with the size of cyanine dyes and porphyrins. Accurate calculations involving collections of these molecules interacting with each other are still unrealistic as it would be necessary to propose a structural model that is already sufficiently close to the real form of the aggregate. A discussion on the optical coherence length of molecular excitons will be presented that will rely on intrinsic structural properties of the molecules to demonstrate how these factors can limit the coherence length even if there are no defects in the aggregate structure.

In addition to the cyanine dyes three porphyrins, TSPP, Fe-TSPP and Co-Protoporphyrin were studied with the intent of determining the feasibility of using the J-aggregating properties of TSPP and metal cation analogues of TSPP as an initial step in a process for the selective formation single-walled carbon nanotubes. Currently carbon nanotubes are being investigated for a multitude of nanotechnological applications because of their multifunctional nature[31]. The combination of chirality-specific conduction properties, high tensile strength and relative lightweight easily make carbon nanotubes the primary materials of interest in nanoscience. As such, finding methods for selectively synthesizing carbon nanotubes depending on what type of system for which they are

needed are very important and are an area of active research[32]. Metal nanoparticles have been used as catalysts in many synthetic processes however one of the problems with using this method to form carbon nanotubes is that because of the large size-distribution of these nanoparticles a large variety of carbon nanotubes are formed and there are as yet no generally applicable methods for separating them. There are other challenges to overcome before carbon nanotubes can be fully utilized in nanotechnology and among those is the problem of dealing with carbon nanotube bundles. The attractive forces between carbon nanotubes are very strong and as a result they do not readily dissolve in conventional organic or aqueous solvents and current methods of dissolution usually require some kind of chemical modification of the surface[33]. One way of avoiding the aforementioned challenges in synthesizing and separating carbon nanotubes is to find a method to obtain them in a manner that allows their synthesis to be type-specific and that keeps them somewhat apart from each other. In this chapter, a model of the J-aggregate of TSPP will be proposed that is based on concepts introduced in previous chapters that agrees with all known qualitative conformational features of protonated and aggregated TSPP. Absorption spectra will be presented for all three porphyrins in both acid and base and cyclic voltammograms will be presented for Fe-TSPP and Co-protoporphyrin in acid on a platinum electrode. Results will be analyzed as they pertain to surface coverage and to the location and nature of the bonding between the porphyrins and the electrode.

In chapter six all results will be summarized and future research ideas will be proposed. The combined data obtained from absorption, Raman, and NMR spectroscopies will be shown to provide new and important information on cyanine dye molecular structure and on J-aggregation.

Chapter 2: Spectroscopic Techniques and Experimental Systems

Background information is provided for each experimental technique used. All data obtained with each experimental technique was acquired on the same instrument.

2.1 Electronic absorption spectroscopy

Electronic absorption spectroscopy of liquids samples has long been used to characterize the optical properties of cyanine dyes and is still the first technique considered when gathering preliminary information on them. At low concentrations, spectra of analytes that absorb between the near ultraviolet to near infrared region can be acquired with absorbance intensities following Beer's Law where the absorption is proportional to the concentration of analyte in the solution.

$$A = \varepsilon c l \qquad [2.1]$$

In Beer's Law A is the absorption of the molecule of interest, ε is the molar absorptivity, also known as the extinction coefficient, c is the molar concentration of the analyte, and l is the path length of light in the sample cell. Absorption spectroscopy is very useful in tracking the change in composition of a solution when changes are made for instance to the pH or ionic strength of the sample, or when the absorption of one species is proportional to the decrease in absorption of another. Such is the case during the formation of a J-aggregate where a decrease in the molecular absorption intensity is concomitant with an increase to that of the J-band absorption. Additionally cyanine dyes absorb even at micromolar concentrations making absorption spectroscopy a very practical technique as well in regards to sample size requirements.

Experimental procedure

Absorption spectra for all molecules presented here were acquired using a Perkin Elmer Lambda 18 spectrophotometer, usually in non-absorbing 1 cm path length quartz cells that allow for spectral acquisition into the UV region down to 200 nm. Methanol solutions were prepared with ultra-high purity methanol and aqueous solutions were prepared with high-resistivity deionized water. Colloidal suspensions of silver were prepared by Dr F. Jean-Mary using the standard silver nitrate reduction method[1].

2.2 Vibrational spectroscopy

Raman spectroscopy is a type of vibrational spectroscopy and is the quantum mechanical complement to infrared spectroscopy. Qualitatively, the infrared signal is sensitive to the strength of polarization of a bond, i.e., the strength of an infrared signal can be modeled using a Hooke's Law-type model whereas the Raman signal is sensitive to the polarizability of a particular bond. The polarizability is a tensor that relates the surrounding electric field to the dipole moment of a species.

$$\vec{\mu} = \alpha \vec{E} \qquad [2.2]$$

$$\begin{bmatrix} \mu_X \\ \mu_Y \\ \mu_Z \end{bmatrix} = \begin{bmatrix} \alpha_{XX} & \alpha_{XY} & \alpha_{XZ} \\ \alpha_{YX} & \alpha_{YY} & \alpha_{YZ} \\ \alpha_{ZX} & \alpha_{ZY} & \alpha_{ZZ} \end{bmatrix} \begin{bmatrix} E_X \\ E_Y \\ E_Z \end{bmatrix} \qquad [2.3]$$

Conceptually the polarizability is a measure of how much the electronic distribution in a bond or in a molecule can be modified from that of its equilibrium configuration upon interaction with either a persistent or transient electromagnetic disturbance. Quantum mechanically the polarizability can be represented as the orbital overlap between two vibrational energy levels summed over all intermediate electronic and vibrational states. The generalized Raman cross-section can be represented in different ways but for the purposes of this work, two representations will be particularly useful:

$$\sigma_{R,i\to f}(\omega_L) = \frac{8\pi^2 M^4 \omega_L \omega_s^3}{9\hbar^2 c^4} \sum_i P_i \left| \sum_v \frac{1}{\pi} \frac{\langle f|v\rangle\langle v|i\rangle}{\omega + \omega_i - \omega_0 - \omega_v + i\gamma/2} \right|^2 \qquad [2.4]$$

$$\sigma_{k\to k',r} = -\left(\frac{\hbar c}{2\varepsilon_0}\right)(nkk')^{\frac{1}{2}} \sum_r \left[\frac{(\vec{\mu}^{mr}\cdot\bar{e}')(\mu^{rp}\cdot\bar{e})}{E_{rp} - \hbar ck} + \frac{(\vec{\mu}^{mr}\cdot\bar{e})(\vec{\mu}^{rp}\cdot\bar{e}')}{E_{rp} + \hbar ck'} \right] e^{i(k-k')\cdot\bar{R}} \qquad [2.5]$$

In equation [2.4], the electronic transition dipoles are grouped together and removed from the summation over initial vibrational states and intermediate vibrational states that have sufficient overlap with the initial and final states. The imaginary term $i\gamma$ is a damping term that prevents the expression from increasing without bound in a resonance excitation. In equation [2.5], both the electronic and vibrational components of the wavefunction are in the summation along with the local electric fields and the sum is over all intermediates. In the latter equation *k* and *k'* are wave vectors and serve as the energy propagators in the scattering process[2]. Conceptually the wave vectors perform the same role as the vibrational intermediates do in equation [2.4].

Experimental procedure

All nonresonance Raman spectra were acquired using a Coherent Innova 200 argon-ion laser as pump source and resonance Raman spectra were acquired using a Coherent CR-599 dye laser. Spectra acquired for aggregated species were done on smooth silver electrode in an electrochemical cell designed such that the electrode surface was oriented at 45 degrees to both the incident laser light and the detector resulting in a Raman signal that is perpendicular to that of the incident light.

2.3 Nuclear magnetic resonance spectroscopy

Nuclear magnetic resonance or NMR spectroscopy is an experimental technique that is used to detect atomic nuclei with non-zero magnetic quantum number m[3]. In the presence of a strong magnetic field $\vec{B}_0$ the population of a nucleus of interest splits into its $2I+1$ orientations, where I represents the spin angular momentum quantum number, and the values of m go in integer steps in the interval of $[-I, I]$. The spin angular momentum $\vec{I}$ is related to the magnetic moment $\vec{\mu}$ of the nucleus by a proportionality factor called the gyromagnetic ratio γ.

$$\vec{\mu} = \gamma \vec{I} \qquad [2.6]$$

The gyromagnetic ratio is a measure of the response or susceptibility of a nucleus to a magnetic field and this quantity is dependent on both the magnetic spin and the mass of the nucleus. NMR is extremely useful in organic chemistry, especially proton or ^{1}H NMR as this nucleus is the most responsive to the presence of a strong magnetic field and the

^{1}H nucleus, appears in a large number of organic compounds. Followed by ^{13}C, these two remain the most widely used nuclei for NMR work. In the case of ^{13}C NMR, although its abundance relative to ^{12}C is extremely small and the magnetic susceptibility of the ^{13}C nucleus is much weaker than that of ^{1}H, the fact that most molecules are carbon compounds makes ^{13}C NMR in many ways just as important as ^{1}H NMR. The source of the NMR signal is a transition from a higher energy orientation of the magnetic spin to a lower energy orientation with

$$\Delta m = \pm 1 \qquad [2.7]$$

and

$$E = \vec{\mu} \cdot \vec{B} \qquad [2.8]$$

E is the energy of a nucleus in the presence of a magnetic field. Because the magnetic moment of a nucleus is very sensitive to local electric field effects, a nucleus that appears in different regions of a molecule can exhibit different peaks in its NMR spectrum depending on the effective shielding σ_{eff} provided by neighboring electrons. The differences in response of the nucleus of interest when in a particular molecule from that of a reference is called the chemical shift δ and it is expressed in parts per million.

$$\delta = 10^{6} \frac{\nu - \nu_{ref}}{\nu_{ref}} \qquad [2.10]$$

where

$$v = \frac{\gamma \vec{B}_0 \left(1 - \sigma_{eff}\right)}{2\pi} \qquad [2.11]$$

The energy difference between spin orientations relative to the applied magnetic is proportional to the strength of the field and the gyromagnetic ratio of the nucleus of interest.

$$\Delta E = \frac{h\gamma \vec{B}_0}{2\pi} \qquad [2.12]$$

The energy difference obeys the Boltzmann distribution of the relative populations of the spin orientations and the greater the energy difference, the stronger the relaxation transition and thus the stronger the NMR signal.

$$\frac{n_{upper}}{n_{lower}} = e^{-\Delta E/\ kT} \qquad [2.13]$$

and approximately

$$\frac{n_{lower} - n_{upper}}{n_{lower} + n_{upper}} = \frac{\Delta E}{2kT} \qquad [2.14]$$

Similarly to infrared absorption spectroscopy NMR peaks that appear in a region of the spectrum provide information on the functional groups and the type of bonding that are in the vicinity of the nucleus. Additionally not only does NMR offer qualitative information on a molecule but also quantitative information as the relative areas under each peak is equal to the relative magnitudes of the nucleus of interest in different parts of the molecule. Another feature of NMR that helps deduce the immediate environment of a nucleus is the splitting of a peak caused by interference by another NMR-active nucleus;

typically the strongest splitting will occur if a similar nucleus is in the vicinity. The degree of splitting between peaks of neighboring nuclei is the same and this spacing is called the coupling constant ***J***. One can obtain information on conformations from NMR data using the Karplus equation:

$$^{3}J = A + B\cos\theta + C\cos^{2}\theta \qquad [2.15]$$

Where A, B, and C are the first, second, and third order coupling constants, respectively, and θ is the dihedral angle between the interacting nuclei[4].

Experimental procedure

NMR spectra were obtained using a Varian Mercury Plus 300 which operates at 300MHz and produces a magnetic field of just over 7 Tesla. Samples were prepared in deuterated solvents D_2O and CD_3OD and spectra were acquired at room temperature typically over 512 or 1024 repetitions, with 1 second relaxation delay between scans, in order to obtain results with a sufficient signal-to-noise ratio that all peaks of interest could be properly identified.

2.4 Electrochemical methods

Some of the more interesting properties of molecules are best observed in an electrochemical system where an applied potential can alter the energy of a molecule in such a way as to make it interact more strongly with a surface, make it react faster, or even make it arrange itself in a system in a desire manner. When electrochemical methods were coupled to Raman spectroscopic measurements, surface-enhanced Raman

spectroscopy, or SERS, became an almost indispensible tool to study the structure of many molecules. Molecules responded differently at different applied potentials allowing for the relative enhancement of certain types of vibrations compared to others as well as allowing for the overall enhancement of the Raman spectrum. Roughened surfaces provided locations where local fields could be much greater than the applied field thus strengthening the scattering response of the molecule. Another enhancement phenomenon was observed in Raman spectra of J-aggregated molecules on smooth surfaces where SERS concepts did not apply. This new enhancement mechanism was termed Aggregate-Enhanced Raman Scattering, or AERS and it revealed yet another spectroscopic property of J-aggregates that differentiate them from their respective molecular spectra. Another method that provides essential information on surface deposition is cyclic voltammetry and it was used to study the metalloporphyrins in this work. Cyclic voltammetry is a Nernstian (reversible) sweep reversal method where usually a symmetrical triangle potential wave, i.e., the potential changes at a constant rate, acts on the electrode double-layer[5]. These variable potentials make it possible to observe adsorption and desorption patterns and in some systems to track changes in molecular energetics.

Experimental systems

Potential dependent Raman experiments were performed using a BAS CV27 potentiostat. Molecules were allowed to equilibrate with the electrode surface for some minutes after setting a new potential before Raman spectra were recorded. For this work Raman experiments in electrochemical systems were comprised of a SCE or Ag/AgCl reference electrode, a platinum wire auxiliary electrode and a smooth surface silver electrode. A KCl-saturated agar gel served as a salt bridge. Cyclic voltammograms were collected on a

CHI 660 Workstation with a 1-second delay between cycles. The electrochemical system was the same as that used in the Raman potential-dependent experiments.

Chapter 3: Structural Analysis of PIC and 2,2'-Carbocyanine by Raman and NMR Spectroscopy

3.1 Introduction

Of the many cyanine dyes that are used to study J-aggregation there is no dye that has been more extensively used than 1,1-diethyl-2,2-cyanine also known as pseudoisocyanine or PIC[1]. PIC, shown in figure 3-1, is one of the more structurally simple cyanine dyes and because of the extensive volume of data that is available for it, this dye is often among the first ones used when applying a new experimental or computational technique to studying cyanine dyes and J-type aggregation.

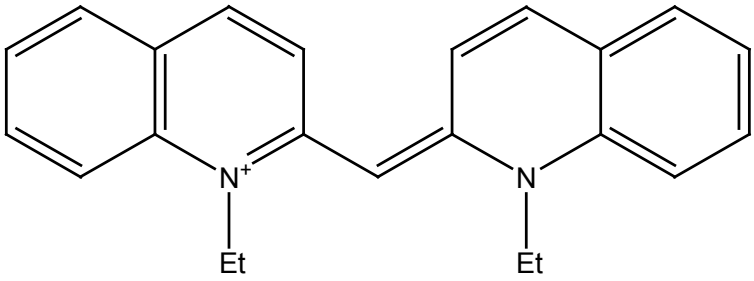

Figure 3-1. Molecular model of PIC.

Previous vibrational and quantum chemical studies on PIC have focused on peak assignments[2] for the monomer as well as on what types of vibrations are enhanced upon aggregation and may perhaps contribute or participate in aggregate formation. More specifically, as was determined through Raman spectroscopy and density functional theory (DFT), the peaks located in the lower-energy region of the Raman profile are mainly produced by out-of-plane vibrations, whereas, higher-energy peaks are produced

by in-plane vibrations. The energetic differences between in-plane and out-of-plane vibrations are indicative of not only the affect of ring structure but also of conjugation and aromaticity in organic molecules, providing some insight into the distribution of energy released through vibrations.

According to quantum mechanical calculations the structure of PIC was suggested to have an equilibrium configuration of nearly C_2 symmetry with the quinoline moeties being structurally identical albeit differently oriented in space with a twist angle of approximately 46 degrees between them[3]. The large angular separation between the two quinoline moieties is in large part caused by steric hindrance because of the H_{14} protons on both moieties that would have occupied the same space had the molecule been totally planar. H^1 NMR spectroscopy has long been used to study the structure of organic molecules and to provide particularly useful information concerning for instance the immediate electronic environment of a proton, the planarity of a ring and the rigidity of a chain. In using NMR spectroscopy to study PIC it may be possible to reach conclusions on its structure, even if in a qualitative manner, more directly and more easily than with quantum chemical calculations that are reliable but require a significant amount of time to acquire. Additionally NMR can be used to gather data on structurally similar molecules making it an excellent tool to identify trends and relative tendencies for bonds in pi-conjugated regions to undergo addition or substitution reactions along with providing some information on the relative orientations of neighboring groups.

The carbocyanine analogue of PIC is 2,2'-carbocyanine, shown in figure 3-2. It has a relatively modest history in the literature[4]. The two molecules differ in structure only by the extra ethylene bond along the conjugated bridge in 2,2'-carbocyanine and as such are

expected to have very similar UV-Visible absorption profiles. Likewise, they are expected to have similar fluorescence and infrared absorption profiles.

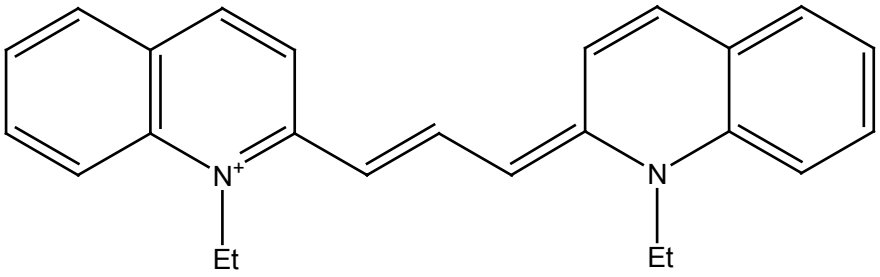

Figure 3-2. Molecular model of 2,2'-carbocyanine.

The Raman and NMR spectra of these dyes however are expected to show some differences that may indicate qualitative differences between the two molecules and provide information that is useful to understand their structural properties. The characteristic sharp and red-shifted peak that normally appears in the absorption spectra of J-aggregated molecules sometimes does not appear at low concentrations if the aggregate is not formed on a surface such as for instance a nanoparticle, an electrode, or another type of substrate. When Raman spectroscopy was first used to study J-aggregates it was shown that, similarly to the case for UV-Visible absorption spectra, new and sharp peaks appeared in the lower energy region of the spectrum when the aggregate was excited with light that was resonant with the aggregate's absorption maximum. These peaks were ascribed conceptually to the intermolecular coupling of molecular motions in a manner similar to that of lattice modes that would be found in crystals. Beyond that qualitative assignment of vibrational motion in J-aggregates no further explanation has been presented to account for these new peaks. Because the vibrations that produce these peaks are the product of intermolecular interactions it is even more difficult to determine what types of molecular motions are involved in this coupling. For instance it is unknown

if these vibrations come from coupled molecular vibrations or if instead they are the product of coupled rotational or translational motions. Furthermore, it is unclear what relationship these motions have with respect to J-aggregate formation, if any.

As mentioned before in chapter 1, NMR is one spectroscopic technique that is capable of providing information on the structures of these two molecules that clearly distinguishes them because of the technique's inherent sensitivity to local and extended electric fields. Furthermore, NMR is a very useful spectroscopic technique in ways similar to that of infrared spectroscopy. Just as infrared spectroscopy allows one to identify the presence of functional groups in molecules because of their location in the spectrum, the magnetic spins of protons in a particular electronic environment will be affected in such a way as to have that proton's NMR transition appear within a certain region in the NMR spectrum. Once the gross assignment of peaks is completed, a more detailed study of each peak including analysis of the splitting and the specific location of each peak can lead to a highly detailed picture of the structure of the molecule. Qualitative assessments can therefore be made concerning not only structure but also the electronic and chemical properties of different regions of a molecule.

In this chapter absorption, UV-Vis, Raman and NMR spectra will be presented of monomeric PIC and 2,2'-carbocyanine and the two molecules will be studied in a comparative manner in order to make qualitative assessments on the planarity and twist angle between the two methine-linked quinoline moieties. A discussion will also be presented on the relative tendency of the two molecules to undergo substitution or addition reactions along with where those reactions would likely take place.

3.2 Experimental

PIC and 2,2'-carbocyanine iodides, shown in figures 1 and 2, respectively, were purchased from Kodak and were used without further purification. Absorption spectra of PIC and 2,2'-carbocyanine were obtained by preparing methanolic solutions of both dyes and adjusting the concentrations such that the absorption maximums would be less than 2 absorption units. Raman spectra of monomeric PIC and 2,2'-carbocyanine were obtained from millimolar solutions of each in methanol. Preparations of PIC and 2,2'-carbocyanine for NMR measurements were made in deuterated methanol and their concentrations were in the order of 10 mM to ensure a strong magnetic resonance signal.

3.3 Results and Discussion

3.3.1 Characterization of PIC and 2,2'-Carbocyanine by UV-Vis Spectroscopy

The absorption spectrum of PIC in methanol is shown in figure 3-3 and the main peak at 521 nm is the Soret band with the strong peak at 480 nm corresponding to the 1-0 transition. The absorption profile of 2,2'-carbocyanine is very similar to that of PIC and is shown in figure 3-4 and the main difference between the two is the overall shift of the profile to the lower energy region of the visible spectrum. Again, the main peak at 604 nm is the Soret band of 2,2'-carbocyanine and the strong peak at 560 nm corresponds to the 1-0 vibronic transition.

One can apply particle-in-a-box concepts to understand the relative position of their respective absorption spectra because the length of the chromophore affects the energy of the excited state. The longer polymethine chain in 2,2'-carbocyanine leads to a lower

energy for the excited electron in the chromophore that resides between the two nitrogens on each side of the chain. The strong vibronic bands found in both molecules suggest that the rings in both are very flexible and can easily produce out-of-plane vibrations. Evidence of strong out-of-plane vibrations coming from the ring structures of the quinoline moieties will be provided by the respective single-molecule Raman spectra of the two dyes, particularly in the low-energy region.

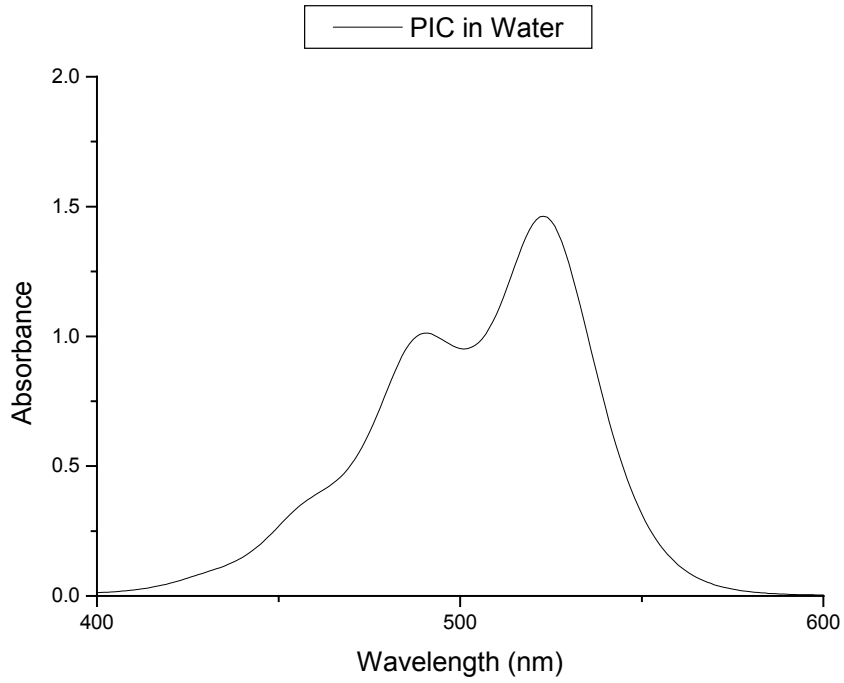

Figure 3-3. Absorption spectrum of PIC monomer in neutral water. PIC was first dissolved in a small amount of methanol before adding water. At low concentration and low ionic strength, PIC does not aggregate in water.

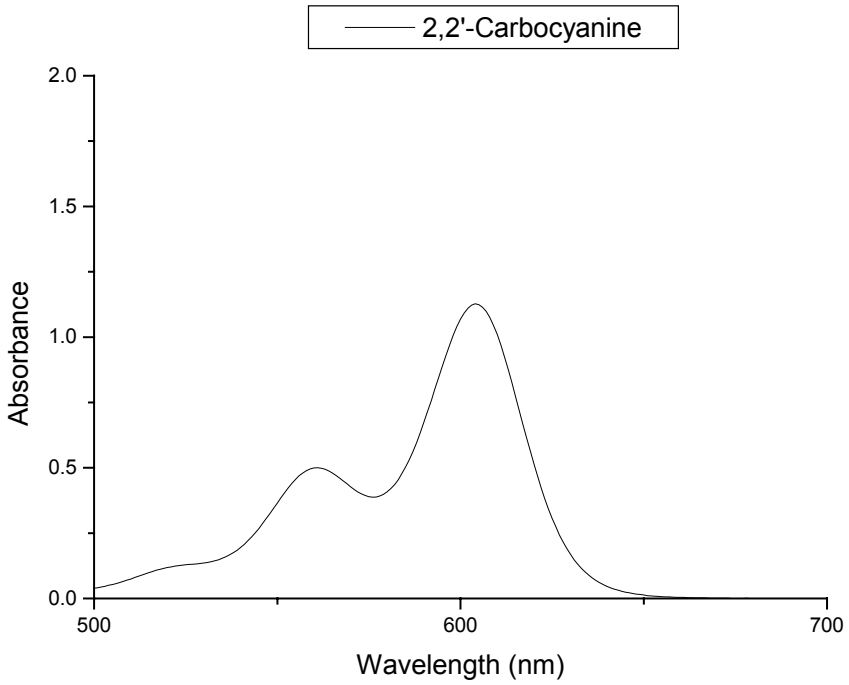

Figure 3-4. Absorption spectrum of 2,2'-carbocyanine in methanol.

3.3.2 Raman Spectra of PIC and 2,2'-Carbocyanine

It is useful to compare the Raman spectra of PIC with 2,2'-carbocyanine particularly because the two molecules are so similar in structure and could be expected to have very similar Raman profiles. An examination of the vibrational assignment of the PIC Raman spectrum can be used to analyze any difference in relaxation energy distribution between the two molecules. Ab-initio quantum chemical calculations on one half of the PIC monomer provided indispensible data to perform normal mode calculations and obtain a relatively accurate assignment of the Raman peaks. These quantum chemical calculations went a long way in helping to relate specific motions to individual Raman bands. In general, it was determined that out-of-plane vibrations preponderated in the lower energy

region below 600 cm^{-1} whereas in-plane vibrations preponderated above 600 cm^{-1} and this difference in energy between in-plane and out-of-plane vibrations will be important in understanding certain aspects of J-aggregate structure and formation.

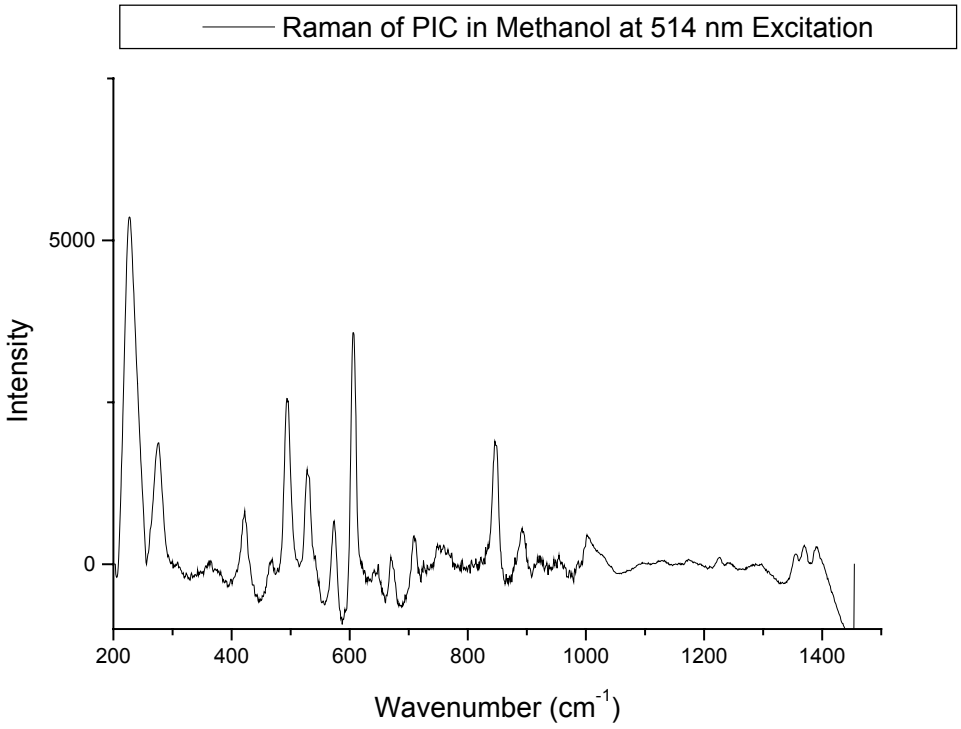

Figure 3-5. Raman spectrum of PIC in methanol with 514 nm laser excitation.

The Raman spectrum of PIC in methanol is shown in figure 3-5 and immediately one can see that there are many relatively strong peaks in the region below 600 cm^{-1} and not too many strong peaks above. The Raman spectrum of 2,2'-carbocyanine can be seen in figure 3-6 and it is evident that the relative intensities of the peaks below 600 cm^{-1} are virtually identical to those of PIC; furthermore, it is apparent that these peaks are not only a product of out-of-plane motions but also that these are vibrations that occur within the quinoline moieties. It can be argued that the nearly identical appearance of the two spectra in the low-energy region shows that the motions of the quinoline moieties in 2,2'-

carbocyanine are essentially not affected by the motions of the c-c bonds along the polymethine chain, i.e, the vibrations, and possibly other properties of this molecule can be separated by region.

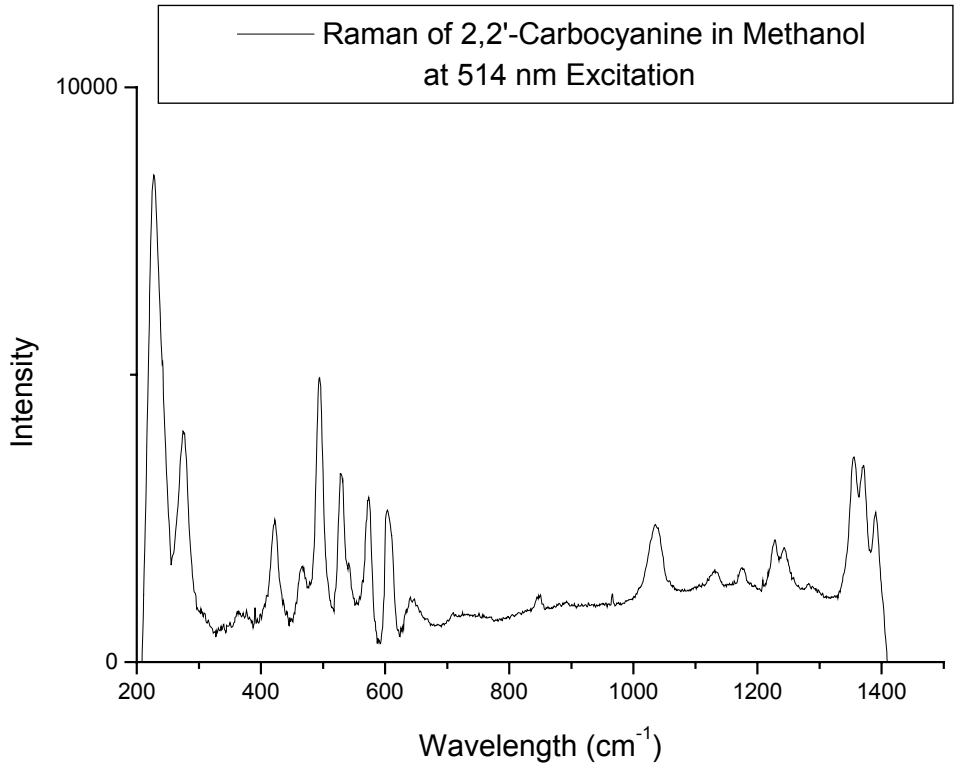

Figure 3-6. Raman spectrum of 2,2'-carbocyanine in methanol at 514 nm excitation. Raw spectrum was background corrected to remove fluorescence.

It was already shown how the longer length of the polymethine chain in 2,2'-carbocyanine shifted to the red the location of its absorption spectrum relative to that of PIC while at the same time not truly affecting the overall absorption profile. Similarly, the Raman spectra of the two molecules show that while the relative intensities coming from the out-of-plane vibrations in the low-energy region of both molecules are nearly identical, the relative intensities of the peaks coming from in-plane and coupled vibrations are noticeably different. It appears that the longer chain in 2,2'-carbocyanine

has a damping effect on the some of the higher-energy vibrations in molecule. One possible reason why there would be a damping effect to the higher-energy vibrational motions of 2,2'-carbocyanine is if the bonding character of the c-c bonds along the polymethine chain is irregular or at least not uniform. In the classical sense, the consequence of differing bonding character of the c-c bonds along the chain is that there is a less efficient longitudinal transfer of vibrational energy between the quinoline moieties and an absence or reduction of constructive interference between individual motions in 2,2'-carbocyanine relative to that which may be found in PIC. In the following section NMR spectroscopy will be used to offer qualitative evidence that indeed the c-c bonds in the polymethine chain of 2,2'-carbcyanine are not of uniform character and that in turn there are chemical differences between the protons associated with these carbons.

3.3.3 NMR Analysis of PIC and 2,2'-Carbocyanine Structure

A numbering system is used to facilitate the characterization of PIC and 2,2'-carbocyanine by NMR and it is shown in figure 3-7. Only half of each molecule is shown as both molecules are symmetric with respect to a perpendicular plane that goes through the C_{13} and C_{14}, carbon atoms in PIC and 2,2'-carbocyanine, respectively. When referring to the atoms residing on the other half of each molecule, that atom will be assigned a "prime" designation.

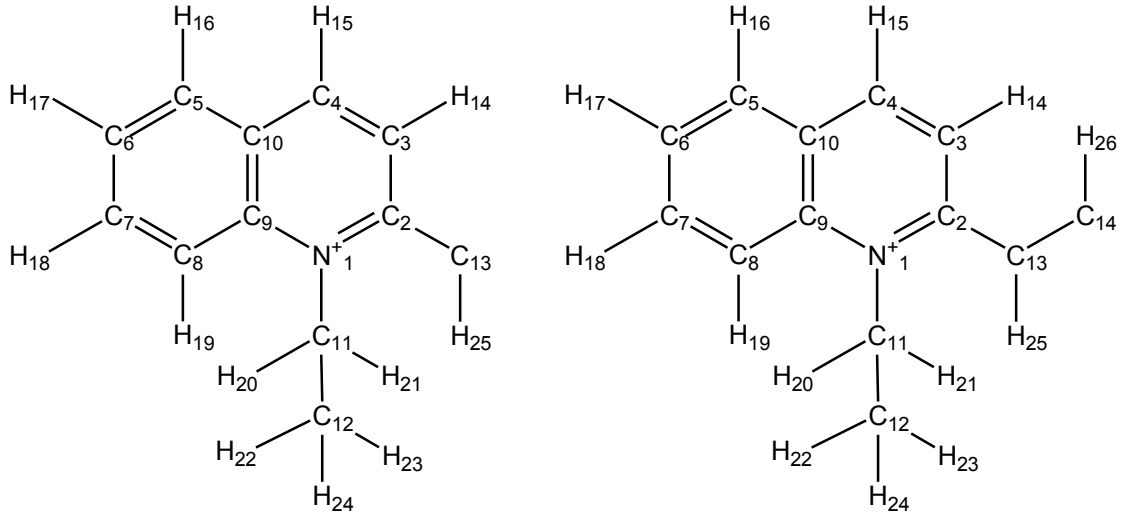

Figure 3-7. Atomic numbering scheme for a.) PIC and b.) 2,2'-Carbocyanine. Only one half of both molecules is presented as PIC is symmetric about C_{13} and 2,2'-carbocyanine is symmetric about C_{14}.

The NMR spectrum of PIC is shown in Fig 3-8 and on first inspection three regions of interest can be identified immediately. The peaks in the region that is below 5 ppm are attributable to the aliphatic protons that are found in the two ethyl groups and are readily assignable. The peak at 5.6 ppm is attributable to the proton on the methine bridge that links the two quinoline moieties. The four sets of peaks found above 7 ppm are in the aromatic region and are attributable to the protons on the quinoline moieties. Although the peaks are very close to each other it is plausible that four sets of peaks would be found. The protons on C_4, $C_{4'}$ and C_5, $C_{5'}$ experience essentially the same local electric field and are expected to produce doublets while the protons on C_6, $C_{6'}$ and C_7, $C_{7'}$ are expected to produce triplets. The protons on C_8, $C_{8'}$ would have been expected to produce a doublet in the same manner as the protons on C_4, $C_{4'}$ and C_5, $C_{5'}$ except that the ethyl groups attached to N_1, $N_{1'}$ can periodically interfere with them and lead to a triplet instead. Finally the protons on C_3, $C_{3'}$ are expected to produce a doublet and not a triplet

because the twist angle between the quinoline moieties is large enough for those two protons not to interfere with each other. The actual spectrum of PIC was largely what was anticipated qualitatively; there are doublets at 7.8 and 8 ppm, and triplets at 7.5 and 7.9 ppm.

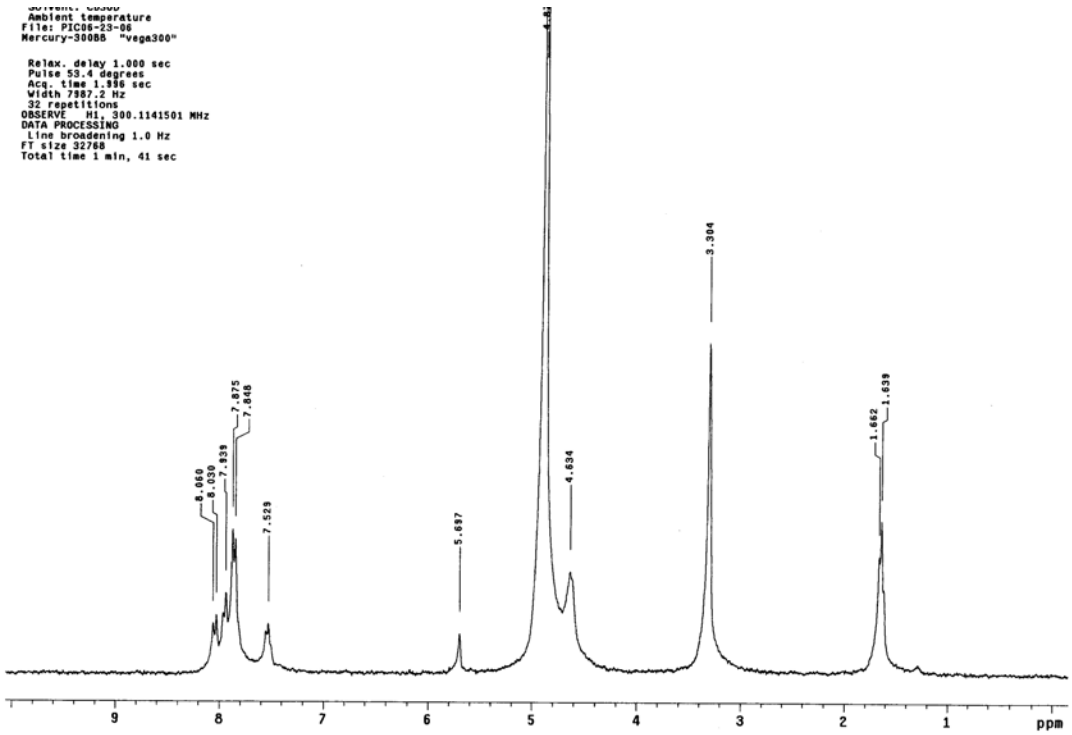

Figure 3-8. Proton NMR spectrum of PIC in deuterated methanol.

Because the peaks are not well separated it is difficult to make definitive conclusions as to which peaks correspond to which protons however, as mentioned before, one of the benefits of using NMR spectroscopy can be seen when studying similar molecules because even small differences in local electric fields can produce noticeable changes in an NMR spectrum. With 2,2-carbocyanine it is possible to use its NMR spectrum to further characterize PIC while at the same time making qualitative comparisons based on the differences in their NMR spectra. The fact that the proton that is bonded to the central carbon in PIC experiences a local electric field that is very different from that of the

protons bonded to the carbons on the quinoline moieties is significant because it means that the conjugation is not uniform throughout the molecule.

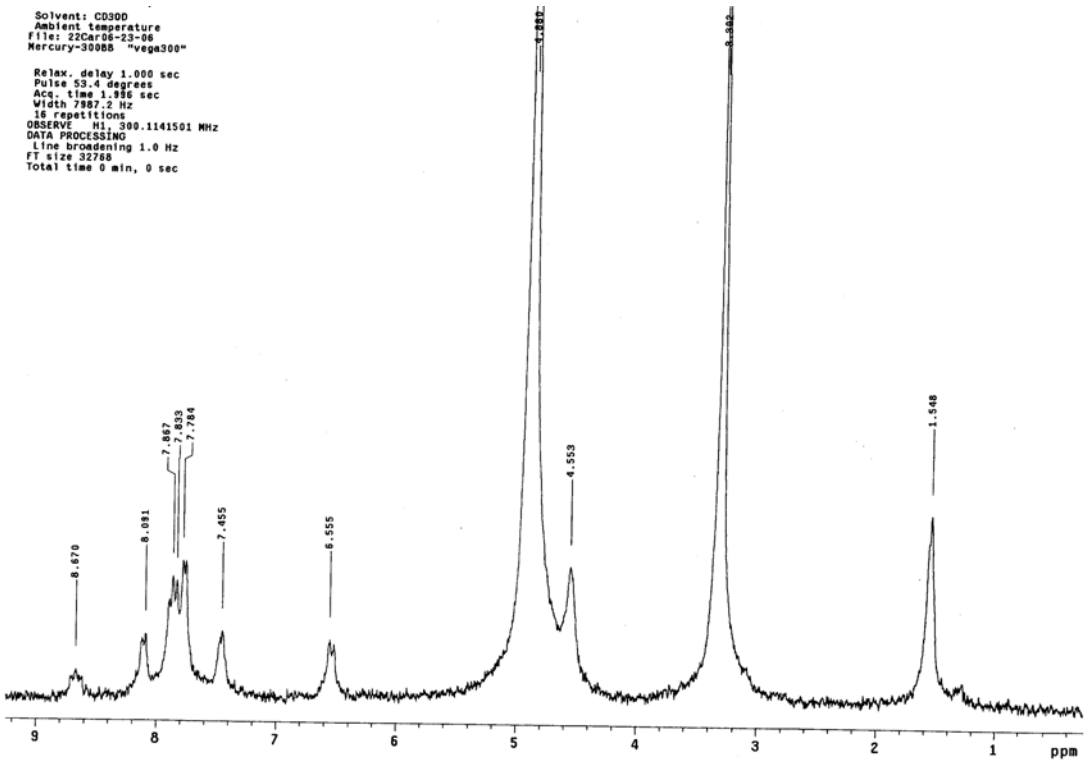

Figure 3-9. Proton NMR spectrum of 2,2'-carbocyanine in deuterated methanol.

The NMR spectrum of 2,2'-carbocyanine is shown in Fig 3-9 and one can immediately observe that unlike their respective Raman spectra, the NMR spectra of PIC and 2,2'-carbocyanine are sufficiently different to easily distinguish one from the other. The three sets of protons in the aromatic region are more easily distinguishable in 2,2'-carbocyanine and it should be noted that in the same manner that the spectrum of PIC was predicted, the anticipated spectrum for the protons on the quinoline rings is what is basically observed. In relation to PIC, there is an additional peak in the 2,2'-carbocyanine spectrum in the aromatic region at 8.3 ppm, and this peak is attributable to one of the two types of protons on the polymethine chain, i.e., either the middle proton or the two vicinal protons. It is unclear why the peaks in the aromatic region are so close to each other in

the case for PIC and more distinguishable in the case for 2,2'-carbocyanine however the peaks maintain a similar profile. The remaining two peaks, the triplet at 8.3 ppm as well as the doublet at 6.5 ppm correspond to the protons on the polymethine chain. The peak corresponding to the proton bonded to the central carbon in the methine chain of PIC appears at 5.9 ppm and it would be similarly expected that the central proton in the case for 2,2'-carbocyanine would appear somewhere in the same area and the same would be expected for the vicinal protons. The actual spectrum is different from that which was anticipated. As it is clear that the two peaks at 6.5 ppm and 8.3 ppm correspond to the two types of protons and because of the multiplicity of the two peaks it can be determined that the doublet belongs to the vicinal protons and the triplet belongs to the central proton. It is remarkable that the two types of protons experience such different electronic environments and this means that the character of the carbon atoms to which these protons are attached have not only different reactivity but also that the pi electrons along the polymethine chain are not evenly distributed along the chain. The pi electrons are apparently more likely to concentrate in the vicinity of the central carbon. This distribution of electrons leads to a greater sigma-bond character for the C_2-C_{13} and $C_{2'}$-$C_{13'}$ bonds and greater pi-bond character for the C_{14}-C_{13} and C_{14}-$C_{13'}$ bonds. The greater sigma-bond character of the C_2-C_{13} and $C_{2'}$-$C_{13'}$ bonds in principle makes it easier for rotation about those bonds relative to rotation about an evenly conjugated carbon chain. The fact that those bonds are fundamentally different from those of C_{14}-C_{13} and C_{14}-$C_{13'}$ corroborates the information gathered from the Raman spectrum of 2,2'-carbocyanine and the relative reduction of intensity of the in-plane and coupled vibrations compared to PIC. The fact that the proton on the central carbon in PIC is observed at 5.9 ppm

indicates that this carbon is vulnerable to proton addition in the presence of an acid. Regarding 2,2'-carbocyanine, the peak corresponding to the proton on the central carbon is in the aromatic region while the protons on the vicinal carbons produce a peak just outside the aromatic region meaning that the vicinal carbons are vulnerable to addition reactions in the presence of an acid while the central carbon is more likely to undergo a substitution reaction. This fact is important to note because the relatively strong basic conditions in which J-aggregates of these molecules form leaves the potential for reactions or strong electrostatic interactions to take place that could serve as precursors to the formation of the aggregate.

3.4 Summary and conclusion

Absorption, Raman and NMR spectra of PIC and 2,2'-carbocyanine were analyzed and it was found that while PIC and 2,2'-carbocyanine are very similar molecules the conjugation and length of their respective chains affected their spectra in significant ways. The longer chain of 2,2'-carbocyanine lead to not only a red shift in its absorption profile relative to that of PIC but also to a difference in its Raman spectra. The relative intensities of in-plane and coupled vibrations compared to those of PIC were reversed indicating that there was a relatively different pi-character of the central C-C bonds on the chain in the two molecules. The relative difference in location of the NMR peaks of the protons bonded to the central and vicinal carbons in 2,2'-carbocyanine pointed to the fundamental difference in reactivity of those carbons and these differences were thought to have important consequences in the formation of the J-aggregate.

Chapter 4: Structural Analysis of TTBC and TDBC-4

4.1 Introduction

There are many cyanine dyes that can aggregate as long as certain environmental conditions are met; in some instances solutions need the necessary ionic strength or pH, other instances where systems having surfaces have the necessary properties to attract the molecules of interest. Some dyes offer greater opportunity for study of aggregate morphology and molecular structure in different environments because those conditions can be met more easily. Two molecules that can aggregate relatively easily in aqueous and colloidal solutions as well as on surface sunbstrates are TTBC and TDBC-4. Both molecules are carbocyanines just as 2,2'-carbocyanine, however unlike it, have benzimidazole rather than quinoline moieties. As is common with most photosensitive dyes previous studies on TTBC have included steady-state and time-resolved fluorescence measurements. It was determined that some dyes, including TTBC, exhibited super-radiance at levels that were orders of magnitude greater than conventional systems suggesting for instance that TTBC could serve as an important component in systems designed for mirrorless lasing[1-5].

Studies of surface properties of cyanine dyes have included studies conducted on PIC on functionalized glass surfaces as well as subsequent studies using TTBC and TDBC-4 as surface sensitizers for gold and silver noble metal nanoparticles. Based on the height differences between experiments done on nanoparticles with and without dye coverage, AFM (atomic force microscopy) and DLS (dynamic light scattering) studies suggested

that the dyes preferentially aggregated on top of the nanoparticle "islands" rather than over areas not covered by the nanoparticles[6]. The combination of ease of aggregation, promising dynamical properties, similar aggregate structures and morphologies to PIC and 2,2'-carbocyanine make both TTBC and TDBC-4 logical candidates for structural analysis with Raman and NMR spectroscopy just as was done on PIC and 2,2'-carbocyanine. The fact that the two molecules are similar to each other make them equally useful to compare to each other as PIC and 2,2'-carbocyanine were previously. Furthermore, the fact that TTBC and TDBC-4 are carbocyanines make their NMR spectra interesting to compare to that of 2,2'-carbocyanine particularly in regards to where the central and vicinal protons on the polymethine chain will appear.

In addition to the Raman and NMR studies, UV-Visible studies done on TTBC in silver colloid will be presented in this chapter and they will provide some qualitative information on the manner of stacking of the aggregated molecules and the curvature of the surface of the nanoparticles. A discussion will be presented concerning the role of the silver surface as a stabilizer for the aggregate when in solution along with an analysis of surface coverage by the aggregate on the silver nanoparticles.

Raman spectra of TTBC will be shown that not only demonstrate the difference in the distribution of vibrational energy between an aggregate and a monomer species but also will hint at a possible molecular structure within the aggregate. Differences between the Raman spectra of molecular and aggregated TTBC will be discussed and special attention will be paid to the difference in the types of vibrations that are affected upon aggregation. Raman spectra will also be shown for aggregated TDBC-4 in colloidal solution and will be compared to the Raman spectra of aggregated TTBC on silver smooth electrode.

These comparisons will be done to demonstrate the similarities between the two dyes and to support the argument that the optical coherence length of the aggregate is sufficiently short that the molecules within experience the same field as they would on a smooth surface. Said differently, the curvature of the surface of the nanoparticle can be considered to be small compared to the optical coherence length of the aggregate and this fact is important because this opens new possibilities to develop nanoscale materials through these aggregate-nanoparticle interactions.

NMR spectra will be used to study the benzimidazolo rings as well as the polymethine chain in both TTBC and TDBC-4 and these results will be compared to those previously presented for the spectra of PIC and 2,2'-carbocyanine. The issue of isomerism, not a factor in analyzing PIC or 2,2'-carbocyanine will have to be addressed in this chapter to explain the presence of a greater number of peaks than would have ordinarily been predicted. Finally, the NMR spectrum of monomeric TDBC-4 will be compared to that of its aggregate. TDBC-4 is one of the few dyes that can form a J-aggregate in neutral pH water, as opposed to most cyanine dyes that need strongly basic solutions, making it an excellent candidate to study J-aggregates with NMR spectroscopy. Many potential problems are avoided such as issues with solution homogeneity and the potential interference by the presence of other proton-carrying species. The differences in splitting and peak location in the NMR spectrum for aggregated TDBC-4 from that of its monomer will provide a picture of the molecule within the aggregate. The list of possible conformational changes that take place in the molecule that allow it to aggregate is very large however and the information that NMR provides will help to narrow this list.

Structural factors that limit the exciton coherence length will be studied and it will be shown how structural data obtained from NMR can be used together with dynamics studies to more rigorously address the issue of the exciton's coherence length. Collectively these studies will provide extremely useful information concerning the structural and conformational changes that take place in a molecule upon aggregation.

4.2 Experimental

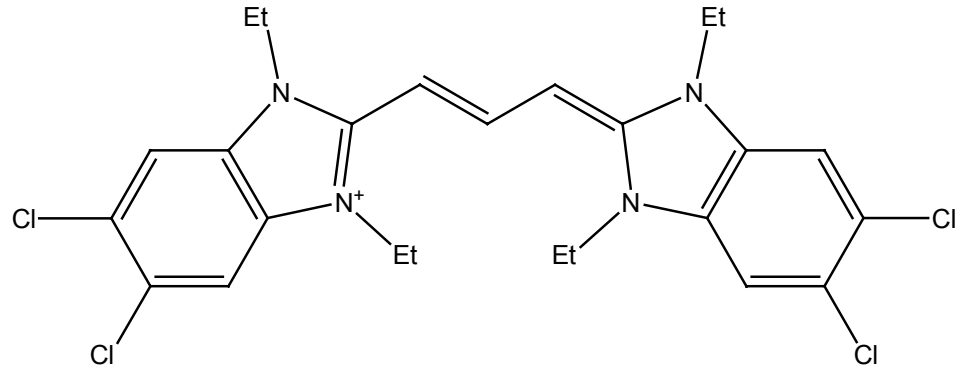

Figure 4-1. Molecular structure of TTBC, the ionic charge is evenly distributed among the four Nitrogen atoms. The counter ion is not shown but is usually a chloride or iodide anion.

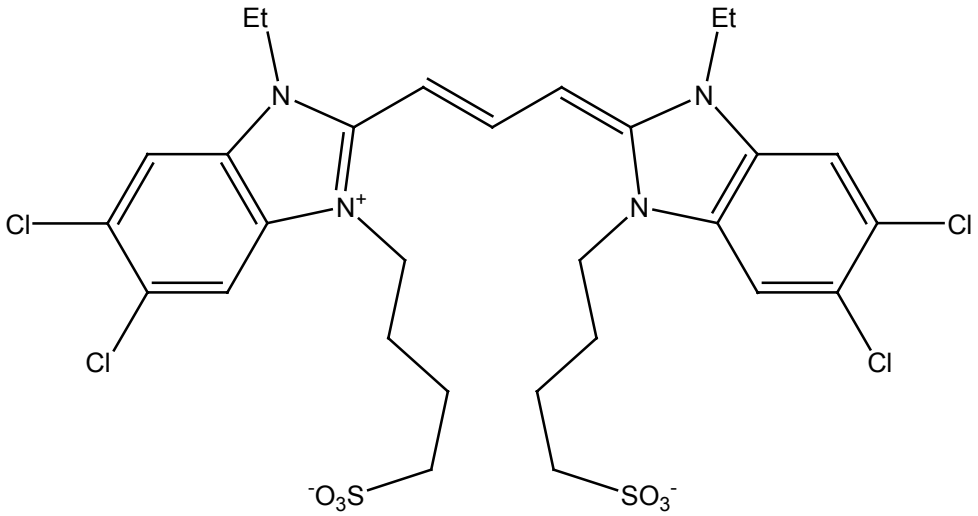

Figure 4-2. Molecular structure of TDBC-4.

TTBC, shown in figure 4-1, was purchased from Accurate Chemical and Scientific Company and was used as received without further purification. TDBC-4, shown in figure 4-2, was purchased from Few Chemicals and was also used as received. Sample solutions were dilutions from more highly concentrated stock preparations. Surface potential Raman studies were conducted in neutral water solutions where NaCl was added to obtain a 1mM salt concentration in order to ensure proper electrical conductivity.

4.3 Results and Discussion

4.3.1 Characterization of TTBC and TDBC-4 by UV-Visible spectroscopy

The absorption spectrum of TTBC in methanol can be seen in figure 4-3 with the Soret band appearing at 514 nm and there is a shoulder attributable to the 1-0 electronic transition at 480 nm. The absorption spectrum of TDBC-4 in methanol can be seen in figure 4-4 and its profile is very similar to that of TTBC with the Soret band and 1-0 transition appearing at nearly the same location.

Among the questions that have yet been answered concerning J-aggregation are for instance ones concerning the role of a surface in aggregate formation and stability and what are the conditions for aggregate stability in aqueous solutions. While it is clear that the aggregating molecule interacts through electrostatic interactions with the surface it is not clear why this interaction leads to the aggregated species. Furthermore as mentioned before, it is unclear what role the solvent or other solutes play in the formation of the aggregate and its stability.

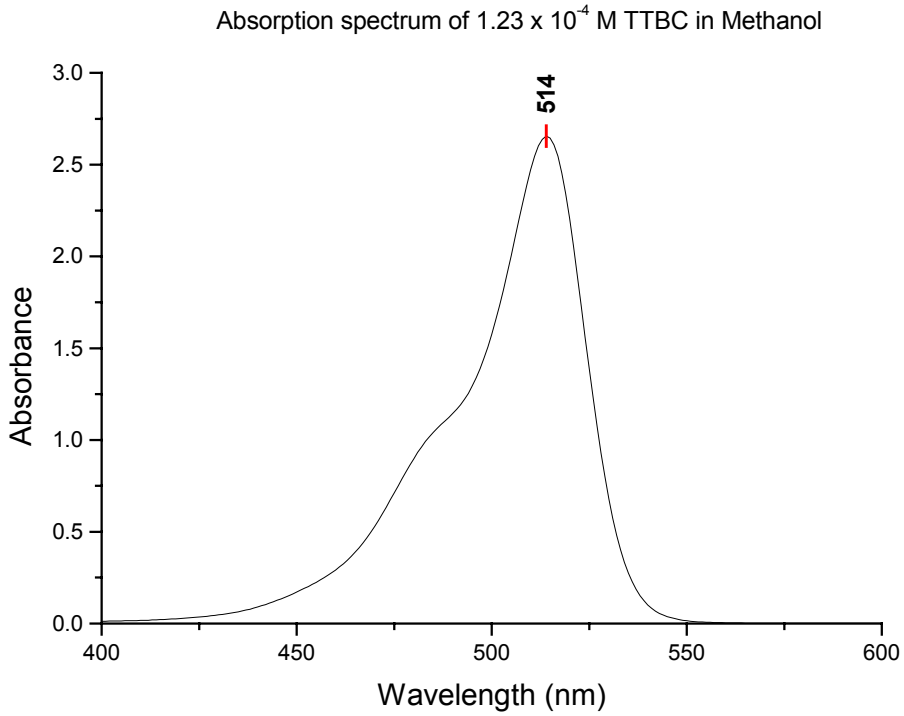

Figure 4-3. Absorption spectrum of TTBC in Methanol. The monomer band appears at 514 nm and a shoulder corresponding to a 1-0 transition can be seen at around 480 nm.

In figure 4-5 the absorption spectrum of J-aggregated TTBC in basic solutions can be seen with the J-band appearing at 592 nm. Dissolution of TTBC in water is achieved by initially dissolving it in slightly acidic media and the J-aggregate is obtained by adding base to that solution. All the spectra of TTBC in aqueous solutions obtained through this method show a third peak in the ultraviolet region that decreases in intensity along with an increased formation of the aggregate. The additional peak shows that there is a chemical change in the molecule in the acidic medium that is reversed when base is added and this peak is likely caused by, in essence, a shortening of the conjugation in the polymethine chain. This peak also serves as a control in monitoring the formation of the

aggregate by helping to verify that the change in intensity of the aggregate peak is not merely a change in the solution's dielectric properties.

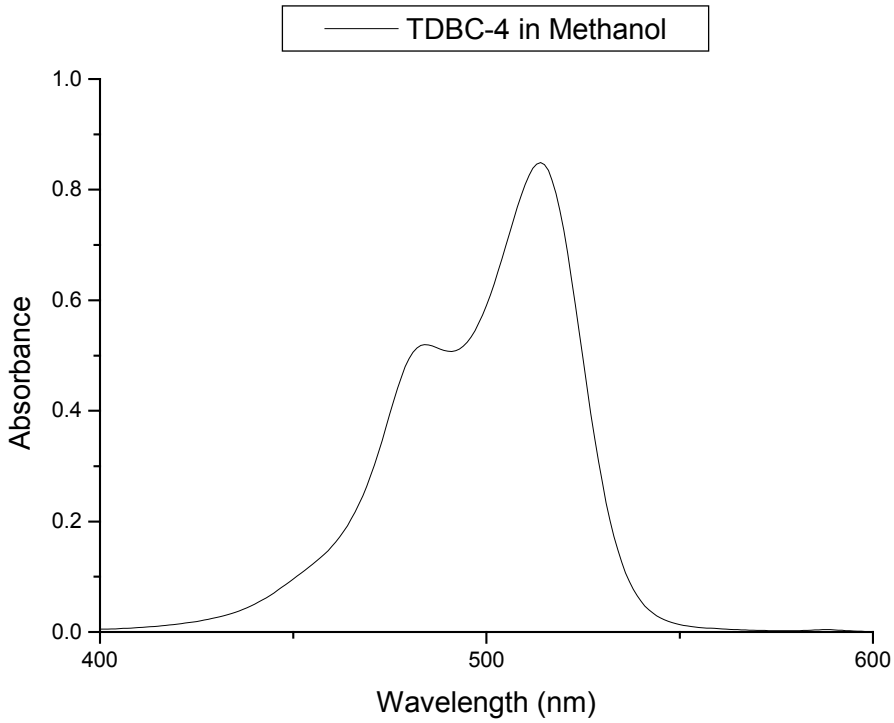

Figure 4-4. Absorption spectrum of TDBC-4 in Methanol. The monomer band can be seen at 518 nm and the 1-0 transition can be seen at 480 nm.

As mentioned before in the case of 2,2'-carbocyanine, the chromophore in TTBC is located on the chain linking the two benzimidazole moieties and the particle-in-a-box concept applies reasonably well in this case as well where the shortening of the chain leads to an increase in energy for the chromophore. Another interesting feature of these spectra is that the shape of the monomer peak does not show the characteristic shoulder that was found in methanol other than at pH 10 when the monomer and aggregate peaks reappear. Additionally the monomer peak is blue shifted with the maximum moving from 510 nm to 504 nm. It is unclear whether this blue-shift is a product of a different

dielectric environment in the solution or because of some kind of physical change in the dye monomer.

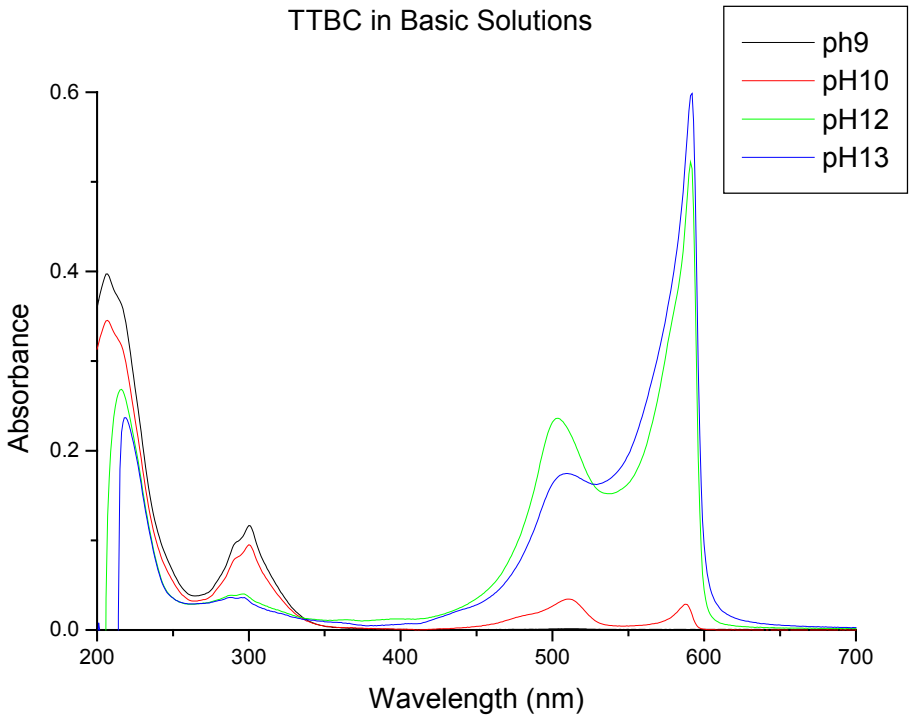

Figure 4-5. Absorption spectra of TTBC in basic solutions. At neutral to mildly basic pH there is neither monomer nor J-band. Beginning at pH 10 both bands appear, initially at equal intensity but as the pH increases the sharp J-band begins to dominate.

Both TTBC and TDBC-4 can aggregate in colloidal solutions of silver nanoparticles and in figure 4-6 the absorption spectra of TTBC in colloidal silver at pH 9 can be seen where the solutions are mixtures of water alone and water with methanol. These spectra were referenced to a blank of silver colloid in water. It can be seen that a negative peak appears at 400 nm at the plasmon resonance peak of colloidal silver, and over time the methanol/water mixture, from the initial spectral acquisition at zero time, shows an increase in the J-band's intensity concomitant with a greater dip in the plasmon resonance peak. This indicates that the dye is selectively aggregating on the nanoparticle surface

rather than in the solution. In methanol/water mixtures with addition of base the J-aggregate spectrum of TTBC differs somewhat from that of TTBC in water. In the basic mixtures the monomer and J-aggregate peaks are completely separated whereas in water the two peaks are not and the J-band is not symmetric; the aggregate peak seems to represent in some respects a band edge with the absorption maximum appearing to resemble a cusp.

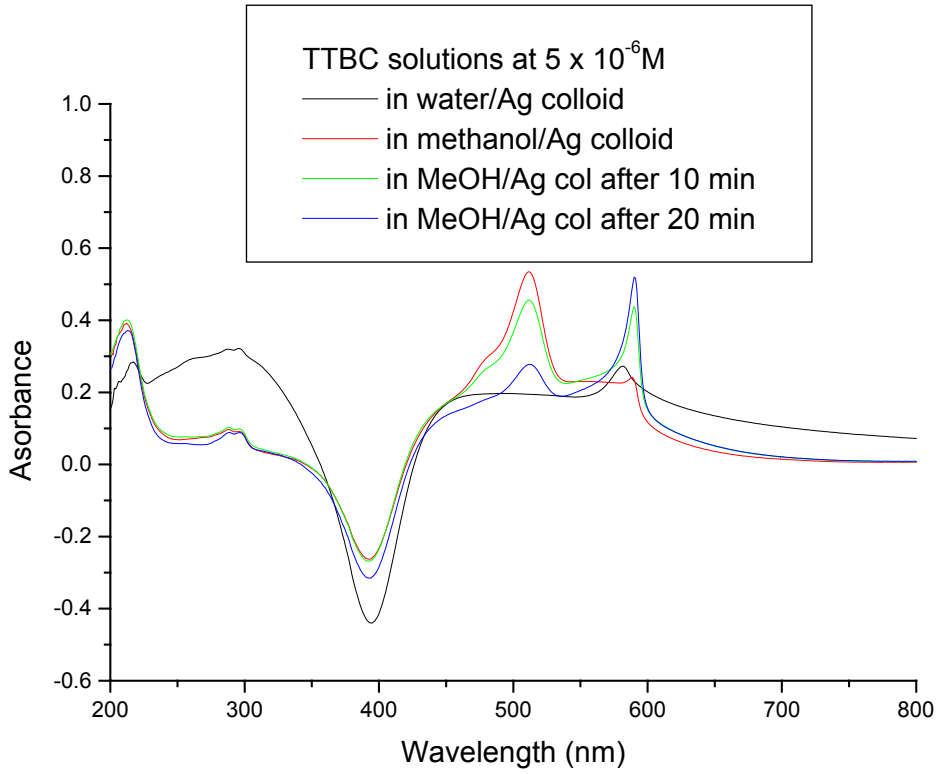

Figure 4-6. Absorption spectra of TTBC in solutions of silver colloid and methanol. All spectra were referenced to silver colloid as the blank.

The lack of complete separation between monomer and aggregated TTBC in base is indicative of a structural disorder manifested by the presence of alternate aggregate configurations that approach but do not attain or maintain for sufficient time the necessary configuration for J-aggregation.

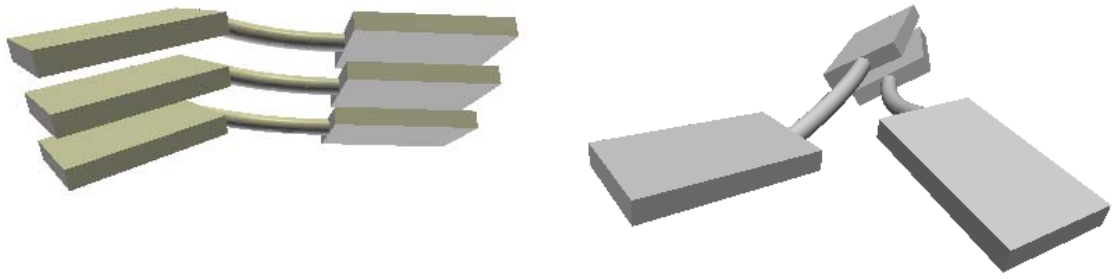

Figure 4-7. a.) An ordered cyanine dye trimer and b.) A disordered cyanine dimer.

In figure 4-7 two proposed models of an ordered aggregate that leads to the J-band and a disordered aggregate that does not, are shown to illustrate the possible structural differences between the two. The presence of both monomer and J-type aggregate species in silver colloidal mixtures of methanol/water suggests that there is an equilibrium between the two, and may also indicate the presence of different forms of monomeric TTBC, possibly not all of which lead to the J-aggregate. Lastly, the coexistence of both monomer and aggregate dye in the methanolic colloidal mixture suggests that there are local inhomogeneieties where monomers of TTBC are more likely to be surrounded by methanol molecules and water molecules are more likely to surround the silver nanoparticles, upon which the dye has aggregated. The J-aggregate of TDBC-4 on a silver nanoparticle film is shown in figure 4-8; it should be noted that the TDBC-4 J-aggregate can be obtained simply by direct dissolution in neutral pH water.

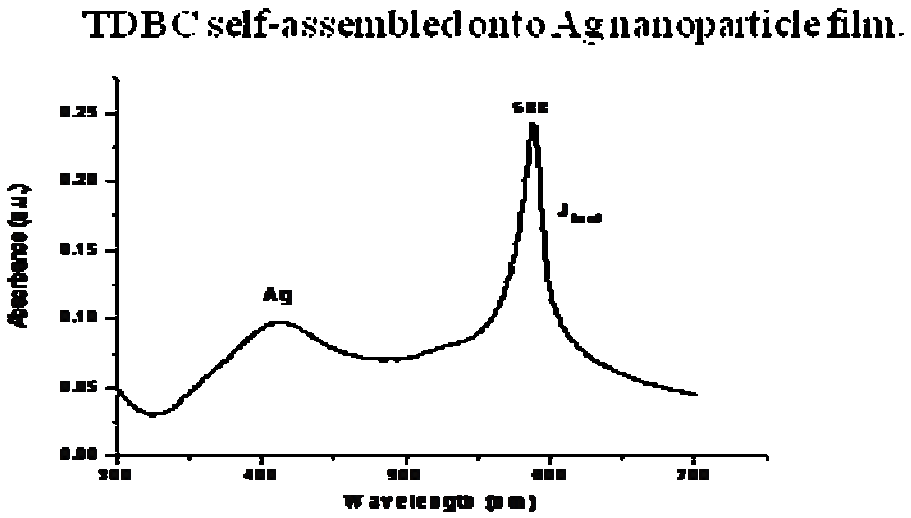

Figure 4-8. Absorption spectrum of TTBC-4 on silver nanoparticles. Spectrum was referenced to a blank glass slide.

Similarly to the case of TTBC in colloidal silver, the relatively low intensity of the silver plasmon shows that the dye molecules are preferentially aggregating on the nanoparticle surface. Ease of aggregation and stability are two factors that suggest that both TTBC and TDBC-4 can have long coherence lengths compared to other typical cyanine dyes and it can be postulated that the structural properties of each play an important role in this regard. Although absorption spectra of J-aggregated cyanine dyes are used at times with empirical methods for estimating the aggregate's optical coherence length based on the ratio of full-width-at-half-maximum of the monomer and the aggregate, these methods are not independently verifiable and will not be used here.

4.3.2.1 Surface potential dependence of the Raman spectrum of TTBC

When it is difficult to obtain solution-based Raman spectra of certain molecules a practical alternative is to deposit the molecule on an electrode surface. Surface-enhanced Raman spectroscopy (SERS) has been used for a long time in order to augment the

relatively weak Raman signal from low-concentration solutions by using the enhanced field effects generated by uneven surfaces with sharp protrusions. When molecules J-aggregate, they too are able to produce enhanced Raman spectra without the need for roughened surfaces. The augmentation of the Raman signal through aggregation was termed aggregate-enhanced Raman spectroscopy (AERS) and this phenomenon holds true for aggregated TTBC where the off-resonance spectrum is very strong even at low dye concentrations. It should be stressed that the TTBC solution used, though at neutral pH was obtained by diluting an acidic stock solution of monomeric TTBC. The aggregation of TTBC therefore clearly took place spontaneously on the electrode surface, at open circuit, and not in the solution. The fact that aggregation occurs on both the electrode surface and in colloidal silver on the nanoparticle surface suggests that silver has an inherent electron-donating character to it that allows it to interact with cyanine dyes in such a way as to create the necessary local conditions for J-aggregation.

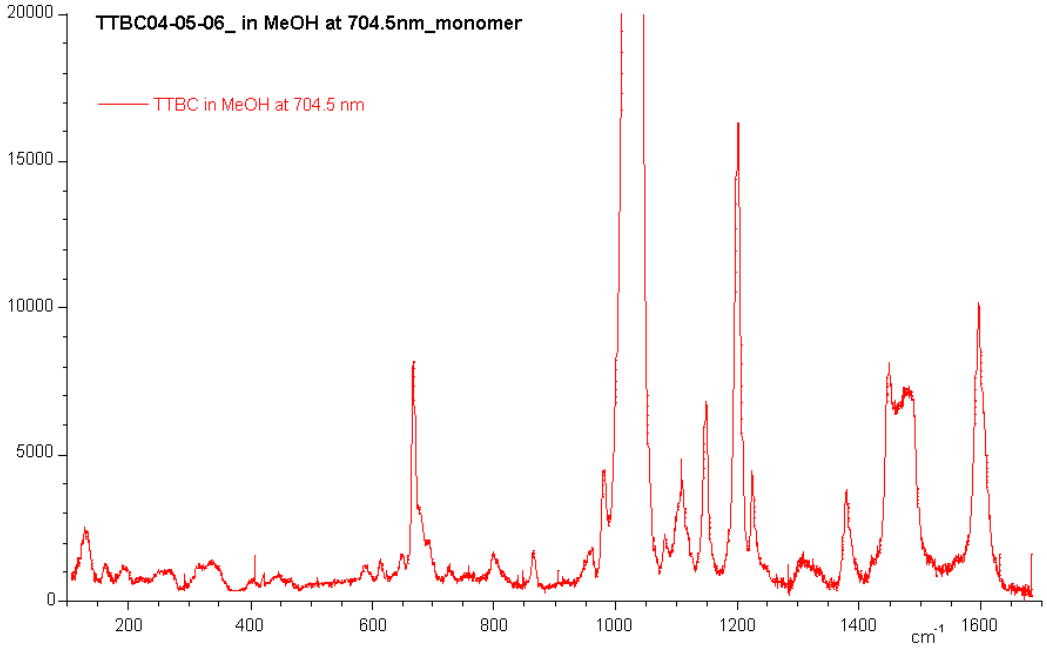

Figure 4-9. Raman spectrum of TTBC in methanol at 704.5 nm laser excitation.

Figure 4-9 shows the off-resonance Raman spectrum of TTBC in methanol and figures 4-10 and 4-11 show the off-resonance and resonance Raman spectra on smooth silver electrode at 0 applied potential for aggregated TTBC, respectively. It is apparent by comparing the two spectra that there are not only marked differences in the relative intensities of the Raman bands but also that there are new lower-energy peaks that appear in the resonance case. Of particular note is that fact that TTBC exhibits a trio of new peaks in the low energy region whereas most J-aggregating molecules usually show only one or two such peaks. This additional vibro-excitonic peak comes from an additional vibrational motion in the TTBC aggregate that does not occur in the conventional case where only two peaks appear and this motivates an interest on the nature of these motions. The main obstacle in determining what these motions are is that it is not known in sufficient detail how the molecules are arranged in the J-aggregate and how a molecule's particular structural properties affect these arrangements.

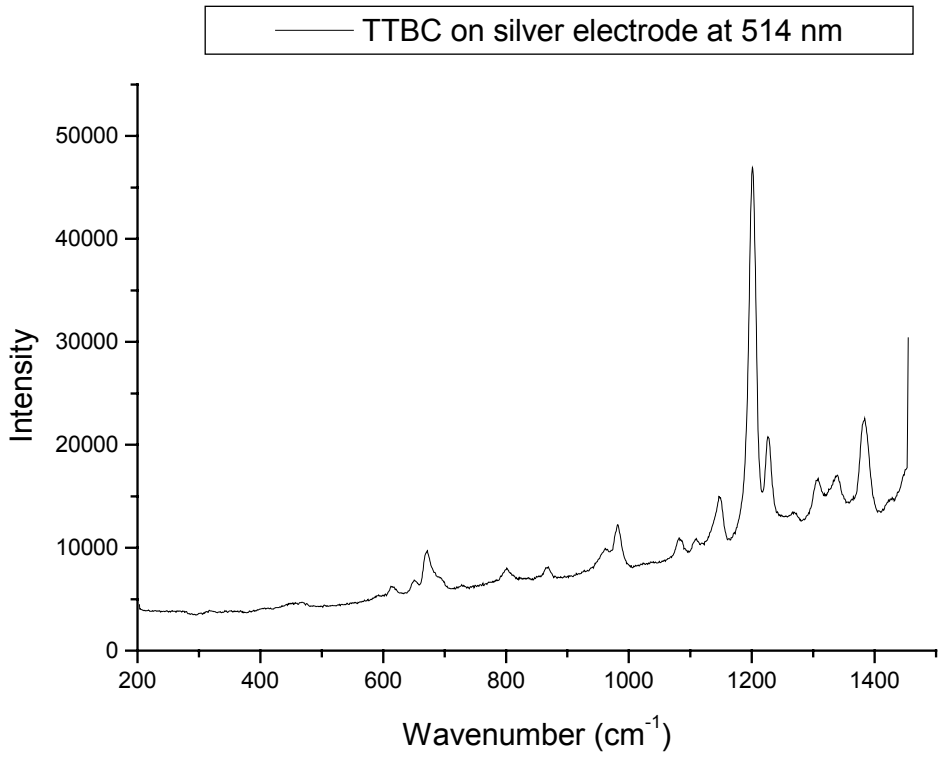

Figure 4-10. Raman spectrum of aggregated TTBC on silver electrode with laser excitation at 514 nm.

Figure 4-12 shows the resonance Raman spectra of aggregated TTBC on silver electrode and on colloidal silver, the striking similarities of the two spectra complement the results obtained by UV-Visible spectroscopy. In essence the electric field that emanates from the silver nanoparticles is essentially uniform, i.e. the curvature of the surface is negligible compared to the optical coherence length of the aggregate.

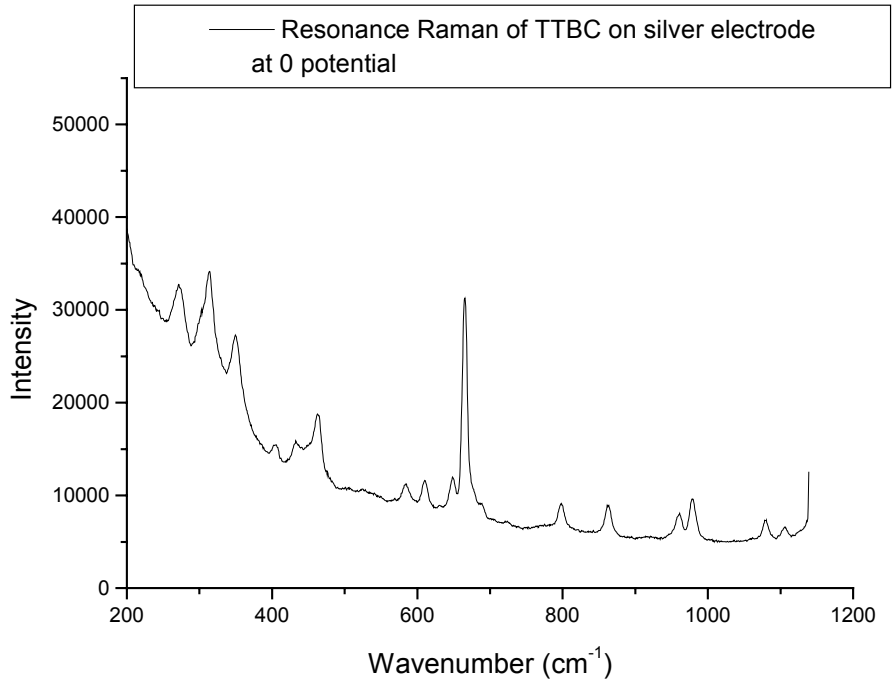

Figure 4-11. Resonance Raman Spectrum of aggregated TTBC on silver electrode with laser excitation at 592 nm.

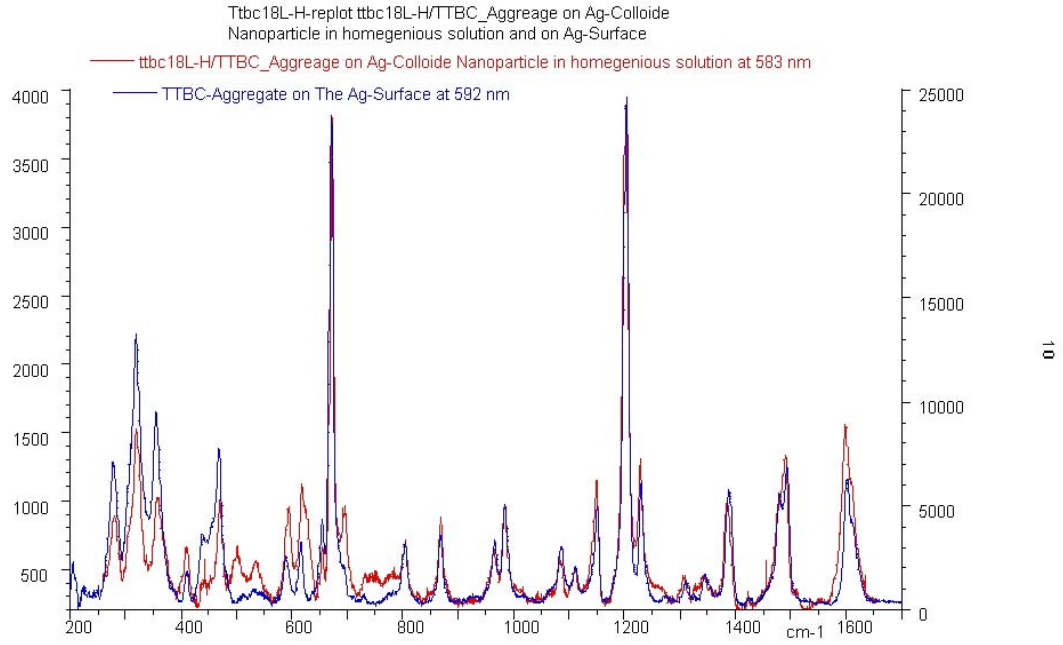

Figure 4-12. Resonance Raman spectra of TTBC in Silver Colloid and on Silver Electrode. Laser excitation was at 583 nm for TTBC on silver electrode and at 592 nm laser excitation on silver electrode.

4.3.2.2 Raman Spectrum of TDBC-4

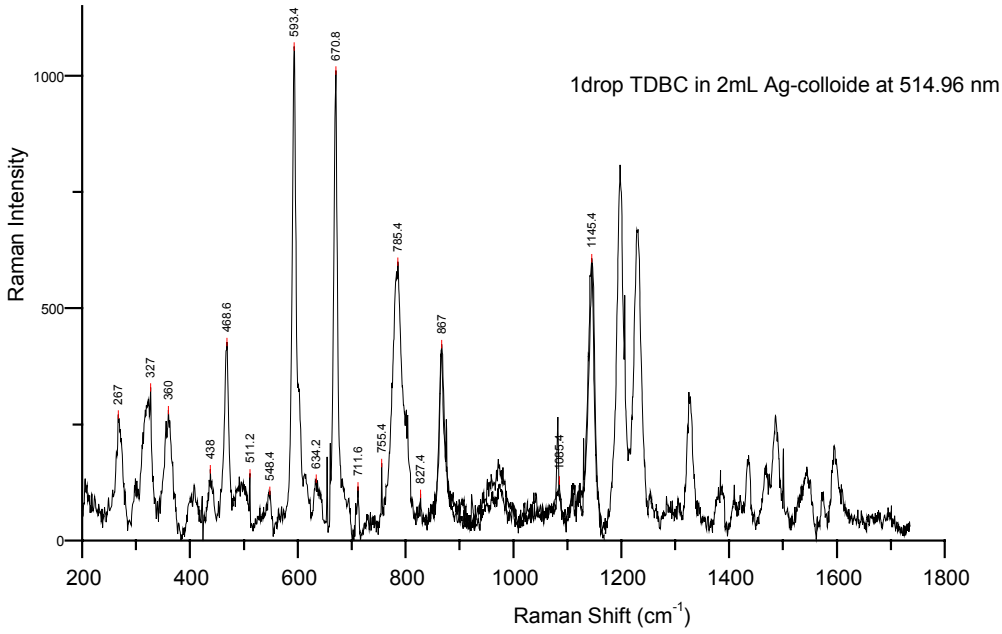

Figure 4-13. Raman Spectrum of TDBC-4 in silver colloid at 514 nm laser excitation.

The off-resonance Raman spectrum of aggregated TDBC-4 in colloidal silver suspension is shown in figure 4-13 and of immediate interest is the fact that, as in the case for the resonance spectra of TTBC, there is a trio of peaks in the low energy region. The fact that these peaks appear in the off-resonance spectrum of TDBC-4 is suggestive of the relative strength of pi orbital coupling. More specifically, because TDBC-4 molecules aggregate so readily in water without the need for increased solution pH or ionic strength this indicates that the vibro-excitonic lattice modes are more easily accessed pathways following excitation to the virtual state than in the case for other J-aggregates. It is reasonable to assume that the more rigidly held in place within the aggregate are the individual molecules, the more strongly will scattering occur from the lattice modes.

Viewed from a different perspective a weak aggregate would be one where it would be expected that the Raman spectrum would strongly resemble that of the monomer and that only under exceptional circumstances, as in the case with resonance excitation, would there be vibro-excitonic relaxation through lattice vibrations. A natural extension of this argument would be a discussion as to the difference in optical coherence length between a molecule such as TDBC-4 and PIC, the latter being unable to produce a J-aggregate as easily as the former. It is understood that the limiting factor in determining the aggregate's optical coherence length is the degree of pi orbital overlap between neighboring molecules. Because the relatively weak Van der Waals forces are what hold a J-aggregate together, at least to a first approximation, the less planar the molecule and the greater the flexibility of the molecule, the less able are these forces to maintain these molecules together under normal conditions in solutions at room temperature where molecular collisions occur with great frequency. In the case of PIC, steric hindrance from the protons in the ortho position relative to the methine link, and the relative sigma character of the two c-c bonds in the chain reduce the degree of molecular packing that can occur through Van der Waals interactions. In turn, the pi-orbital overlap is reduced and therefore so is the optical coherence length of the aggregate. TDBC-4 aggregates so readily that it is likely the optical coherence length of TDBC-4 is greater than that of PIC. Although these assertions do not go past the point of conjecture at this stage, the data is suggestive of TDBC-4 having a greater coherence length than PIC and the forthcoming NMR data serves to strengthen this argument.

4.3.3 NMR Analysis of TTBC and TDBC-4 Structure

The NMR spectra of TTBC and TDBC-4 are expected to be very similar to each other particularly as regards the protons on the polymethine chain. Of interest is where the proton on the central carbon will appear and where the protons on each side of it will appear as well. The location of those peaks will provide a picture of their relative degree of aromaticity, i.e., the tendency of those bonds to undergo substitution reactions rather than additions reactions in the presence of an electron acceptor. The pi orbital character of the c-c bonds on the polymethine chain will offer clues as to the degree of twisting between the benzimidazole moieties as well.

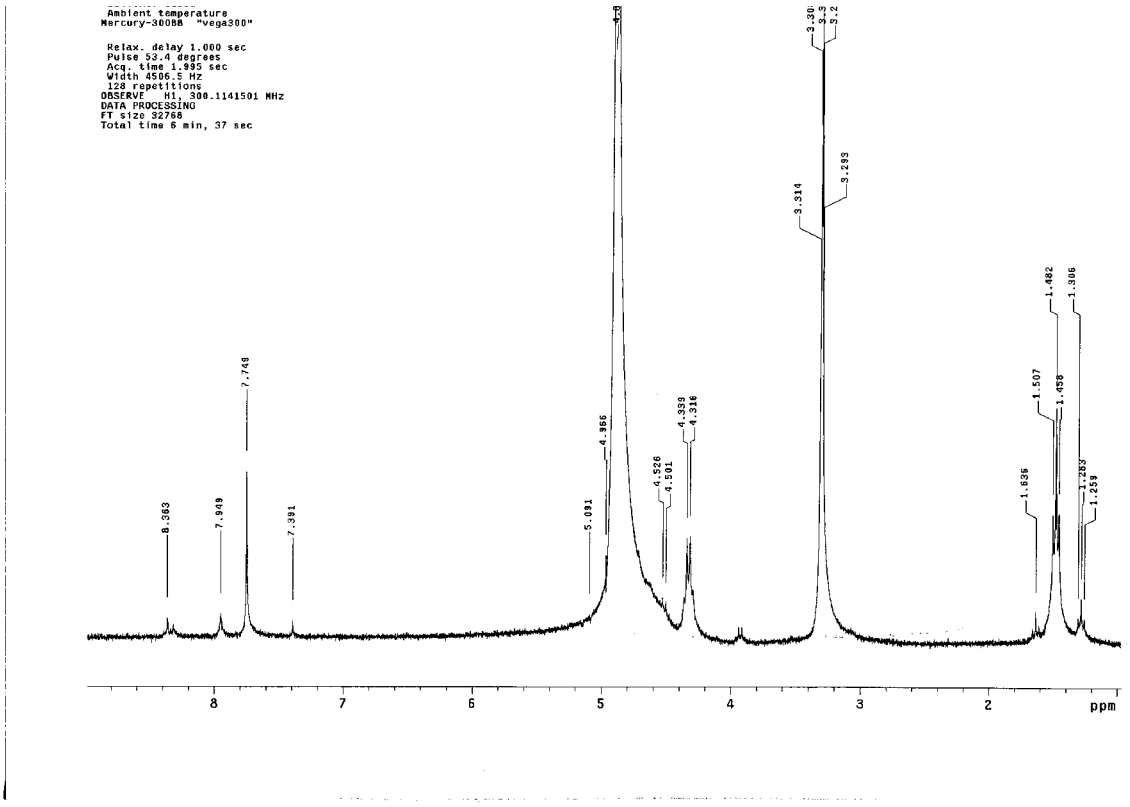

Figure 4-14. NMR spectrum of TTBC in deuterated methanol.

Figure 4-14 shows the NMR spectrum of TTBC in deuterated methanol. It is interesting to note that all of the peaks that are downfield are all below 7 ppm. The fact that all the

protons that belong to c-c bonds with pi-bond character are in the aromatic region is significant in that now it would seem that TTBC, relative to 2,2'-carbocyanine is a more rigid molecule, i.e., there is less likelihood that the c-c bonds along the polymethine chain allow rotation about their axis. This fact has a special consequence that becomes apparent only after realizing that there are more peaks in the downfield region of TTBC's NMR spectrum than would be assumed given a cursory look at a model of the molecule. Based on the structure of the molecule it would have been assumed that there would be three peaks downfield, two corresponding to the protons on the chain and one larger peak belonging to the four protons attached to the benzimidazole rings. At 7.8 ppm there is a peak that is not only relatively large and sharp but also very close in location to the protons found on the outer ring in PIC and 2,2'-carbocyanine. This peak is likely attributable to the four protons on the outer rings of the benzimidazole moieties. The difficulties occur when assigning the remaining peaks and this is for two reasons. Firstly, as mentioned before, there are more peaks than would ordinarily be expected and secondly there are no obvious indicators in terms of the splitting of those peaks as was the case for 2,2'-carbocyanine. Again, as was done with PIC and 2,2'-carbocyanine, the NMR spectrum of TDBC-4 offers important clues as to the identity of the peaks located downfield. The NMR spectrum of TDBC-4 in deuterated methanol is shown in figure 4-15 and one can see that while there is the same number of peaks in the aromatic region as was found for TTBC there is actually one less peak that needs assignment. Because TDBC-4 has two ethyl and two n-butyl groups, the protons on the outer ring of each benzimidazole moiety are not equivalent and are expected to experience, however slight, different electric fields.

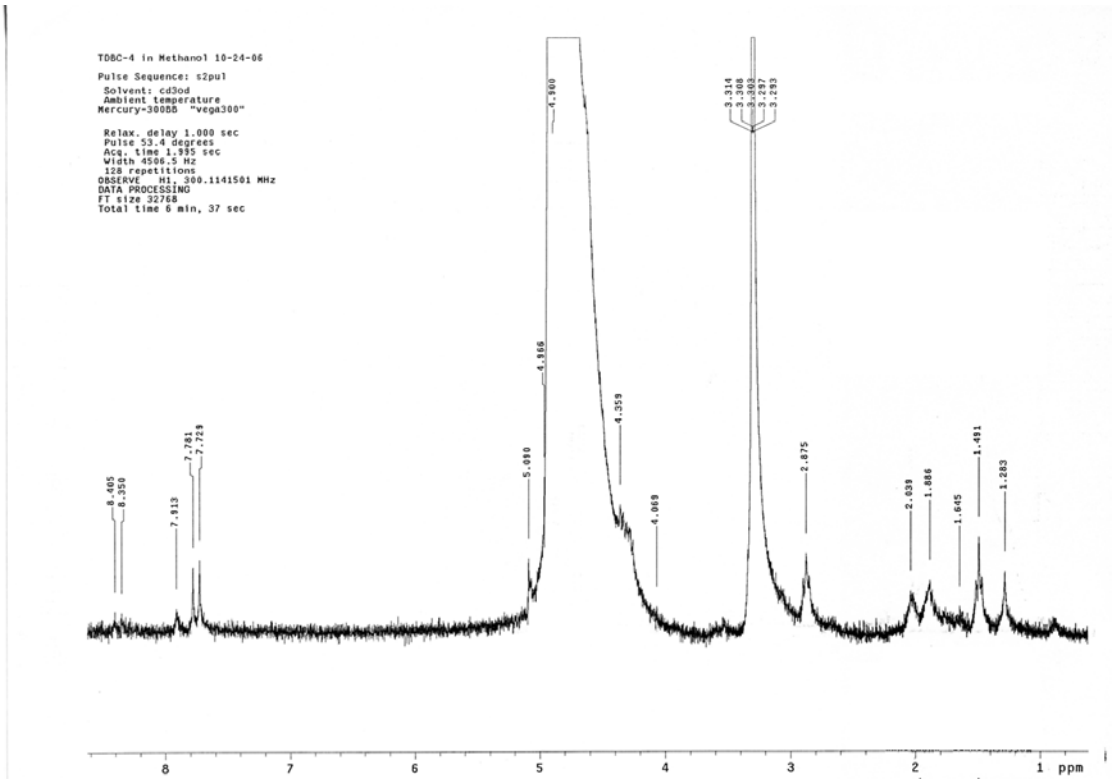

Figure 4-15. NMR spectrum of TDBC-4 in deuterated methanol.

It is apparent that the two peaks at 7.7 ppm and 7.8 ppm are attributable to those two sets of protons and this assignment is also consistent with the assignment of those same protons on TTBC. Interestingly those two peaks in TDBC-4 are equidistant from the corresponding peak in the NMR spectrum of TTBC although it is not clear why that is the case. Concerning the peak found at 7.9 ppm in the spectra of both TTBC and TDBC-4 and the pair of peaks at 8.36 ppm and 8.31 ppm, and 8.4 ppm and 8.3 ppm for TTBC and TDBC-4, respectively, it is clear that they belong to the protons on the polymethine chain. More specifically because of the apparent total area under the peaks, the pairs of peaks above 8 ppm are attributable to the central proton on the chain and the slightly wide peak at 7.9 ppm is attributable to the vicinal protons. The question of why those peaks do not show as triplets for the central proton and as doublets for the vicinal protons

is answerable by allowing for the possibility of stereoisomerism in both TTBC and TDBC-4 due to the aforementioned rigidity of the c-c bonds along the polymethine chain of both molecules.

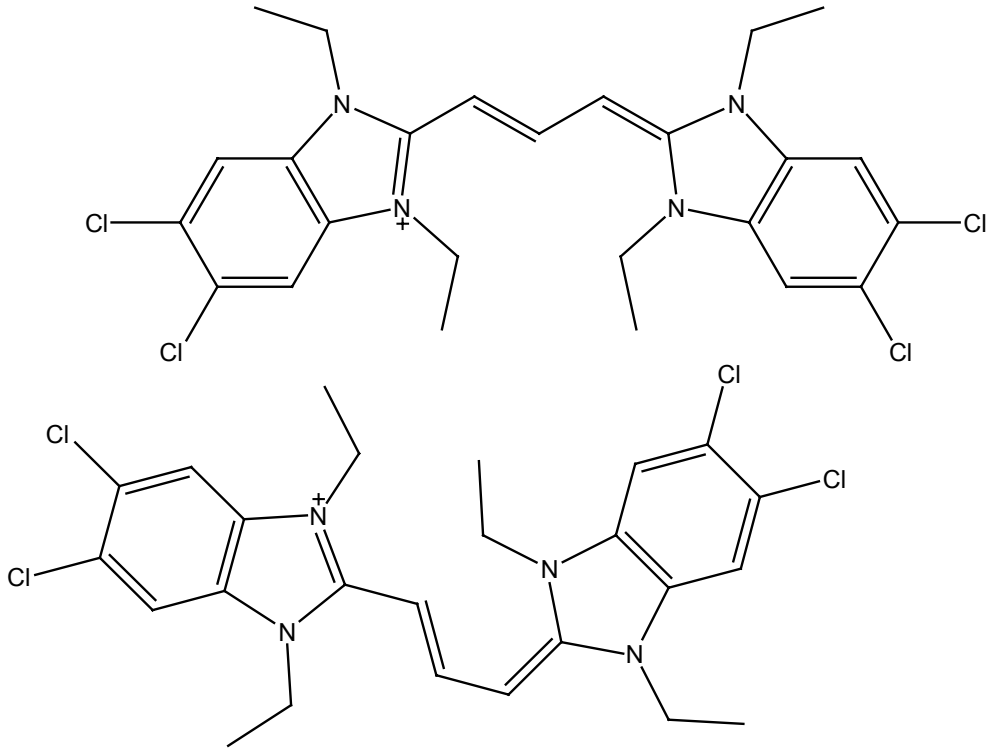

Figure 4-16. Different configurations of TTBC.

Because of the degree of pi bond character along the length of the chain it is reasonable to assume that there is very little possibility for rotation about those bonds. There are two possible conformations for TTBC; the protons on the polymethine chain can be in the all-trans configuration or one of the vicinal protons can be in the cis-configuration with the central proton. In the case of TDBC-4 there are two additional configurations that come from the relative arrangement of the ethyl and n-butyl sulfate groups on the two benzimidazole moieties where the like groups can be either cis or trans to each other depending on the pairing of the side chains.

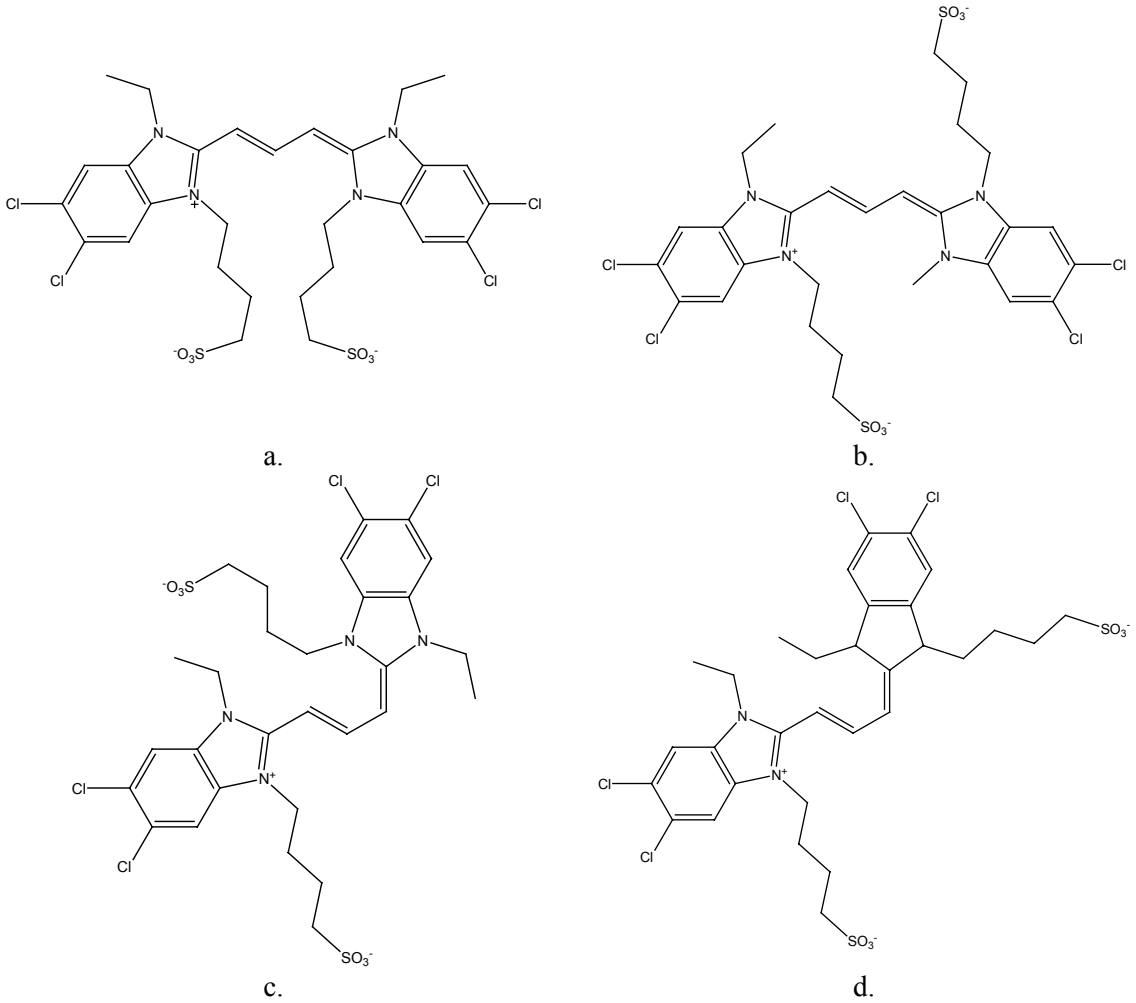

Figure 4-17. Different configurations of TDBC-4 where we see two isomers where the polymethine chain is in the all-trans configuration and the side groups are cis in a.) and trans in b.). The other two isomers have the side groups in cis and trans configurations, c.) and d.) respectively, also but the polymethine chain is not all-trans. The configurations where the c-c bonds on the polymethine chain are all-cis are not shown.

Those conformations are shown in figures 4-16 and 4-17 for TTBC and TDBC-4, respectively. It should be noted that the fact that the peaks on the polymethine chain are more easily identifiable in 2,2'-carbocyanine is a direct result of the relative discontinuity in the pi character if the c-c bonds along the chain compared to that of TTBC and TDBC-4. The fact that the vicinal protons on the polymethine chain in the NMR spectrum of 2,2'-carbocyanine are found further up-field than in the case of TTBC and TDBC-4

indicates that there is greater sigma bond character to the c-c bonds that link the chain to both quinoline moieties. The low-field appearance of the vicinal protons also shows that the pi-electrons found in the center of the polymethine chain are not shared equally by the three carbon atoms. There is a greater concentration of pi electrons and therefore weaker electron shielding for the central proton.

Although there are different configurations of both TTBC and TDBC-4 in these solutions they are not equally represented. It is apparent that the ratio of the all trans configuration to the other is 1 to 2 and this number can be predicted by simply allowing for a fair distribution of configurations. The peak at 7.3 ppm in the spectrum of TTBC is attributable to the vicinal protons in the all-trans configuration with the central proton for that configuration appearing just in-between the two larger peaks at 8.36 ppm and 8.31 ppm. Those two peaks correspond to doublets of the central proton and not two triplets because in the configuration that is not all-trans the vicinal protons do not interfere with the central proton's electric field equally. The vicinal protons in the other configuration appear at 7.9 ppm and it is reasonable to believe that two doublets are not seen in place of the broad peak because the differences between the vicinal protons are extremely small. The NMR spectrum of aggregated TDBC-4 in deuterated water is shown in figure 4-18 and it is important to note several differences between this spectrum and the previously presented spectra of the carbocyanine dyes in methanol. Firstly one should note that the largest peak is located further downfield than all the other peaks. Secondly there is an appearance of small peaks below 7 ppm while there were none for the monomer in methanol.

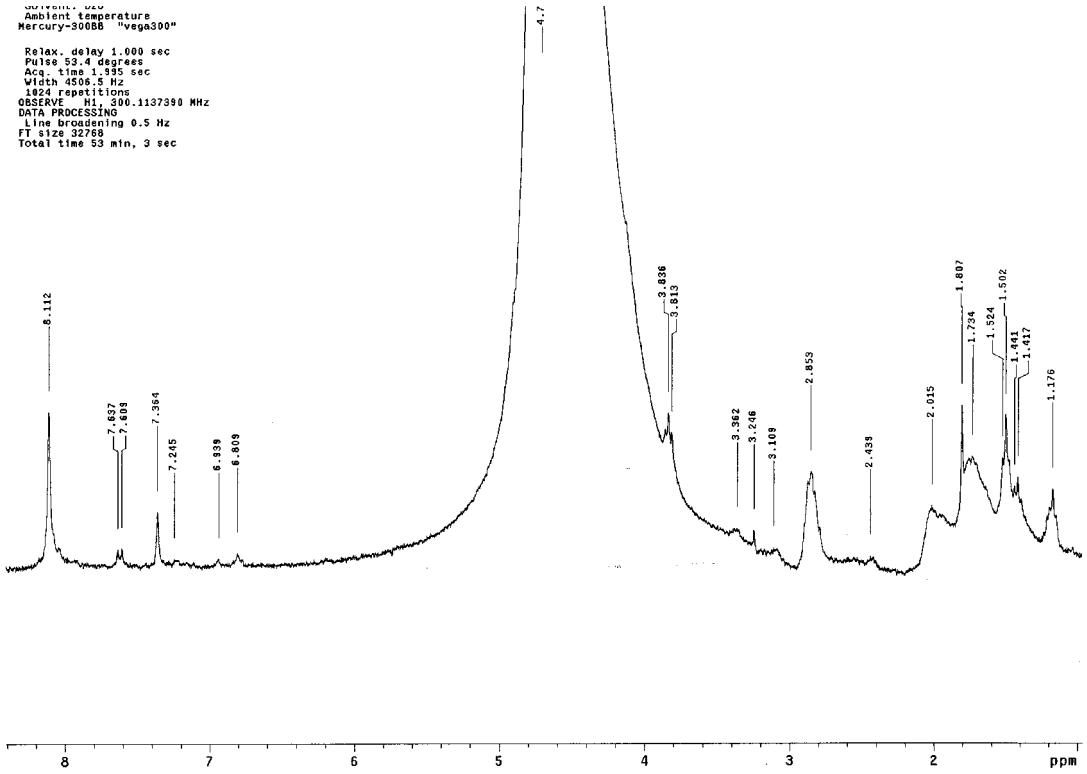

Figure 4-18. NMR spectrum of TDBC-4 in deuterated water.

Essentially the aromatic region of the spectrum of aggregated TDBC-4 in water looks in many ways as the spectrum of molecular TDBC-4 in methanol with the peaks shifted upfield. The difference lies in the downfield shift of the protons on the outer ring of the benzimidazole moieties and the fact that they form essentially one peak and not two. This fact offers some clues as to the possible arrangement of the TDBC-4 molecules in the aggregate. The four protons on the rings appear as two peaks in the NMR spectrum of the single molecule because of the extended-field affect of the two side chains. For there to be only one peak, even if the peak were in reality two peaks very close together, it would have to be because the two pairs of protons now experience a virtually identical field influenced by both the ethyl and tert-butyl sulfate side chains. Figure 4-19 shows a

possible configuration of the aggregate of TDBC-4. A very important question rises as to the aggregation of the different isomers of TDBC-4 as well as the isomers of TTBC.

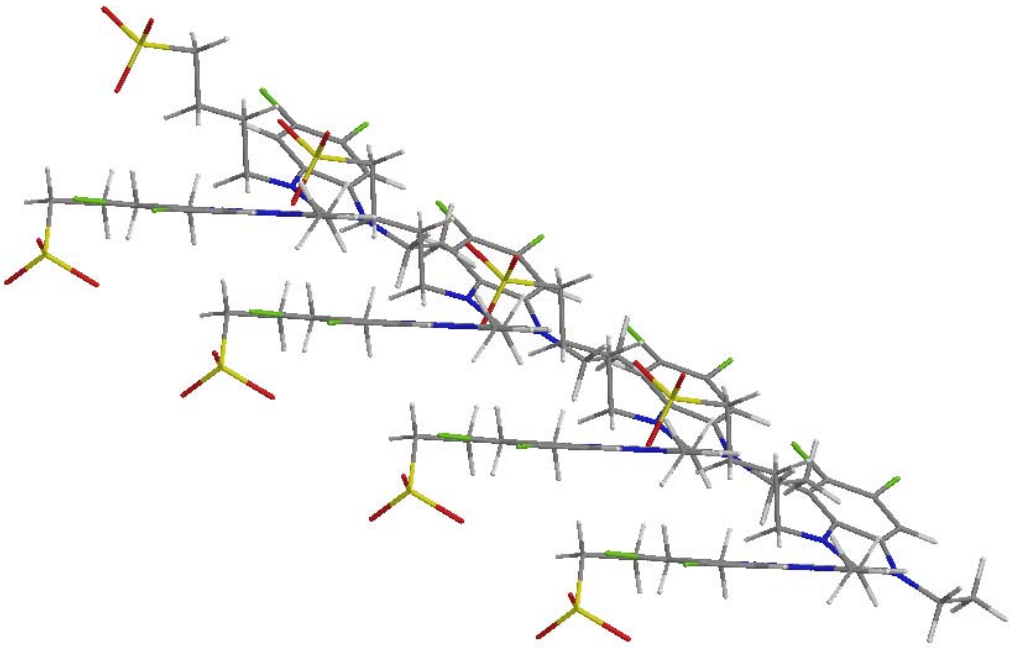

Figure 4-19. Possible model of aggregated TDBC-4. The protons along the polymethine chain are all-trans and the side groups are cis to each other.

Concerning the aggregation of TTBC it is very likely that the species that actually forms the aggregate is the all-trans even though it is apparently not initially the most abundant species. As noted before TTBC aggregates in aqueous solutions after it has been dissolved in acidic media and upon addition of base the aggregate forms. It is very probable that the change that occurs in TTBC from whatever species exists in the acid leads to the formation of the all-trans species. Furthermore, it should also be noted that in the absorption studies conducted in methanol/water mixtures although the aggregate was formed the monomer peak was stronger indicating that most of the TTBC had not aggregated. It is clear from the additional information provided by the NMR data that the TTBC molecules that did not aggregate were from the more abundant isomer. In the case

of TDBC-4 the aggregate forms so easily in neutral water that it seems very likely that all the isomers are able to form the aggregate. That said, it is not suggested at all that there are different aggregates for each isomer. It is assumed that there is only one aggregate that is formed but that some type of transformation takes place that is mediated by water molecules that facilitate the aggregate formation. The fact that TDBC-4 dissolves so easily in water means in other terms that the molecule is very easily solvated and that it interacts strongly with water molecules. The triplet at 6.8 ppm belongs to the central proton in monomeric TDBC-4. This shift upfield for that proton means that the pi character of the central c-c bonds in the polymethine chain is sufficiently lowered in water to allow for rotations about those bonds and therefore allows all the possible isomers of TDBC-4 to aggregate.

4.3.4 Molecular structure and J-aggregate models

Since their discovery, proposed J-aggregate models have been as varied as the imagination allows and because of the dearth of actual physical and spectroscopic evidence that conclusively supports a certain molecular arrangement, many proposed models that can easily be grossly inaccurate go unchallenged. One such model, shown in figure 4-20, is of the dye molecules aligning along their long axis in one of many configurations where the dye molecules are arranged such that the chromophores of the individual molecules are separated from each other by the physically overlapping moieties.

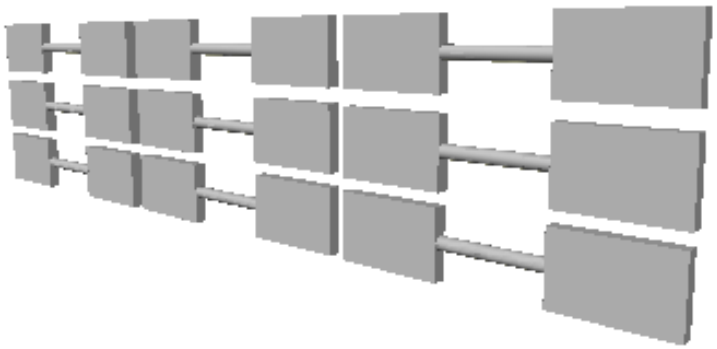

Figure 4-20. Dye molecules aligned along their long axis.

This model is essentially arbitrary and unjustified because the transition dipoles of those molecules do not necessarily align in this way; in fact, the transition dipoles may align orthogonally to the long axis of the molecule in some instances resulting in a J-aggregate model that in no way reflects the true configuration. In assuming that the chromophores of each unit do not physically interact, it is possible to a first approximation to view the aggregate as a collection of weak-interacting units held together by Van Der Waals and other weak forces, and to view the exciton as a perturbation that does not alter the physical characteristics of the individual molecules. Furthermore, resonance Raman spectra of J-aggregates shows that there is enough physical proximity between the molecules to produce vibrations that are not observed in the Raman spectra of either the monomer or the aggregate in the off-resonance case. Based on Raman data alone one

must conclude that some orbital overlap must occur between the molecular units when the aggregate is electronically excited.

The combined data from absorption and NMR spectroscopy validates this claim as not only do both TTBC and TDBC-4 aggregate more easily in many environments compared to PIC, but because of this ease of aggregation, TTBC and TDBC-4 J-aggregates are also more practical systems with which to study the superradiant properties of cyanine dyes.

4.3.5 The optical coherence length

The optical coherence length of a J-aggregate can in many ways be considered as an indirect measure of its physical characteristics. Theoretical models that are used to determine optical coherence lengths, though they are increasingly more sophisticated and incorporate more of the factors involved in exciton dynamics, are still incomplete. The most obvious missing element in these models relates to the absence of structural considerations that are specific to the molecules being studied such as for instance their symmetry, their pi orbital characteristics and degree of conjugation, etc. For now, fluorescence decay rates are largely considered as more determinative of optical coherence lengths than other factors. Similar to the variety in J-aggregate structural models, there is a variety in theoretical exciton dynamics models that produce different results. Coherence lengths for PIC for instance have been calculated to be as short as two molecules long to as long as thirty molecules. Intrinsic structural factors may play a large role in limiting optical coherence lengths, yet this area of investigation has not been explored in the literature. While simplified J-aggregate models use parallel-aligned transition dipoles, a more plausible non-parallel, or offset, model may actually be more useful to analyze. As shown previously in section 1.2.2 , equation [1.2], the energy for

the generalized point-dipole expression can be represented with a simple point-dipole expression. In a three-dimensional scenario α is the angle between a plane formed by one of the transition dipoles and the molecular line of centers and the projection onto that plane of the second transition dipole. One of the interesting features of this expression is that it is not necessary to alter it to represent a trimer, tetramer or any larger aggregate. A simple model of a larger aggregate can be represented as a sum of dimer point-dipole expressions:

$$\Delta E = \sum_{i \neq j}^{n} \Delta \varepsilon_{ij} \qquad [4.2]$$

In this expression *i* refers to the initial exciton host molecule and *j* refers to all the other molecules that are part of the coupled state. The coherence length in this model is limited by the number of molecules on either side of the initial excited host molecule whose transition dipole projects within an angle α of 90^{o} to the plane formed at the host molecule between its transition dipole and the line of centers between it and the adjacent molecule. It is clear that the actual physical arrangement of the molecules in the aggregate can play a large role in limiting the optical coherence length without there being a need to rely on environmental factors or internal defects in the aggregate to explain it. This is an important fact because a J-aggregate that forms in different environments and produces the same absorption and emission profiles must be relatively insensitive to externals influences and mainly have intrinsic factors that determine its optical properties. An example of such an aggregate is that of TTBC whose absorption maximum in figure 4-5 and 4-6 appears between 592-595 nm in both basic and colloidal

solutions. The J-aggregate in colloid was shown to form primarily on the silver nanoparticles, therefore not only should the optical coherence length of TTBC be the same in both environments but it should be clear that the optical properties should principally be determined by internal structural factors that are specific to it. It should be noted that because TTBC is so well conjugated the molecule is less susceptible to molecular conformational distortions caused by environmental influences and this means that if a structure can be deduced, this structure is enough to provide the necessary information to improve the accuracy of coherence length calculations.

4.4 Summary and conclusion

Absorption spectra were presented of aggregated TTBC and TDBC-4 in solution and it was shown that these molecules aggregate preferentially on silver surfaces, whether on colloidal silver or on a smooth silver electrode surface rather than in the solution itself. Raman spectra of aggregated TTBC and TDBC-4 showed that there are three intermolecular modes that appear in the low-energy region and that these motions are mainly caused by out-of-plane vibrations. NMR spectra of TTBC and TDBC-4 monomer and aggregated TDBC-4 provided evidence for the presence of different isomers of both molecules also offered clues as to why relatively little TTBC aggregated in methanol/water compared to the amount of aggregate obtained from basic water solutions of initially acidic TTBC. The sharpness and intensity of the peak representing the protons on the outer ring of the benzimidazole moieties in the spectrum of aggregated TDBC-4 is suggestive of the formation of only one type of aggregate despite the presence of different isomers of the single molecule in methanol. It is assumed that the interaction of

water with TDBC-4 leads to the formation of the aggregate from all its isomers. Furthermore it was shown that by pairing structural and spectroscopic data certain erroneous models could be eliminated. By using the generalized point-dipole equation, it was possible to use a simple expression to provide more information on the structural factors that affect the optical coherence length.

Chapter 5: Structural Analysis of TSPP and Electrochemical Studies with Fe-TSPP and Co-Protoporphyrin

5.1 Introduction

Porphyrins are compounds that are important elements in various biological processes including being the primary light-harvesting components in photosynthesis[1,2] and are therefore very important molecules for basic scientific research. In the area of photosynthesis porphyrins play a determinative role in capturing light and converting that light into energy that drives a plant's cellular cycle. Although it is still not fully understood how this multi-step process of energy transfer and conversion occurs it is known that aggregation of the porphyrin does take place and is crucial to the completion of the overall reaction. One of the simplest molecules available that can be used to study many general properties of porphyrins and in particular J-type aggregation is meso-tetrakis(p-sulfonatophenyl)porphine also known as TSPP shown in figure 5-1.

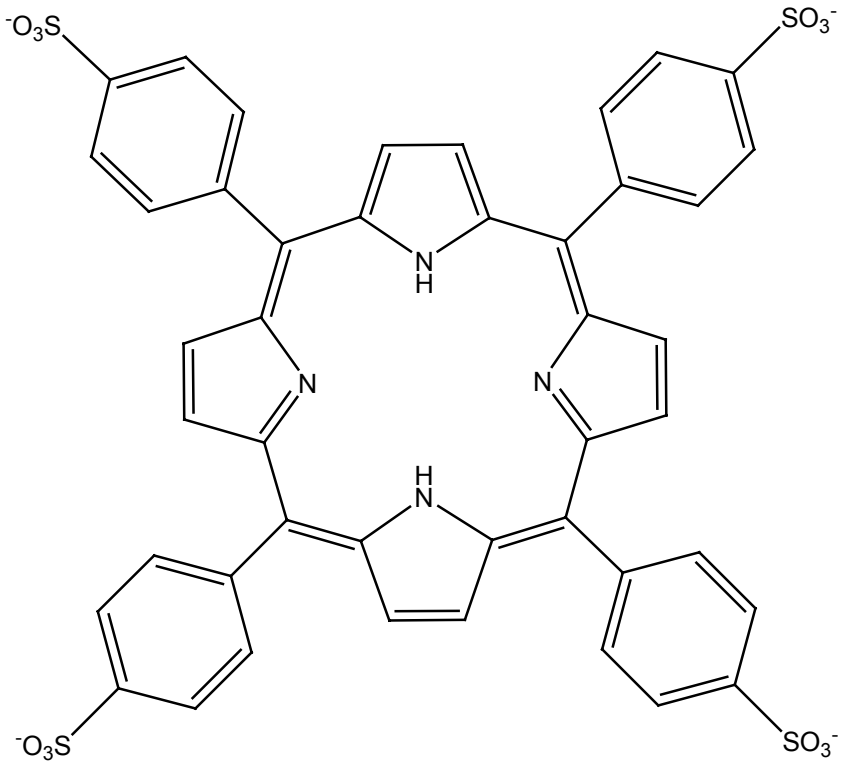

Figure 5-1. Molecular model of H_2TSPP.

While it is known that the TSPP J-aggregate forms in acidic media by proton addition to the pyrollic nitrogens in the inner ring of the porphyrin[3], just as is the case for the cyanine dyes that J-aggregate, it is not known how the single molecule's structure and conformation is modified upon aggregation. There are two possible conformations that can be representative of protonated TSPP that also addresses potential steric factors. Models of these conformers, shown in figure 5-2, show the molecule with a "ruffled" conformation and in both, pairs of the protons in the core shift above and below the plane of the molecule.

a) b)

Figure 5-2. Ruffled models of TSPP; in a) the proton opposite to each other are paired and in b) the protons that are paired are adjacent to each other.

No experimental method has been found to definitively demonstrate what occurs in the porphyrin core upon aggregation however this matter remains a topic of great interest and scientific value. What is known is that TSPP forms a one-dimensional structure[4,5] and through the use of scanning probe techniques such as AFM it has been proposed that the TSPP aggregate is actually a helical nanotube-like structure[6,7].

Molecular J-aggregates share many properties of both single molecules and molecular crystals and because of this seemingly dual nature that they have, they are very interesting systems to study from a conceptual and theoretical viewpoint; the interactions that trigger self-assembly, and ultimately form the aggregate, have both structural and spectroscopic consequences. Because the J-aggregate of many molecules has numerous attractive properties for nanotechnological applications, it is essential for practical purposes to determine conclusively not only how the molecules arrange themselves, but also how they change conformation to adapt to the pseudo-polymeric and kinetically restrictive environment. In this chapter structural characteristics of the molecular J-aggregates will be discussed using that of TSPP as a test model, and a systematic

approach will be used to obtain a stucture that satisfies both spectroscopic and structural requirements. Additionally, electrochemical methods will be used to take advantage of the aggregating properties of TSPP.

There are many metalloporphyrin analogues to TSPP such as Mg-TSPP, Cu-TSPP, etc, and these metalloporphyrins are also able to form the same J-aggregate as TSPP under the same acidic conditions through ejection of the cationic metal found in the core and the replacement of that metal cation by four protons[8].

The fact that this occurs offers a great opportunity to investigate the feasibility of using TSPP aggregation as a method for forming metal nanoparticles. Under proper conditions, once the metal cation has been expelled from the porphyrin's core, conventional methods for nanoparticle synthesis specific to that metal can be employed.

Coupling the aggregation of TSPP to an electrochemical process affords the possibility of controlling the nanoparticle size because the metal cations could be deposited and reduced on an electrode in an ordered array. By definition, J-aggregates always form by self-assembly and if it is possible to control the degree and rate of aggregation[9], it may be possible to ensure a homogeneous coverage of the porphyrin over an electrode surface. Metal analogues of TSPP offer the opportunity to investigate the potential of using electrochemical methods for various applications where for instance surface topography, regularity and layer thickness are important. One of the many important uses of chemically modified surfaces is to facilitate reactions or to provide the conditions for targeted synthesis and metal surfaces have a long history of being used as catalysts. The prospect of disposing of an ordered array of size-specific metal nanoparticles opens the

door to many possible applications including the use of iron nanoparticles for the controlled synthesis and growth of carbon nanotubes.

As mentioned before in chapter 1, there are many challenges that confront scientists in the synthesis of type-specific carbon nanotubes and metalloporphyrins have the potential of serving as important components in their catalytic formation. A metalloporphyrin analogue of TSPP that is of particular interest as an initial step to synthesizing type-specific carbon nanotube synthesis is Fe-TSPP shown in figure 5-3.

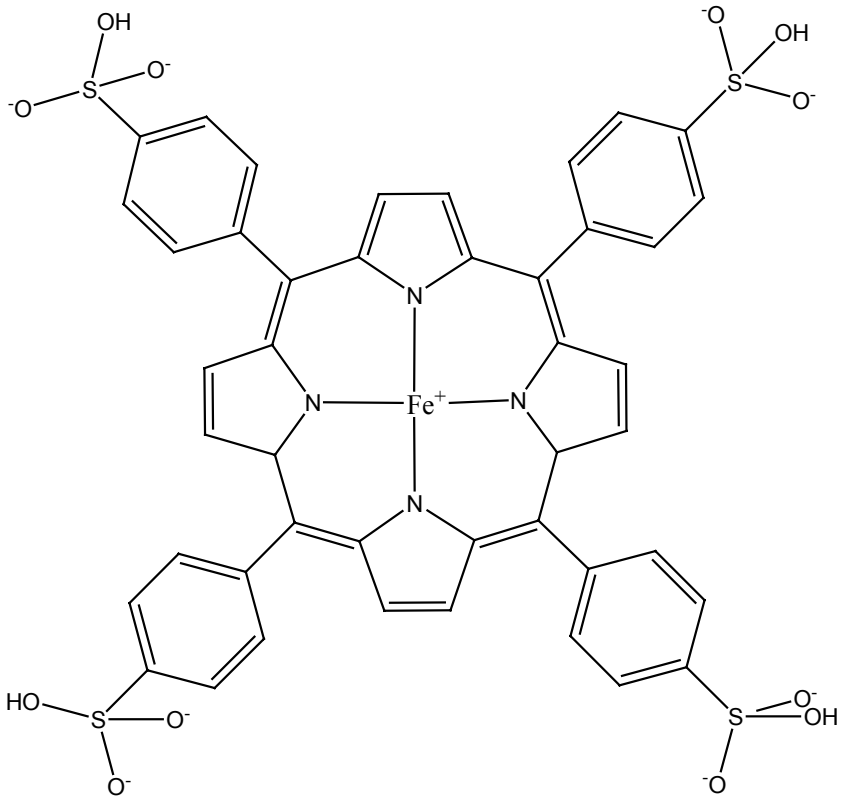

Figure 5-3. Molecular model of Fe-TSPP.

Fe^0 nanoparticles serve as excellent catalysts for single-walled carbon nanotube synthesis[10,11] and methods for synthesizing these nanoparticles are relatively economical. While the Fe^0 nanoparticles greatly facilitate single-walled carbon nanotube synthesis and research has been done to synthesize uniform-sized metal nanoparticles, conventional

methods still lead to nanoparticles of different sizes and in turn these nanoparticles lead to nanotubes of varying diameter and chirality. A method that could narrow the distribution of nanoparticle sizes would also lead to nanotubes with more uniform size and chirality, i.e., nanotubes with more uniform properties. If it is possible to develop a method to use Fe-TSPP and deposit Fe^0 nanoparticles on an electrode surface by using the TSPP J-aggregation as a facilitating process, this method would not only solve a critical problem in carbon nanotube synthesis but also open the possibility of using this method for other nanoparticle species with catalytic properties. In addition to Fe-TSPP, another porphyrin that was used in this study for comparative purposes was Co-protoporphyrin shown in figure 5-4.

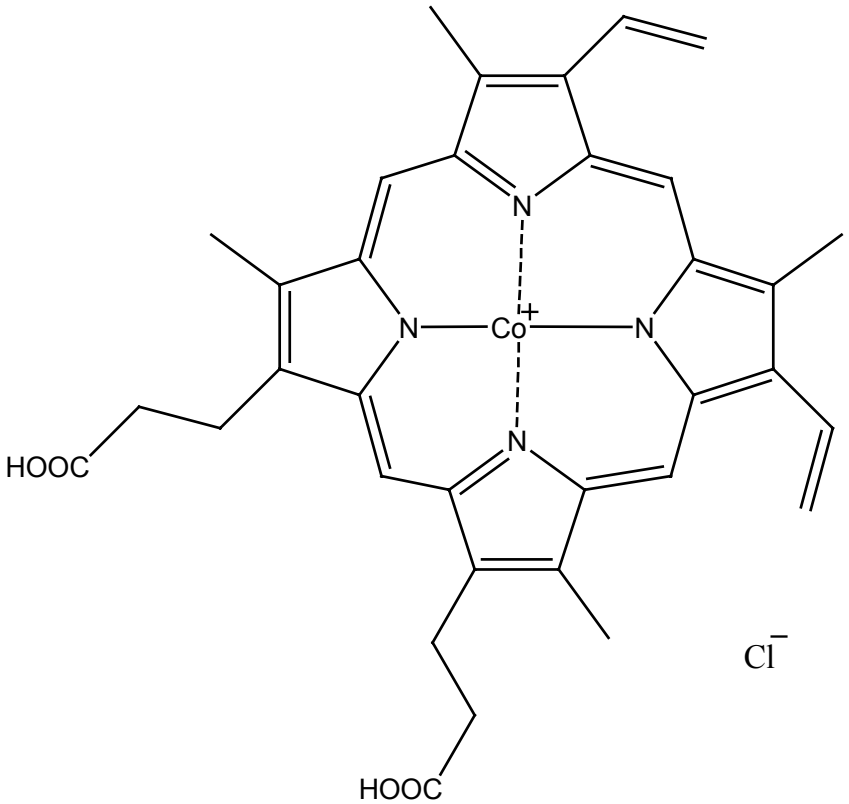

Figure 5-4. Molecular model of Co-Protoporphyrin.

Protoporphyrin and its analogues are different from TSPP and its analogues in that the symmetry of those species is lower and this contrast is helpful because aggregation of such species upon deposition on an electrode surface under the influence of an applied potential may perhaps occur in a more oriented manner than it would in solution. Even if the protoporphyrin were not to form a J-aggregate, applying a potential over an electrode surface could still orient molecular dipoles in an ordered fashion and mimic this important physical characteristic of J-aggregates.

Controlling particle size and spatial distribution as well as forming organized arrays of functional molecular units are of paramount importance in nanoscale applications and electrochemical methods may be the bridge that joins these two processes. Absorption spectra will presented on pH dependence for TSPP, Fe-TSPP, and Co-protoporphyrin in solution to determine the formation and conditions for formation of aggregate species. Cyclic voltammograms on platinum electrode will be presented where the relative strength and type of absorptivity of the metalloporphyrins, whether of the electrostatic or chemical nature, will be investigated and these results will be discussed within the context of possible metal nanoparticle formation and electrode surface coverage.

5.2 Experimental

TSPP, Fe-TSPP and Co-Protoporphyrin were purchased from Prophyrin Products and used without further purification. Cyclic voltammetry experiments were conducted in solutions of 0.1M $HClO_4$ and $NaClO_4$ within a range of -0.275V to 0.925V and -0.275V to 0.625V versus SCE. Ultra-pure nitrogen gas was bubbled for at least 30 minutes prior to taking measurements into the solutions of metalloporphyrin to deoxygenate them and

prevent oxygen-poisioning of the platinum electrode. Voltammograms were recorded until no change was observed in successive cycles.

5.3 Results and Discussion

5.3.1 The J-aggregate of TSPP

As demonstrated in earlier chapters, there are essentially two kinds of coupling that occur in a molecular J-aggregate; the physical coupling occurs through a pi orbital interaction between the moieties of neighboring molecules; the optical coupling that leads to the exciton can be argued to be an orbital coupling of the chromophores. Depending on the degree of conjugation in the dye molecules the two types of coupling may be more or less distinguishable and can be treated independently of each other. Conversely, when the conjugation is relatively uniform along the molecule, both physical and optical couplings are facilitated and such a system is expected to not only aggregate more easily but also respond more strongly to excitation. Elucidating the structure of J-aggregate of TSPP is a very important because analysis of its assemblage would very likely help predict the assemblage of most J-aggregates; because of its unique structural characteristics, including a ring comprised of four pyrroles linked together by four methines, it is easier to narrow the list of possible J-aggregate structures for TSPP. It is known that all four pyrollic nitrogen atoms in TSPP are protonated before forming the aggregate, and while it is still not known conclusively how steric factors affect the positioning of the protons in the center it is possible to construct molecular arrangements that can be representative of the true J-aggregate. Classical mechanical concepts are enough to expect TSPP to have a puckered or ruffled arrangement mainly as a response to the mild ring strain. Based on

this initial structure protonated TSPP would be expected to retain a similar topography. Steric and symmetry factors evidently come into play and result in protonated TSPP having presumably near-C_2 symmetry. Because of repulsion between diagonally opposed hydrogens the N-H bonds are predicted to bend away from each other in a clockwise or counterclockwise manner. There is an added consequence to having the protons in the middle bend away from each other in that manner and it is that other molecules that stack accordingly will not only adopt the same structure and conformation but will also be expected to rotate slightly with respect to each other. It should be noted for clarity that a clockwise or counterclockwise arrangement of the protons are both representations of the same molecule; furthermore, there are no indications that there are different kinds of TSPP J-aggregates with different chiralities. Finally, by including a slippage angle between neighboring molecules all the aforementioned factors lead to an aggregate with a helical shape. As stated earlier, it has been reported that the TSPP J-aggregate has a nanotube-like helical structure according to AFM studies and if true, it is important to note that this simple though systematic analysis was enough to construct a fairly accurate image of it. An example of the beginnings of such a structure is shown in figure 5-3 where the rotational slippage between adjacent molecules suggests a coiled, or helical, aggregate.

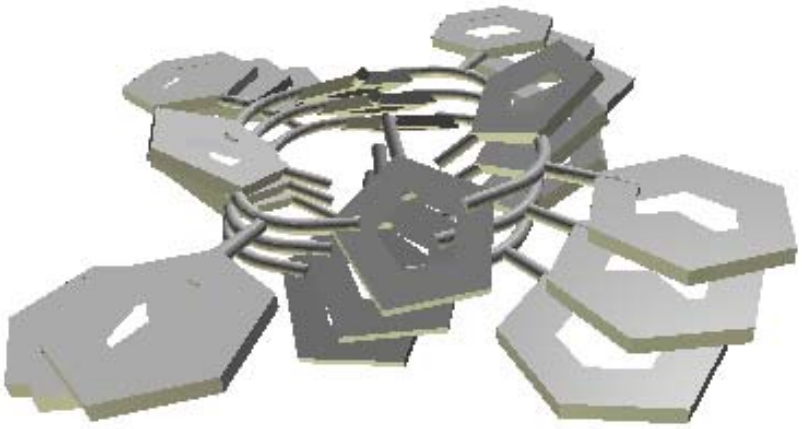

Figure 5-5. Model of aggregated TSPP

If there is a general commonality to the way all J-aggregates form, the assemblage of TSPP described above provides crucial information. Firstly, according to this model, like-groups on adjacent TSPP molecules would be expected to stack preferentially on top of each other and that suggests, for instance, that the chromophores in cyanine dyes would likely stack similarly rather than being separated by the moieties as suggested in other aggregate models. Secondly, the relative angular offset between adjacent TSPP molecules results in a corresponding offset between the molecules' respective transition dipoles. Such an offset would be a structural limiting factor to the optical coherence length that would not depend on any defects or static disorders in the J-aggregate assembly, but rather, on the differences in phase and orientation between transition dipoles. This is important to consider because phase differences between coupled transition dipoles may play an important role in determining a J-aggregate's optical coherence length; this topic is discussed in the following section.

5.3.2 Characterization of TSPP, Fe-TSPP, and Co-protoporphyrin by UV-Visible spectroscopy

The characterization of TSPP and its aggregate by UV-Visible spectroscopy has been done on many occasions however it is useful for the purposes of this work to review some of the salient features. The absorption spectrum of H_2TSPP in neutral water and in acidic solutions is shown in fig 5-6 and briefly, the peak at 410 nm is the Soret band corresponding to the monomeric state of the molecule.

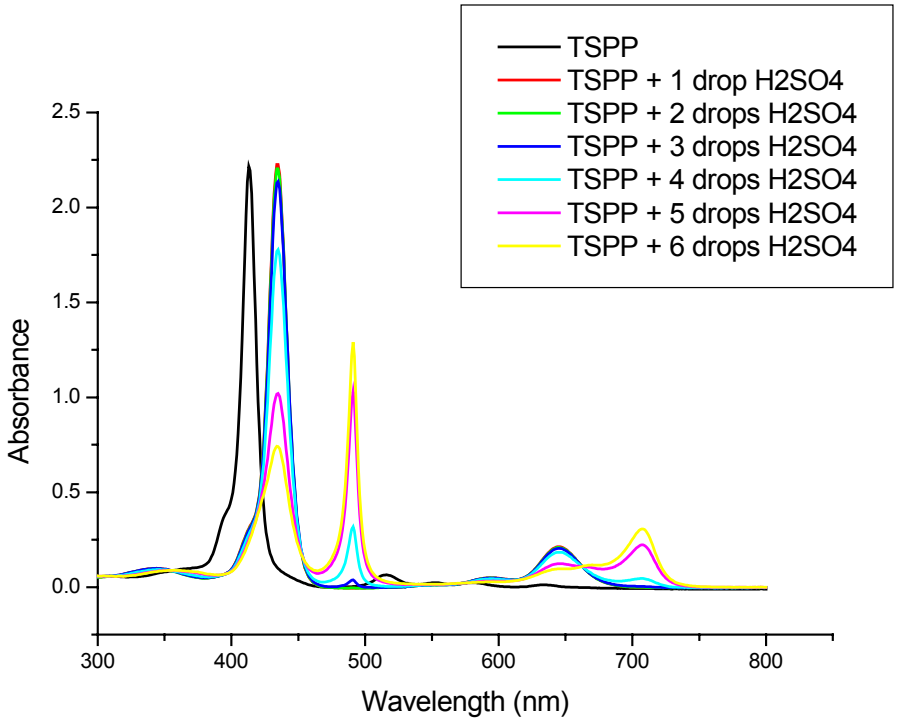

Figure 5-6. Absorption spectra of TSPP and aggregated TSPP in acidic solutions.

In solutions of increasing acidity a peak appears at 440 nm and finally the J-band appears at 480 nm at pH 2. The evolution of the TSPP spectrum shows that the change from monomer to aggregate follows a step-wise process where all the molecules have to enter the same intermediate state before any intermediate enters the final aggregate state of

H_4TSPP. Additionally it is clear from the relative intensities of all three major peaks that TSPP has essentially the same transition dipole in all three species. Whatever changes occur in the molecule do not change the response of the molecular orbitals involved in the electronic transition. This fact suggests that the excited electrons are on the conjugated chains that link the pyrrolic groups. In fact the pi-electrons on the links can be thought to have similar character to those on the methine bridge in PIC as well as those in molecules such as DDPT that have a substituent rather than a proton in the middle of the chain. It is therefore reasonable to believe that proton addition to the nitrogens would not necessarily affect those pi-electrons significantly. Furthermore, because proton addition to the nitrogens leads to the formation of the J-aggregate, it is evident that there are three conditions that must be met to give rise to J-aggregates. Firstly, it is sensible to conclude that for aggregation to occur some type of intermolecular interaction has to take place and in the case of these organic dyes this interaction has to involve the pi-electrons on the aromatic groups on either side of the chain or link. Secondly, the regions of interest in the molecules that produce the molecular exciton in the J-aggregate have to weakly couple as is required in molecular exciton theory. Thirdly, those two regions, the excitonic or exciton-producing region and the pi-electron region that allows for electrostatic interactions and pi-orbital overlap, should be essentially independent of each other. One way of demonstrating that the fundamental character of the molecular orbitals in those regions does not change in any significant way is through NMR analysis. As was shown in the case for monomeric and aggregated TDBC-4, the general location of the protons on the benzimidazole moieties did not change and therefore the properties of the pi-electrons did not change upon aggregation. Another way of demonstrating the relatively

independent character of the pi-electrons in the two regions is through absorption spectroscopy and the pH study that was done with TSPP showed that the magnitude of the transition dipole of the molecule did not change during the process of proton addition and aggregation. A pH study in basic solutions, shown in figure 5-7, was also conducted for TSPP for completeness however the only significant change in the spectrum of TSPP was a diminution in absorption intensity of the Soret band.

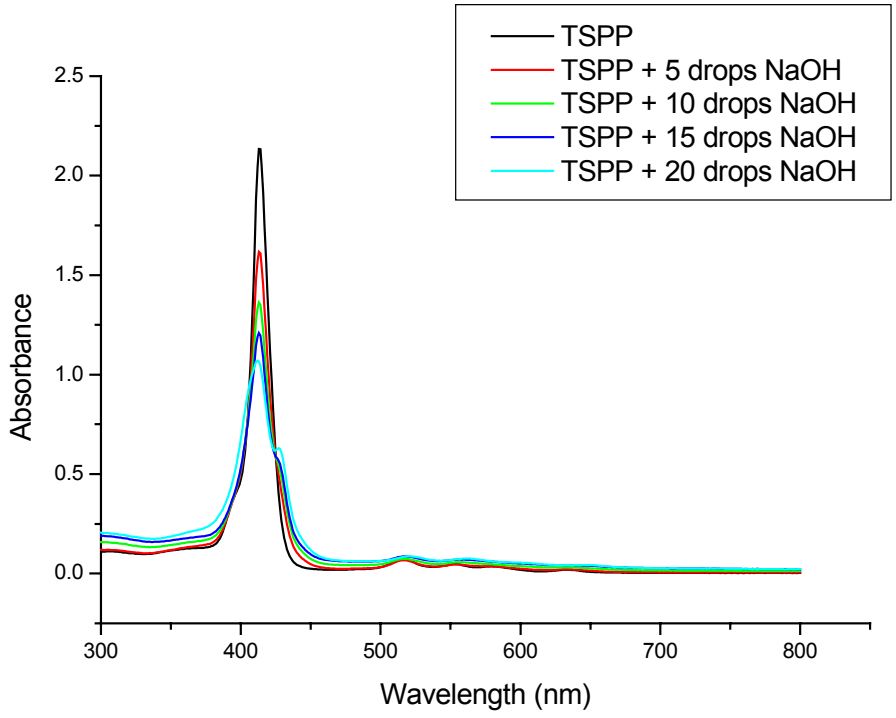

Figure 5-7. Absorption spectra of H_2TSPP in basic solutions.

The beginnings of another peak slightly to the red of the Soret band appears in the most basic TSPP solution and in between the two peaks seems to be an isosbestic point. These results, though interesting and potentially useful in tracking conformational changes in TSPP, need to be combined with special NMR analysis to be adequately discussed and will therefore not be analyzed further. Similar pH studies were attempted with Fe-TSPP

and Co-Protoporphyrin and the results are shown in figs 5-8 and 5-9, respectively. In the case of Fe-TSPP the addition of acid did not greatly change the absorption spectrum with the only change being a modest increase in the Soret band intensity likely caused by the slight change in acidity between the reference and sample solutions.

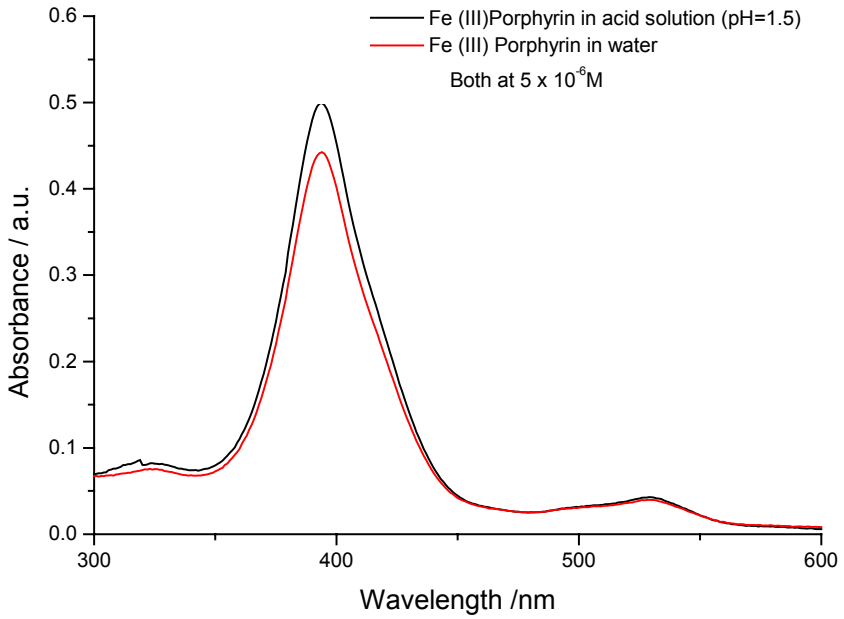

Figure 5-8. Absorption spectra of Fe-TSPP in acidic solutions.

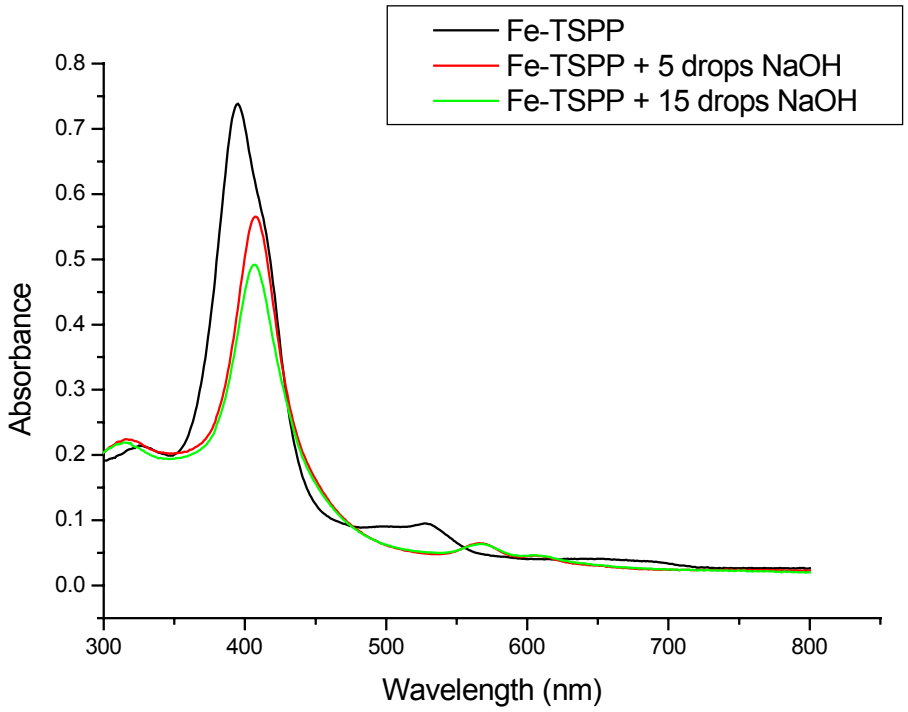

Figure 5-9. Absorption spectra of Fe-TSPP in basic solutions.

The fact that Fe-TSPP, unlike other metal analogues of TSPP, does not readily expel the metal in the core to form aggregated TSPP means that the ligand bonds are very strong in Fe-TSPP. It is reasonable to imagine that because of the strong bonding the molecule is planar and relatively inflexible to certain out-of-plane deformations in the center. In the case of Co-protoporphyrin the addition of acid, shown in figure 5-9, leads to a concomitant appearance of a peak to the red of the Soret and the latter's disappearance. The peak at 417 nm is likely a dimer species but not a J-aggregate because the peak does not show the characteristic narrow line-width and sharpness of J-aggregates. Furthermore the physical link between the two molecules is likely to occur through a ligand bond between the Co atoms rather than by the weak electrostatic interactions or orbital overlap by the surrounding pi-electrons as is the case for J-aggregates.

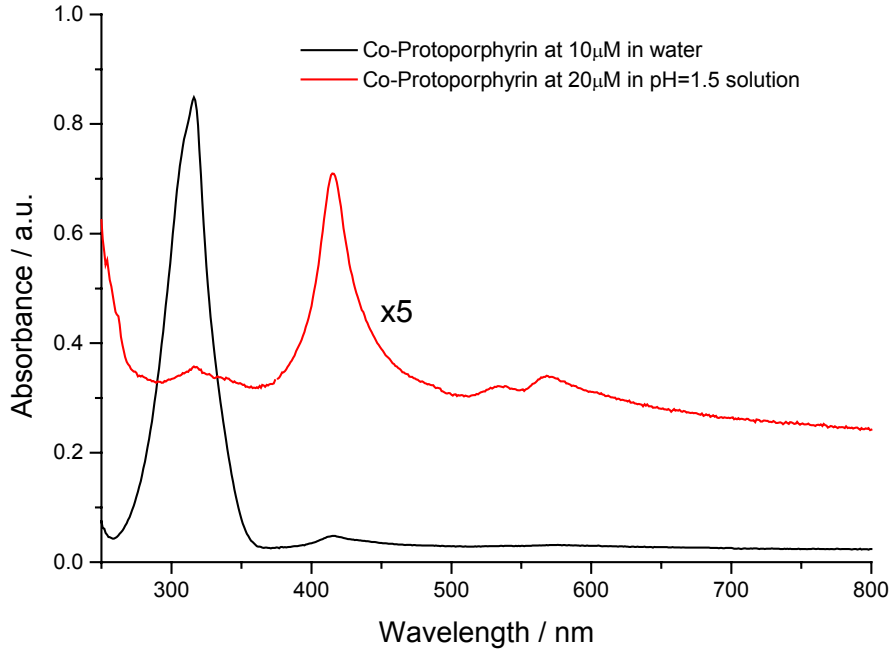

Figure 5-10. Absorption spectra of Co-Protoporphyrin in neutral water and acidic solution.

Although J-aggregates of neither metalloporphyrin were formed, it is still apparent that there are physical changes that take place under varying pH conditions that can be mimicked in electrochemical systems.

5.3.3 Cyclic Voltametry of TSPP, Fe-TSPP and Co-Protoporphyrin on platinum electrode

Cyclic voltammetry (CV) is a very useful electrochemical technique in that many properties of a molecule can be manipulated, often reversibly, by applying a varying potential at different rates of change. For instance, CV provides information on redox levels in a molecule, binding constants, and on electron-transfer rates between the working electrode and the analyte. For the purpose of this work CV is mainly useful as a method to deposit the two metalloporphyrins on an electrode surface as well as to

determine the necessary conditions for aggregation on the surface. It was determined through electrochemical methods that in the hydrogen adsorption/desorption region, H_4^{2+} $TSPP^{4-}$ aggregation occurs on the electrode surface in acidic electrolyte, which is evidenced by a pair of lower-lying bands in its Raman spectrum.

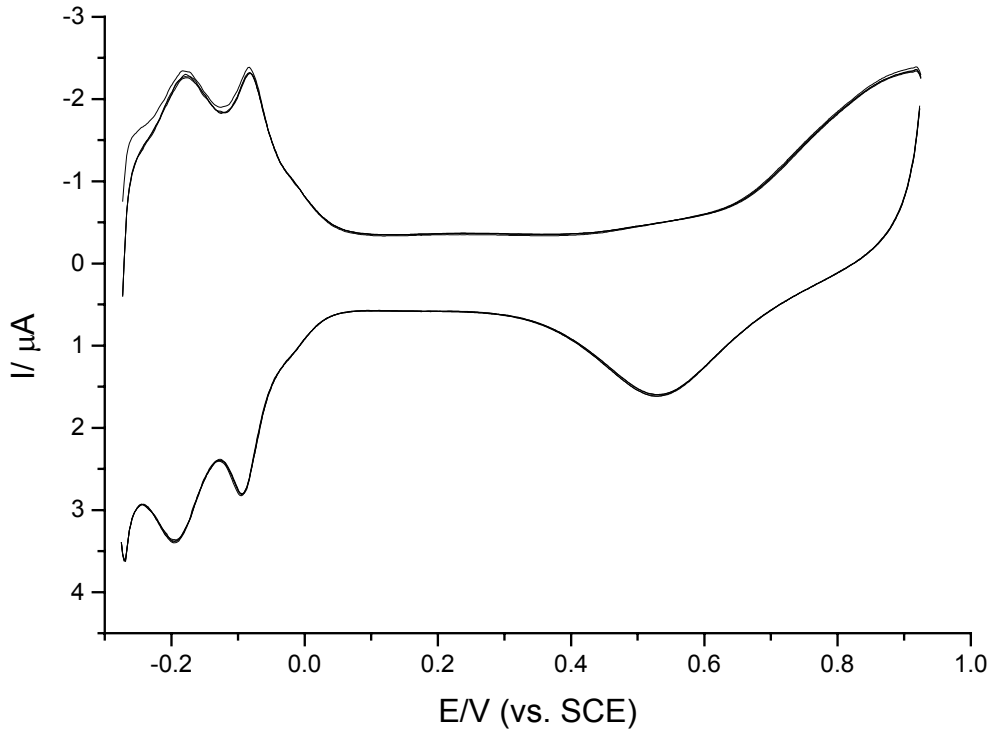

Figure 5-11. Cyclic voltammogram of Pt electrode in $HClO_4$ with a scan rate of 50 mV/s at pH 1.5.

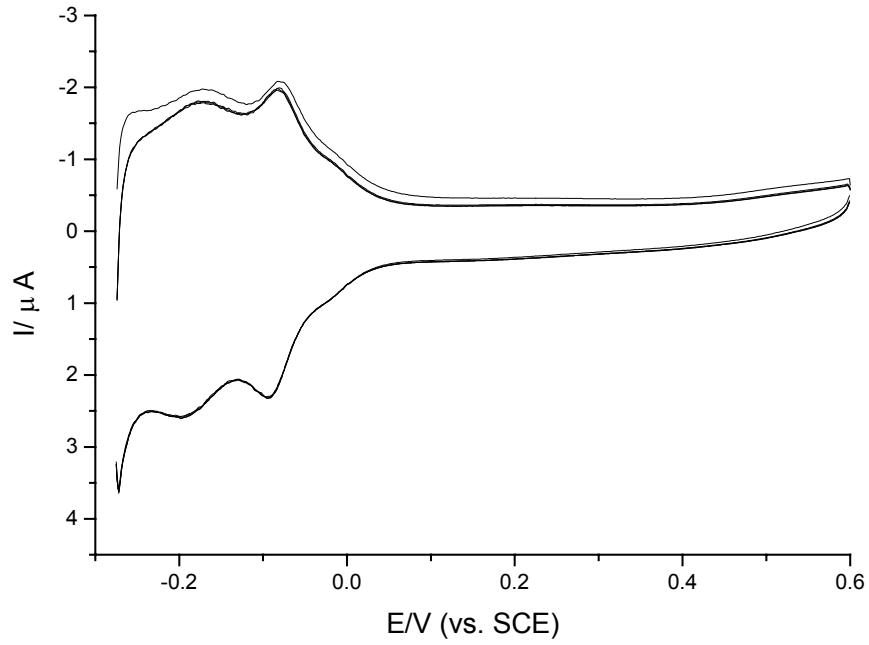

Figure 5-12. Cyclic voltammogram of Pt electrode in $HClO_4$ with a scan rate of 50 mV/s at pH 1.5 over the shorter potential range.

Although absorption spectra showed that Fe-TSPP is relatively resistant to proton insertion in the core cyclic voltammetry can be used to deposit the molecule onto the electrode surface where subsequently the Fe atom can conceivably be separated from the rest of the molecule using other methods. Figures 5-11 and 5-12 show the CVs of Pt electrode in $HClO_4$ at pH 1.5 in a range of –0.275V to 0.925V and –0.275V to 0.600V versus SCE, respectively. Both CVs show two peaks at –0.1V and –0.2V corresponding to hydrogen adsorption/desorption on the Pt surface. CVs were obtained over a range of –0.275V to 0.925V and –0.275V to 0.6V. In a solution of 50 μM Fe-TSPP shown in figure 5-13, the CV of platinum electrode shows a definite change compared to that of platinum in the background solution, of note is the near disappearance of the hydrogen

adsorption/desorption peaks suggesting that some Fe-TSPP molecules are being adsorbed on Pt.

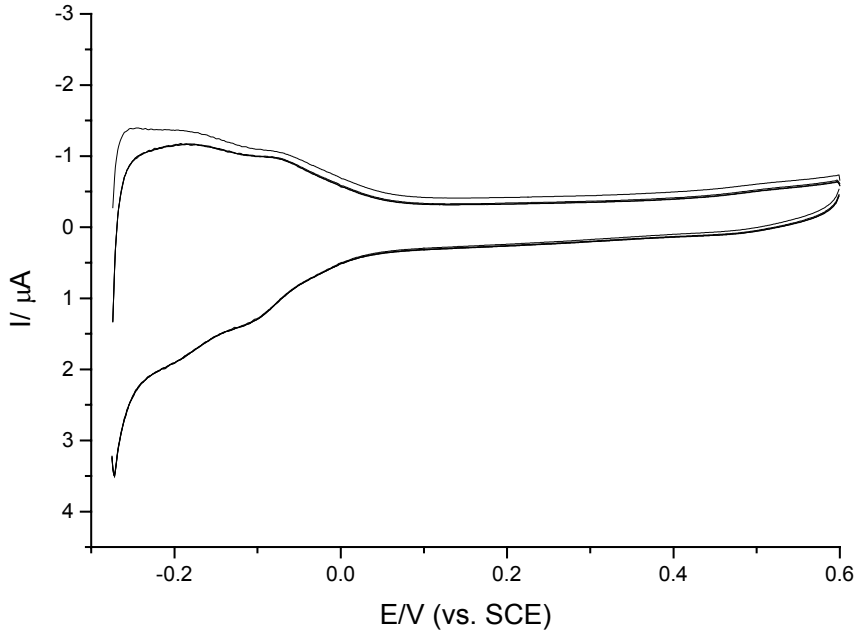

Figure 5-13. Cyclic voltammogram of Fe-TSPP on Pt electrode in $HClO_4$ with a scan rate of 50 mV/s at pH 1.5 over the shorter potential range.

In order to make sure that Fe-TSPP was not being simply physisorbed on the electrode surface, CVs were performed in background solution at least 24 hours after CVs were performed in porphyrin solution. The platinum electrode was stored in water overnight and the CV's in the background solution remained the same as they were in the porphyrin solution clearly showing that Fe-TSPP had chemisorbed onto the surface.

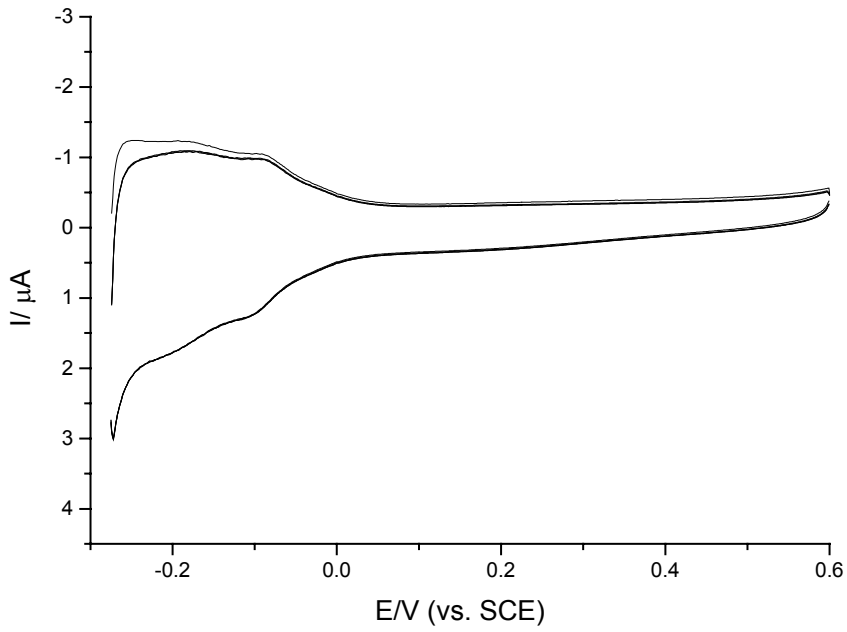

Figure 5-14. Cyclic voltammogram of Pt Electrode with adsorbed Fe-TSPP in $HClO_4$ with a scan rate of 50 mV/s at pH 1.5 over the shorter potential range.

Figure 5-14 is a CV taken of Pt electrode in background solution the day after the CV from figure 5-13 was performed. The CVs with Co-protoporphyrin are very similar in behavior to those of Fe-TSPP as can be seen in figures 5-15 and 5-16. Because it became apparent that for Fe-TSPP, the scans over the longer range of –0.275V to 0.925V led to gradual desorption of porphyrin, voltammograms were recorded over the shorter range to re-adsorb Fe-TSPP. Co-protoporphyrin did not show the same gradual desorption, signifying a stronger interaction between Co atom with platinum and that more positive potentials are needed for desporption to occur. From simply an electrostatic perspective, the additional electron in the Co d-shell orbitals relative to the configuration of Fe is enough to shield the Co atom more and explain its stronger bond to the pt electrode surface.

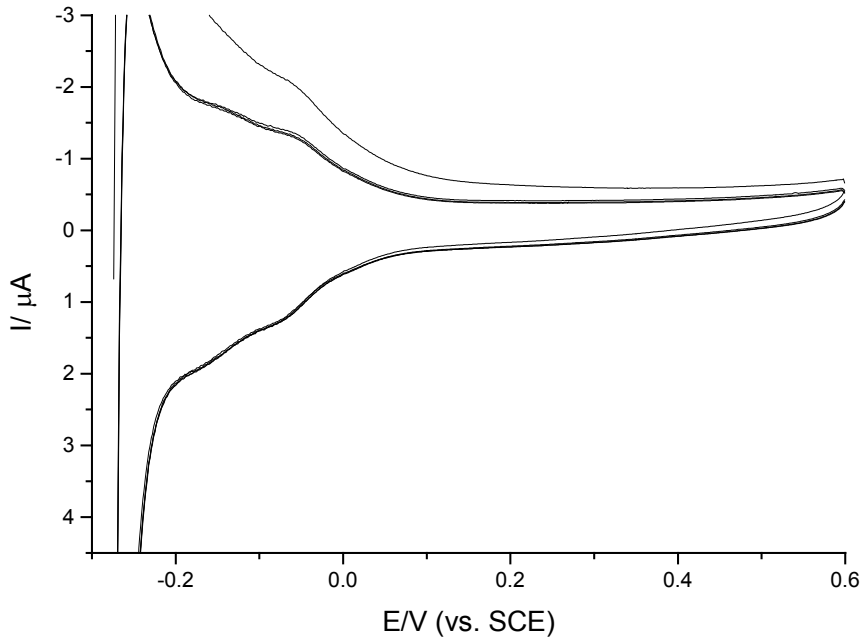

Figure 5-15. Cyclic voltammogram of Pt electrode in 10 mM Co-protoporphyrin in pH 1.5 $HClO_4$ over the shorter potential range.

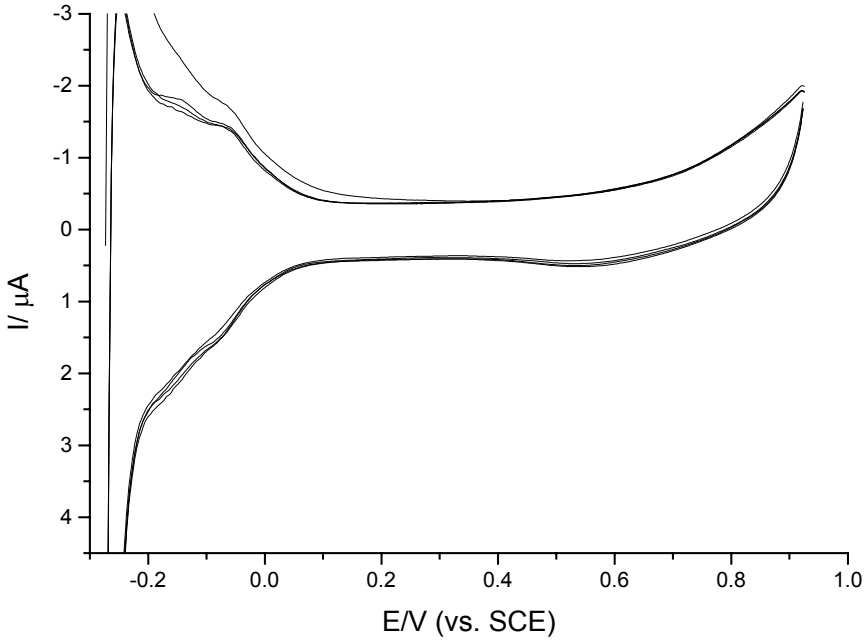

Figure 5-16. Cyclic voltammogram of Pt electrode in 10 mM Co-protoporphyrin in pH 1.5 $HClO_4$.

It is clear that the chemisorptions of the metal porphyrins take place through a bond formation between the electrode and the metal atom at the center of the porphyrin. This fact is very important because ideally one would want the porphyrin ring to interact as minimally as possible with the electrode and thus be available for porphyrin-porphyrin interactions, and possibly, aggregation. By depositing on the platinum electrode through the metal in the core, the porphyrins must deposit along the plane of the molecule and that physical separation between the metal atoms improves the possibility of placing a metal with catalytic properties on a surface in an ordered and well-separated fashion. Because the metal atoms did not separate from the porphyrins in either molecule, it is important to have as the next step in developing a method to use the aggregating properties of porphyrins as a viable technique to synthesize well-separated metal nanoparticles with low size distribution, a more universally applicable way to remove the metal from the porphyrin. It will meanwhile be more practical to try to use the metal porphyrin analogues of TSPP that more easily eject the metal from the core. Raman spectroscopy will be very useful in determining the strength of the metal-to-porphyrin ligand bonds in these molecules and future work in this area will also include NMR analysis. In particular, NMR studies on TSPP can be very informative because changes in peak positions of the central protons upon aggregation can be ascribed to changes in their relative distances. A detailed understanding of how the protons in the TSPP aggregate core arrange themselves would allow for a very credible physical model where all relevant factors such as slippage and offset angles, and molecular packing could be accurately determined. Once this model was obtained the generalized point-dipole

expression could be utilized immediately and an independently determined aggregate coherence length that relied solely on structural parameters could be compared to those obtained through dynamics experiments and simulations. Raman spectroscopy has been used successfully to determine many of vibrational properties of J-aggregates however it has not yet been possible to fully use this data with theory.

5.4 Summary and conclusion

A model of J-aggregated TSPP was constructed using a systematic approach that satisfied both structural and spectroscopic requirements and that model supported the conclusions obtained by AFM studies on aggregated TSPP.

Absorption studies were conducted on TSPP, Fe-TSPP, and Co-Protoporphyrin to examine the behavior of the metal porphyrins in acidic and basic media and to compare that behavior to TSPP. It was concluded that even in very basic media Fe-TSPP was particularly resistant to expulsion of the iron atom thus preventing proton addition to the pyrollic nitrogens and subsequent aggregation of TSPP. It was found that Co-Protoporphyrin did aggregate in acid however that aggregate was likely a Co-Co linked dimer and not a J-type aggregate. Electrochemical studies were conducted using cyclic voltammetry on the metalloporphyrins to determine the manner of deposition on a platinum electrode. Both metalloporphyrins were determined to have chemically adsorbed onto the surface of platinum although Co-protoporphyrin seemed to bond more strongly to the surface than Fe-TSPP as the latter was found to desorb when the potential was cycled over the longer range. Further studies could lead to the determination of the necessary conditions to create an aggregated species near the electrode surface where the

metal atom could both separate from the porphyrin and deposit on the electrode surface in a reasonably well separated and ordered manner.

Chapter 6: Summary and Future Directions

6.1 Summary

6.1.1 Structural characterizations of cyanine dyes

Cyanine dyes were studied to determine their structure and to obtain qualitative information concerning conjugation and its relationship to J-aggregate structure and stability. For the first time Raman and NMR methods were used together to characterize and differentiate similarly-constituted molecules. PIC and 2,2'-carbocyanine were studied together as well as TTBC and TDBC-4. All four cyanine dyes had enough structural similarities that the two pairs could also be compared to each other. Based on the structural data, it was possible to better understand how conjugation played a role not only in aggregate stability but also in aggregate formation.

6.1.2 PIC and 2,2'-carbocyanine monomer structure

Raman and NMR spectra were acquired for both PIC and 2,2'-carbocyanine in methanol solutions and results showed that despite the fact that the only structural difference between the molecules was the additional vinyl link on the bridge in 2,2'-carbocyanine, there were very noticeable and consequential vibrational and orbital differences. Raman spectra were very similar for both molecules and the main differences between the two were generally found in an area in the spectra where out-of-plane vibrations occur. Out-of-plane vibrations were comparatively suppressed in 2,2'-carbocyanine, relative to those

in PIC, in favor of in-plane vibrations. It was evident that the vibrations being produced in that region came from the bonds along the bridge and with the use of NMR spectroscopy it was possible to rationalize those results. Peaks corresponding to the methine and polymethine chain protons in PIC and 2,2'-carbocyanine, respectively, were found to be further up-field from the peaks corresponding to the protons on the moieties with the exception of the proton on the central carbon in the chain for 2,2'-carbocyanine. That proton's peak, along with the peaks corresponding to the protons in the moieties, was found in the aromatic region and though the peaks of the neighboring protons on the chain did not appear in the aromatic region they were nonetheless closer to it than the methine proton in PIC. With the help of this NMR data the nature of the pi orbital character of the bonds on the chains of both molecules was analyzed and used to understand the results obtained through Raman spectroscopy. It was determined that the greater the conjugation between pi orbitals in a molecule, manifested by the relative proximity of NMR peaks in or near the aromatic region, the more likely that the vibrational relaxation during a Raman scatter would occur through in-plane rather than out-of-plane vibrations. These results were also used to study TTBC and TDBC-4, because as carbocyanines, their NMR spectra could be directly compared to that of 2,2'-carbocyanine.

6.1.3 TTBC and TDBC-4 monomer and aggregate structure

Following the characterization of PIC and 2,2'-carbocyanine structure through Raman and NMR spectroscopies it was possible to infer even more information on TTBC and TDBC-4, two carbocyanines with benzimidazole moieties. It was shown through NMR results that unlike the case for PIC or 2,2'-carbocyanine, both TTBC and TDBC-4

monomer samples are composed of structural isomers that are due to the cis- or trans-type connectivity between the vinyl groups along the polymethine chains of both molecules. The presence of these isomers in TTBC and TDBC-4, particularly in light of the fact that isomerism was not apparent in samples of either PIC nor 2,2'-carbocyanine, was determined to be a direct consequence of the greater pi bond character in the bonds along the chains. With the absence of rotation about those bonds isomerism could remain in the samples, contrary to PIC and 2,2'-carbocyanine where molecules in solution could undergo rotations about their chains because of the relatively greater sigma bond character of the vinyl groups. The degree of conjugation within TTBC and TDBC-4 was also found to be a key factor in aggregation of these species. Both molecules self-assemble much more easily than PIC or 2,2'-carbocyanine and it was argued that because out-of-plane motions were so restricted in TTBC and TDBC-4 in favor of their in-plane motions, that the J-aggregate of these molecules formed by a process whereby the individual molecules slid into each other along that plane. In comparing the absorption and Raman spectra of molecular and aggregated TTBC and TDBC-4 it was argued that only one type of aggregate for each was formed even though there were initially several isomers present. It was also determined that in silver colloid, TTBC aggregates formed preferentially on the silver nanoparticles rather than in the solution. In studying the Raman spectra of aggregated TTBC on silver electrode and in silver colloid it was further confirmed that in colloidal suspension the aggregate formed on the nanoparticles rather than in solution. Topographically this suggested that the aggregate deposited on the surface along its length as opposed to depositing in an upright manner and that the optical coherence length of the aggregate was sufficiently short to be unaffected by the curvature

of the nanoparticle surface. J-aggregate structure and the optical coherence length were further discussed and it was argued that structural properties of J-aggregates could be enough to explain limitations to the coherence length.

6.1.4 TSPP J-aggregate and Cyclic Voltammetry of Fe-TSPP and Co-Protoporphyrin

The combined data obtained for the cyanine dyes provided much information to help deduce a structure for J-aggregated TSPP in a systematic manner that satisfied all spectroscopic and structural requirements for J-aggregation. An important concept in deducing the aggregate structure was that its properties were a product of two types of coupling. The first type of coupling was of a physical type where the pi orbitals on the moieties interacted and lead to the new bands that appear in the resonance Raman spectra of J-aggregates. The second type of coupling was an optical coupling of the transition dipoles, primarily by way of the chromophores, that gave rise to the optical coherence length of the aggregates. It was proposed that TSPP aggregate had a somewhat helical structure and this model agreed with a previously published model that relied on AFM data. With the importance of carbon nanotubes in the growing area of nanotechnology and the challenge of developing a method to synthesize nanotubes with uniform structural and electrical properties, metal porphyrins were studied as potential components in this process. It was thought that the aggregating properties of metal porphyrins, particularly of metal analogues of TSPP could be used to deposit metal nanoparticles that could catalyze carbon nanotube synthesis on an electrode surface. Because the nanoparticles were to have uniform size and the surface coverage, it was thought that any carbon nanotubes formed on the electrode would be well-separated and have uniform size and properties.

Two metal porphyrins were studied, Fe-TSPP and Co-protoporphyrin, through absorption spectroscopy and cyclic voltammetry and it was determined in the case of Fe- TSPP the nanoparticle could not be formed before the porphyrin deposited on the electrode surface by chemisorption. Likewise, in the case of Co-protoporphyrin it was determined that although it formed a dimer complex, the metal in the core was not released upon deposition and that no nanoparticle was formed. Although much of the initial objectives were not met with Fe-TSPP and Co-protoporphyrin it was nonetheless important to determine the nature of the absorption of the porphyrins on the electrode surface. It was determined that both Fe-TSPP and Co-protoporphyrin chemisorbed and that the stronger chemisporption of Co-protoporphyrin was likely because of the additional available d-shell electron with which to bond to the surface. It was concluded that further study was necessary and other porphyrins could be used to attempt to form metal nanoparticles on an electrode surface upon porphyrin aggregation.

6.2 Future Directions

6.2.1 Raman and NMR studies of Cyanine Dyes

Using Raman spectroscopy in conjunction with NMR methods was shown to be very useful in gathering very important information on the conformational and orbital similarities between similarly constituted cyanine dyes. Future work with cyanine dyes using both spectroscopies is essential to conclusively determining the structural properties of these dyes and their aggregates. These methods would serve as independent sources of data to which computational data as well as crystallographic data could be

compared. It is conceivable that an exhaustive study of the quinocyanines, carbocyanines and all of their variants will eventually lead to a comprehensive understanding of all the internal and external factors that affect molecular conformational changes and J-aggregate formation.

6.2.2 NMR Analysis of TSPP

One of the difficulties in conclusively determining the arrangement of protons in the TSPP core through NMR spectroscopy is that the formation of the aggregate necessitates acid and the abundance of protons in solution would greatly complicate any analysis. It is nonetheless possible to use deuterated acids to protonate TSPP and track the changes that occur in the NMR peak of that proton pair. A more exotic approach that would yield even more valuable information than a conventional proton NMR method but is perhaps very costly and difficult, is to synthesize TSPP with N14 and perform N14 NMR. In this manner all the conformational changes along the whole process leading to the aggregate would be followed.

6.2.3 Ultrafast Studies

Ultrafast studies of exciton dynamics of J-aggregates are still actively done and remain essential to understanding the lifetimes of molecular excitons and understanding nonlinear phenomena involving them such as exciton-exciton annihilation. In order to fully determine and understand all the properties that differentiate J-aggregate systems from those of their constituent molecules structural data will have to be linked at the theorectical level to the dynamical data.

6.3 Conclusions

For the first time absorption, Raman, and NMR spectroscopy were used together to characterize various structural properties of J-aggregating molecules and to help deduce a model of a J-aggregate. Much information was gathered that helped identify trends between structurally similar molecules and helped determine conditions for aggregation. The optical coherence length of a J-aggregate was studied from a structural perspective and the results showed that coherence lengths could be limited on the basis of simple phase relationships between the transition dipoles of neighboring molecules. These methodologies and results presented provided the foundation for original future work related to dye, porphyrin, and J-aggregate structure.

References

Chapter 1 References

1. Metzger, R, *Acc. Chem. Res.*, **1999,** 32, 11
2. Nolte, R. J. M.; Vriezema, D. M.; Aragone`s, M. C.; Elemans, J. A. A. W.; Cornelissen, J. J. L. M.; Rowan, A. E., *Chem. Rev.*, **2005,** 105, 4
3. Poole, C.; Owens, F. *Introduction to Nanotechnology*; John Wiley; New York, **2003**
4. Periasamy, N.; Koti, A. S. R.; Taneja, *J. Chem. Phys. Lett.*, **2003**, 375, 171; Haddon, R. C.; Niyogi, S.; Hamon, M. A.; Hu, H.; Zhao, B.; Bhowmik, P.; Sen, R.; Itkis, M. E. *Acc. Chem. Res.*, **2002**, 35, 1105
5. Behera, G. B.; Mishra, A.; Behera, R. K.; Behera, P. K.; Mishra, B. K. *Chem. Rev.* **2000,** 100,6
6. Kobayashi, T *Mol. Cryst. Liq, Cryst.*, **1996**, 283, 17
7. Pearlstein, R.M. In *Photosynthesis*, Amesz, J., Ed.; Elsevier: Amesterdam, **1987**
8. Akins, D. L.; Zhu, H-R *Langmuir*, **1992**, 8, 546
9. Akins, D. L.; Zhu, H-R; Guo, C. *J. Phys. Chem.*, **1994**, 98, 3612; Akins, D. L.; Zhu, H-R; Guo, C. *J. Phys. Chem.*, **1996**, 100, 5420; Akins, D. L.; Zhu, H-R; Guo, C. *J. Phys. Chem.*, **1996**, 100, 14390; Akins, D. L.; Zhuang, Y. H.; Zhu, H-R; Liu, J. Q. *J. Phys. Chem.*, **1994**, 98, 1068
10. Akins, D. L. *J. Col. Int. Sci.*, **1982**, 90, 374
11. Akins, D.L.; Ozcelik, S *J. Phys. Chem. B*, **1999**, 103, 8926
12. Israelachvili, J.; *Intermolecular and Surface Forces*; Academic Press, New York, **1992**
13. Akins, D.L.; Guo, H; Xu, W *J. Phys. Chem. B*, **2001**, 105, 1543; Akins, D.L.; Guo, H; Zhang, X; Aydin, M; Xu, W; Zhu, H-R *J. Mol. Struct.* **2004**, 689, 153
14. Akins, D. L.; Akpabli, C. K.; Li, X. *J. Phys. Chem.*, **1989**, 93, 1977
15. Jean-Mary, F. Spectroscopic and Microscopic Studies of Aggregated Molecules Coated onto Nanomaterials; Ph.D. dissertation, City University of New York, 2006
16. Davydov, A. S.; Theory of Molecular Excitons; McGraw-Hill, New York **1962**
17. Kasha, M.; Rawis, H. R.; El-Bayoumi, M. A. *Pure Appl. Chem.* **1965** 11, 371
18. Herz, A. H. *Adv. Colloid. Interface. Sci.* **1977**, 8, 237
19. Ozcelik, S. Spectroscopic and Dynamic Properties of Molecules Adsorbed on Surfaces; Ph.D. dissertation, City University of New York, 1996
20. Kobayashi, T.; Kuroda, M.; Shiraishi, Y.; Yang, A. *J. Chem. Phys.*, **1998**, 109, 8442
21. Bakalis, L. D.; Knoester, J. *J. Lumin.*, **1999**, 83, 115; Meier, T.; Chernyak, V.; Mukamel, S. *J. Phys. Chem. B.* **1997**, 101, 7332;
22. Israelachvili, J.; *Intermolecular and Surface Forces*; Academic Press, New York, **1992**
23. Akins, D. L.; Lombardi, *J. Chem. Phys. Lett.*, **1987**, 135, 495
24. Akins, D. L.; Guo, C.; Zhu, H-R *J. Phys. Chem.*, **1993**, 97, 3974
25. Akins, D. L.; Guo, C.; Ren, B. *J. Phys. Chem.*, **1998**, 102, 8751
26. Li, Q.; Tan, J.; Peng, B-K, *Molecules*, **1997**, 2, 91

27. Feldman, I. H.; Herz, A. H.; Regan, T. H. *J. Phys. Chem.*, **1968**, 72, 6
28. Graves, R. E.; Rose, P. I., *J Phys. Chem.* **1974**, 79, 7
29. Henrichs, P. M.; Gross, S. J., *J. Am. Chem. Soc.* **1976**, 98, 23
30. Egorov, V. V. *Chem. Phys. Lett.* **2001**, 336, 284; Kobayashi, T.; Misawa, K. *J. Lumin.*, **1997**, 72, 38
31. Ajayan, P. M., *Chem. Rev.*, **1999**, 99, 1787
32. Kasumov, A. Y.; Deblock, R.; Kociak, M.; Rewlet B.; Bruchet, H.; Khodos, I. I.; Gorbatov, Y. B.; Volkov, V. T.; Journet, C.; Burghard, M. *Science*, **1999**, 284, 28
33. Weisman, R. B. *Nature Materials*, **2003**, 2, 569

Chapter 2 References

1. Jean-Mary, F. Spectroscopic and Microscopic Studies of Aggregated Molecules Coated onto Nanomaterials; Ph.D. dissertation, City University of New York, 2006
2. Craig, D. P.; Thirunamachandran, R. *Molecular Quantum Electrodynamics*; Academic Press; New York, **1984**
3. Atkins, P. W., *Physical Chemistry*; W. H. Freeman and Company, 7th Ed; New York, **2002**
4. Macomber, R. S., *A Complete Introduction to Modern NMR Spectroscopy*; Wiley-Interscience, 1st Ed; New York, **1998**
5. Bard, A.; Faulkner, L. R., *Electrochemical Methods: Fundamentals and Applications*; Wiley, 2nd Ed; **2000**

Chapter 3 References

1. Herz, A. H. *Adv. Colloid. Interface. Sci.* **1977**, 8, 237; Scheibe, G. *Angew. Chem.*, **1936**, 49, 563; Jelley, E. E. *Nature*, **1936**, 138, 1009; Graves, R. E.; Rose, P. I., *J Phys. Chem.* **1974**, 79, 7
2. Akins, D. L. *J. Col. Int. Sci.*, **1982**, 90, 374
3. Akins, D. L.; Guo, C; Aydin, M; Zhu, H-R *J. Phys. Chem. B*, **2002**, 106, 5447
4. P. M.; Gross, S. J., *J. Am. Chem. Soc.* **1976**, 98, 23

Chapter 4 References

1. Akins, D.L.; Ozcelik, S, *J. Phys. Chem. B*, **1999**, 103, 8926
2. Fidder, H.; Knoester, J.; Wiersma, D.A., *J. Chem. Phys.*; **1991**, 95, 7880
3. Spano, F. C.; Mukamel, S., *J. Chem. Phys.*; **1989**, 91 , 683
4. Misawa, K; Yao, H.; Hayashi, T.; Kobayashi, T., *J. Chem. Phys.*; **1991**, 94, 4131
5. Misawa, K; Machida, S.; Horie, K.; Kobayashi, T., *Chem. Phys. Lett.*, **1995**, 240, 210

6. Jean-Mary, F. Spectroscopic and Microscopic Studies of Aggregated Molecules Coated onto Nanomaterials; Ph.D. dissertation, City University of New York, 2006

Chapter 5 References

1. Pearlstein, R.M. In *Photosynthesis*, Amesz, J., Ed.; Elsevier: Amesterdam, **1987**
2. Creighton, S.; Hwang, J. K.; Warshel, A.; Parson, W. W.; Norris, J. *Biochemistry*, **1988**, 27, 774
3. Akins, D. L.; Zhu, H-R; Guo, C. *J. Phys. Chem.*, **1994**, 98, 3612
4. Akins, D. L.; Zhu, H-R; Guo, C. *J. Phys. Chem.*, **1996**, 100, 5420
5. Akins, D. L.; Zhu, H-R; Guo, C. *J. Phys. Chem.*, **1996**, 100, 14390
6. Nagahara, T.; Imura, K.; Okamoto, H. *Chem. Phys. Lett.*, **2003**, 381, 368
7. Rotomskis, R.; Augulis, R.; Snitka, V.; Valiokas, R.; Liedberg, B. *J. Phys. Chem. B*, **2004**, 108, 2833
8. Akins, D. L.; Guo, C.; Ren, B. *J. Phys. Chem.*, **1998**, 102, 8751
9. Periasamy, N.; Koti, A. S. R.; Taneja, *J. Chem. Phys. Lett.*, **2003**, 375, 171
10. Li, Y.; Liu, J.; Wang, Y.; Wang, Z.-L. *Chem. Mater.,* **2001**, 13, 3
11. Eugster, N.; Jensen, H.; Fermín, D.; Girault, H. *J. Electroanal. Chem.*, **2003**, 560, 143